THE UNIVERSITY OF OKLAHOMA

GRADUATE COLLEGE

PVT PROPERTIES OF GASES TO 10,000 BARS AND 400° C

A DISSERTATION

SUBMITTED TO THE GRADUATE FACULTY

in partial fulfillment of the requirements for the

degree of

DOCTOR OF PHILOSOPHY

BY

STANLEY LUNSFORD ROBERTSON

Norman, Oklahoma

1969

PVT PROPERTIES OF GASES TO 10,000 BARS AND 400° C

APPROVED BY

Stanley E. Babb, Jr.

Harold V. Knuckles

Joe C. Holste

Keith D. Carroll

Gustave A. Day

DISSERTATION COMMITTEE

ACKNOWLEDGEMENT

The author owes an insurmountable debt of gratitude to Dr. Stanley E. Babb, Jr. for his guidance of this research effort, for many illuminating discussions of the problems encountered and the long hours of laboratory work in which he personally took part.

The effort of Gene J. Scott who largely constructed the apparatus and kept it intact and who bailed the author out of many difficulties is gratefully acknowledged.

Special thanks are due to Mary Lou Stokes who typed the manuscript, to my wife for help, encouragement and understanding and to my parents who have encouraged and helped me throughout my life.

TABLE OF CONTENTS

TABLE OF CONTENTS (Continued)

LIST OF TABLES

LIST OF ILLUSTRATIONS

PVT PROPERTIES OF GASES TO 10,000 BARS AND 400° C

CHAPTER I

INTRODUCTION

Of the three common states of matter; solid, liquid and gas, the liquid or dense fluid state is perhaps the least studied and is certainly the least understood. The dense fluid state encompasses the middle range of molecular interactions - between the ideal gas and the solid - and it is precisely this feature which makes a theoretical description extremely difficult. As yet the intermolecular potential functions are only poorly represented and even if they were in fact known one can imagine the difficulty in developing a theory which must on one extreme give the randomness of a dilute gas and on the other, the regularity of a solid lattice. Statistical mechanics may now be developed to an extent which is sophisticated enough to handle the description of the dense fluid state, however, this remains to be seen. The advent of high-speed digital computers has permitted solution of theoretical equations which use assumed representations of intermolecular potentials, but unfortunately there is a paucity of reliable experimental data for comparison in the high-density region.

The experimental results given within this report should alleviate in part the lack of accurate data for pressures above 2000 bars and hopefully they will lead to better theory; better representation of intermolecular potentials, or both.

PVT measurements to 3000 bars have been made and with claims of very high accuracy for several gases at the van der Waals laboratory.[1] Beyond this pressure the experiments have been few in number and sometimes of questionable accuracy. Benedict[2] has studied nitrogen to 5500 bars following Bridgman's[3] earlier measurements on the same gas. Bassett and Dupinay[4] have given a few isolated points to 5000 bars for nitrogen and hydrogen and Blake, *et al*[5] have investigated mixtures of nitrogen and methane to 5000 bars. The measurements of Bridgman cover a slightly larger pressure range than those reported herein but suffer from an apparent systematic error. Since the inception of the present work Tsiklis[6] has published results for nitrogen and argon which cover both the same pressure and temperature ranges as the present work. Comparisons between the results reported within this thesis and those obtained by other workers will be given.

The basic method of the present experiment consists of measuring isothermal volume changes in a fixed mass of gas between an initial pressure and a series of higher pressures. Fiducial densities below 3000 bars corresponding to some of the measured pressures are then used to determine both the initial volume of the piezometer and

the mass of enclosed gas. The reliance upon fiducial densities is occasioned by the presence of a freeze valve which is used to separate the piezometer from the gas loading system which cannot withstand pressures greater than about 4000 bars. Although the volume of frozen gas which plugs the capillary is small it is by no means negligible in comparison with the rest of the sample. The changes in volume of frozen gas between 2000 and 10,000 bars are, fortunately, negligible thus permitting the use of this type valve for change of volume measurements. This point will be discussed in a succeeding chapter. The bulk of the volume of the piezometer is enclosed in a purely hydrostatic environment which thereby minimizes the corrections for compression of its parts and completely eliminates the possibility of plastic distortion. Finally, the apparatus permits continuous readings rather than the discrete Burnett or Amagat-type measurements.

CHAPTER II

APPARATUS

Pressure

The design of the experiment described herein has been largely dictated by a desire for accuracy of 0.1 per cent or better for the experimental measurements of pressure, volume, and temperature. The greatest concession to convenience consists of the use of manganin resistance gauges for the pressure measurements. Previous studies[7] of these gauges and the author's own experience indicate that the gauges become inaccurate on the order of 0.1 per cent at pressures below 2000 bars due to calibration errors although the internal precision of the measurements is seemingly limited only by the Leeds-Northrup G-2 Mueller bridge used for the resistance measurement. The least subdivision of the bridge is 0.0001 ohms and the pressure measurements are internally consistent to a corresponding accuracy which is about 0.4 bars for the gauges used.

For reasons of accuracy, then, most of the measurements presented within this thesis were taken at pressures above 2000 bars. The measurements above 2000 bars, however, only add to the range of experimental knowledge of the gases which have been studied since reasonably accurate data to 3000 bars is available for most of them.

The availability of this fiducial data has permitted this experiment to take advantage of the bellows technique[8] for measurements of gas volume changes rather than absolute volumes. The small spring constants of the bellows used has in turn permitted pressure measurements to be made in the pressure transmitting medium which surrounds the piezometer. The difference in pressure between the inside of the piezometer and the exterior is in all cases less than 0.3 bars and hence within the accuracy of the measurements.

Volumes

The piezometer which is shown schematically inside the pressure vessel in Fig. 1 consists of a constant volume chamber (excepting thermal expansion, etc.) of about 10.2 cc volume connected by a 60 cm long capillary tube of about 0.33 cc volume to a nickel bellows which has a volume which can be varied between approximately 2 cc and 6 cc. These parts of the piezometer account for about 99.4 per cent of the total piezometer volume and are completely enclosed within the pressure vessel thus insuring that the bulk of the piezometer is subject only to hydrostatic stress. The presence of purely hydrostatic stresses both simplifies and lends accuracy to the small corrections which must be applied to volume measurements. With these corrections applied the gas volume changes which occur in the piezometer can be determined to better than 0.1 per cent with an internal precision of about 0.0007 cc.

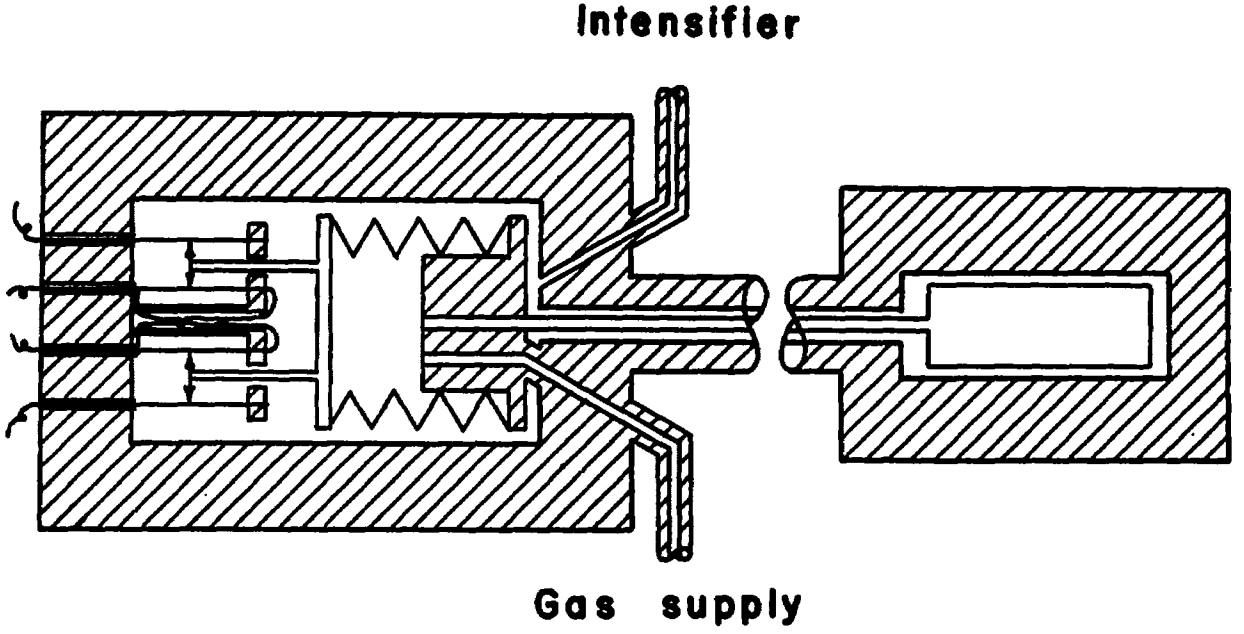

Figure 1. Piezometer and Pressure Vessel

A stainless steel capillary tube of 0.0508 cm I.D. leads from the bellows through the closure of the pressure vessel into a U-shaped freeze valve[9] which is used to isolate the piezometer from the gas loading compressors. The bottom of the U is dipped into liquid nitrogen and if necessary sufficient pressure is applied to the gas to freeze it and plug the capillary. A large temperature gradient exists over a length of about two or three inches between the liquid nitrogen level and the foam rubber cap of the dewar flask. About fourteen additional inches of capillary tube at room temperature are required to reach the pressure vessel. The volume of the capillary between its frozen plug and the bellows is about 0.1 cc. Addition of the volumes of the various parts of the piezometer yields a total volume which is variable between approximately 17 cc and 13 cc. The bellows which are manufactured by the Servometer Corporation are of electrodeposited nickel, 0.750 inches O.D. x 0.570 inches I.D. x 0.0015 inch walls with 28 convolutions. The fragility of the bellows and the difficulty of calibrations dictates the necessity for keeping the bellows portion of the piezometer relatively cool; thus it was separated from the constant volume chamber which is heated to temperatures as high as 400° C.

The most critical part of the apparatus is the electrical system which is used to measure the bellows volume changes. The method of measurement is potentiometric since sliding electrical contacts are part of the scheme. The heart of the electrical system is a Wheatstone bridge which is encased (along with the bellows) in a

brass frame and suspended directly inside the pressure vessel. The bridge and bellows are shown schematically in Fig. 2. The bellows has two stainless steel end plugs which are soft-soldered to the bellows. One plug protrudes into the bellows interior to reduce the enclosed volume and to act as travel limiters while both plugs serve as convenient bosses for attachment to the bridge. One end of the bellows and the electrical wires of the bridge are rigidly attached to the brass case. The "free" end of the bellows is attached to the carriage for the sliding contacts of the bridge. The bridge wires are all of nichrome 1.6 inches long and with individual resistances of approximately 0.88 ohms. The wires are set in tension by set screws outside the brass case and are electrically insulated from the case by means of teflon washers.

Referring to Fig. 2; the leads B and C are connected through a current-limiting resistor to a battery and the potential across the leads A and D is balanced against an external potentiometer. Fig. 2 shows that the central pair of wires of the bridge conduct currents in opposite directions. Thus these two wires from the arms of a Wheatstone bridge and mechanical motion of the bellows produces a voltage change which is double that which could be obtained from a single wire carrying the same current as one of the bridge arms. The hardened steel sliding electrical contact is epoxied to the carriage which attaches to the bellows and moves parallel to the axis of symmetry of the bellows. The bridge wires are pressed by spring-loaded

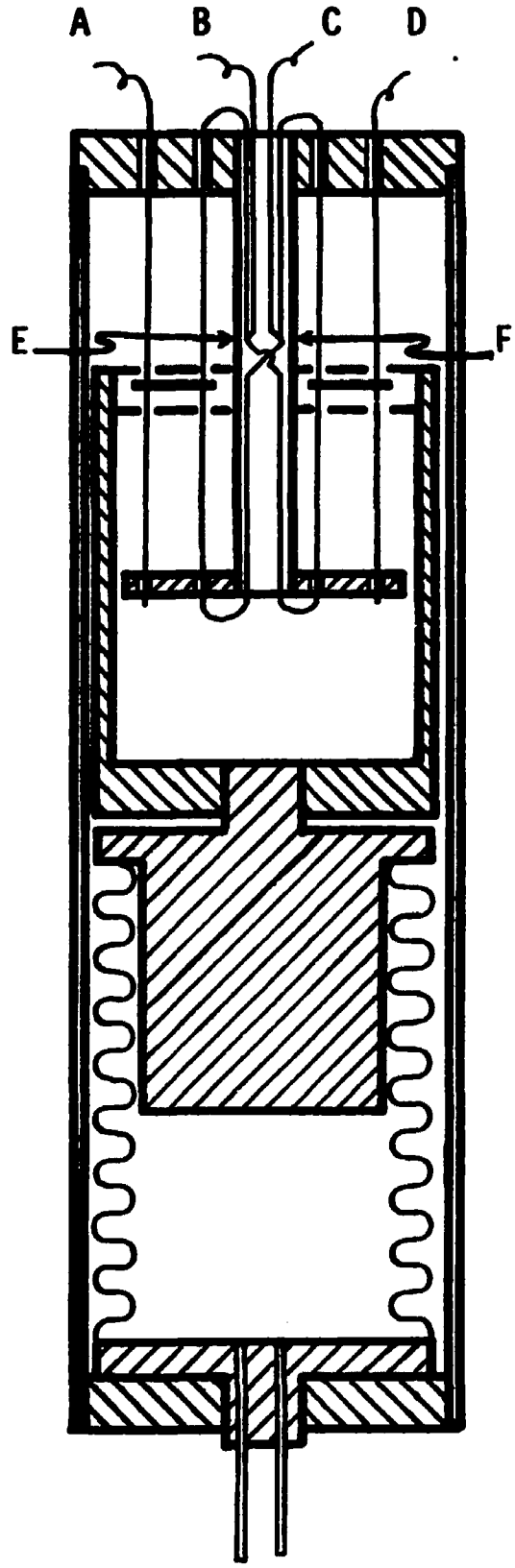

Figure 2. Wheatstone Bridge and Bellows

bakelite pads against the sliding contact. The construction is such that the taut bridge wires are not deflected by motion of the bellows. One other important feature of the bridge arrangement is the equality of the resistances from points E and F to the ends of the slidewires. This construction keeps the null position of the bridge at the same point on the current leads when the bridge is under pressure which causes the wire resistance to change. The external potentiometer circuit consists of a Leeds-Northrup Kohlrausch slidewire, which is suitably shunted. The slidewire resistance of 7.13 ohms is apportioned into 1000 equal length divisions and the resistance of the wire is linear in the scale divisions to about one part in 8000. The slidewire can be interpolated to 0.1 divisions and systematic departures from linearity have a rms value of 0.15 divisions. The useful stroke of the bellows is displayed on about 1500 divisions of the slidewire by reversing the polarity of the Wheatstone bridge output when its sliding contact reaches the null position.

The equivalent circuits of the bellows Wheatstone bridge and external potentiometer are shown in Fig. 3 with the equivalent points A, B, C and D of Fig. 2 appropriately labeled. The dashed line marked "0" represents the null position of the Wheatstone bridge. The operating procedure requires the standardization of the current ratio between Wheatstone bridge and Kohlrausch slidewire. The resistor R_2 is used to standardize the current ratio. The constancy of R_2 is critical for the experiment thus it is specially made of manganin and

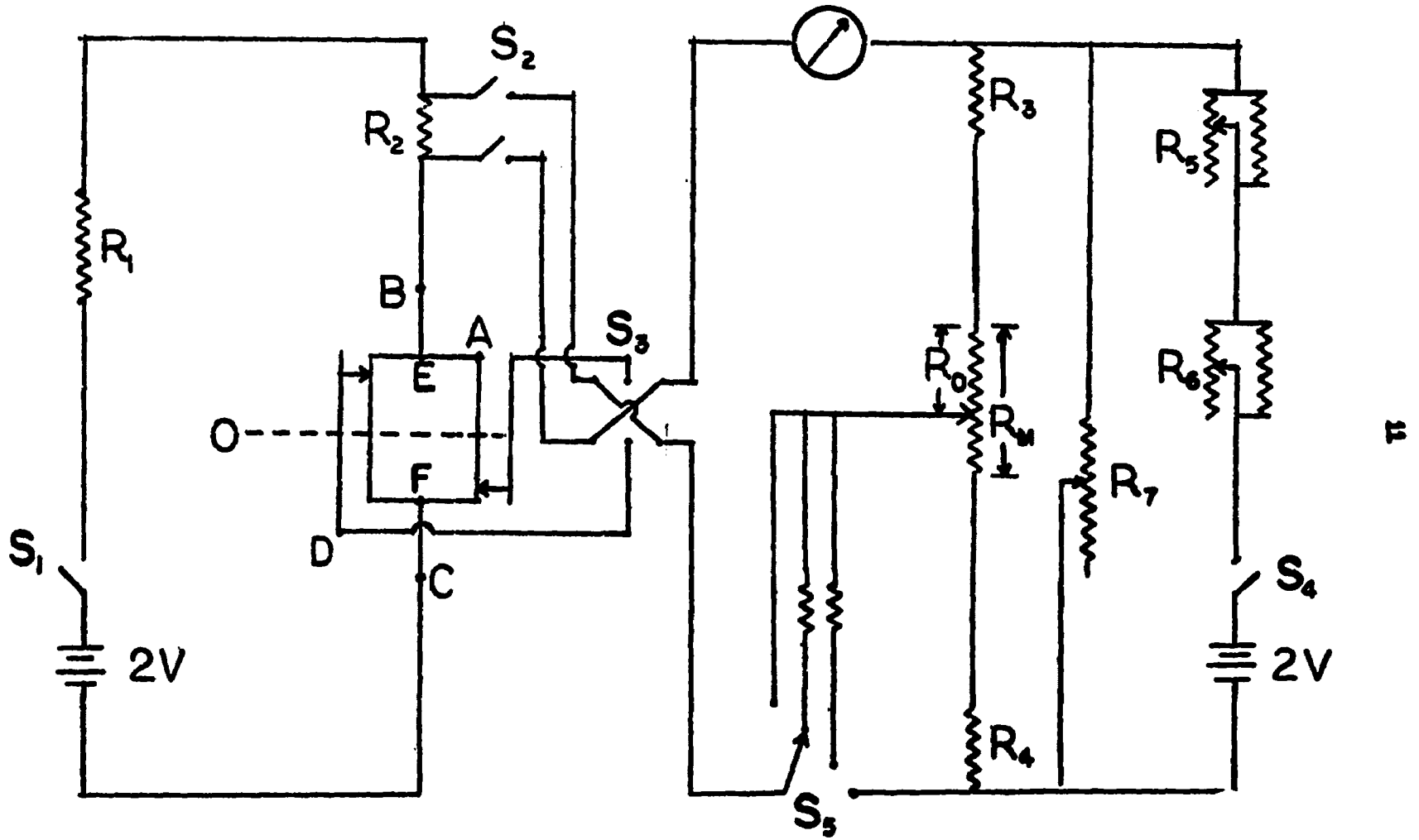

Figure 3. Bridge and Potentiometer Circuit

thermally insulated. The variable resistors R_5 and R_6 are used for the adjustment of the current ratio between Wheatstone bridge and the Kohlrausch slideware. The resistor R_7 is a shunt designed to keep both batteries producing the same current and their discharge rates the same so that the current ratio once balanced doesn't drift rapidly in time. In practice the current ratio is adjusted before each reading of the slidewire position. In addition the switches S_1 and S_4 are double-pole, double-throw switches which permit readings to be taken with both normal and reversed current directions. Averaging the resulting pair of readings then eliminates the effect of all thermal emfs which do not vary during the time of observation.

Temperature

The bellows and its associated sensing equipment is housed in a portion of the pressure vessel which is immersed in a well-stirred oil bath and controlled with heaters and a mercury in glass thermostat at 35.00±0.01° C. The constant volume chamber's cell is housed in a metal block thermostat which can be controlled at various temperatures to 400° C. The cylindrical metal block thermostat completely encases the pressure cell of the constant volume chamber. The block has heater windings on its side and independently controllable end heaters which are used to compensate for heat losses through the pipe which connects the pressure vessels of the constant volume chamber and bellows. The temperature control is exercised by switching a portion of the heater currents with relays which are actuated by photocells

and a galvanometer light. The control element is a nickel resistance thermometer in a Wheatstone bridge. The unbalance voltage of the bridge is displayed on the galvanometer. Control oscillations of about 0.02° C occur at the exterior of the pressure vessel and these are largely damped out in passage into the inner bore[10]. Temperature measurements on the constant volume chamber are made using calibrated thermocouple placed at the outer wall of the pressure vessel.

An important feature of the construction of the pressure vessel is the pipe which connects the cells for the bellows and constant volume chamber. The piezometer is supported at only one point on the cool end of the pipe and the electrical leads for the Wheatstone bridge are passed through the pipe at the same end. It is thus possible to remove the piezometer from the pressure vessel without dissembling the piezometer. This is especially important since it is possible to change the pressure seals when need arises without disturbing a carefully calibrated piezometer. Despite the fragile appearance of the pipe local rumors insist it will endure forever.

The remainder of the apparatus consists of the gas handling system used for loading gas into the piezometer. A block diagram of this apparatus is shown in Fig. 4. The loading is done in three stages. After evacuating to about 10^{-2} mm-Hg, gas is fed into the piezometer through a regulator which permits the pressure to be raised to the full bottle pressure and pressure transmitting fluid (petroleum ether) is pumped either alternately or simultaneously into the pressure

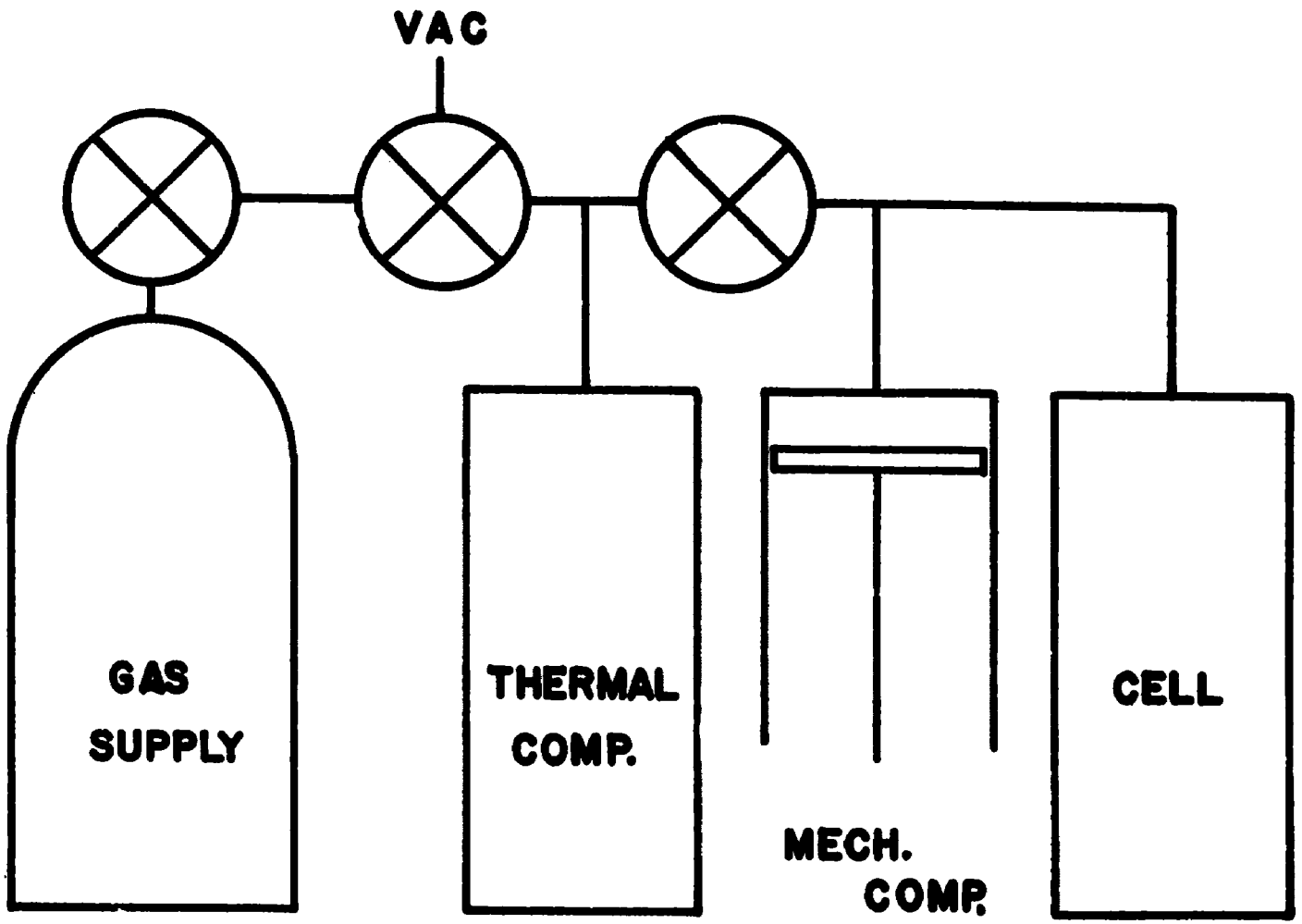

Figure 4. Gas Loading System

vessel but exterior to the piezometer. A second stage of pumping is accomplished using a liquid nitrogen cooled thermal compressor of 64 cc to condense the gas from the bottle and upon heating the gas pressure can be raised to around 300 bars. The final stage of pumping is done by a single stroke piston pump which has a maximum volume of approximately 170 cc. The pump has greaseless teflon and viton packing to prevent introduction of impurities into the gas sample. Pressures up to 4 kbar can be generated with the pump. After pumping to the desired initial pressure the freeze valve is used to seal the piezometer and the piston pump can be relieved of duty until it becomes necessary to unload. The unloading procedure is exactly the reverse of loading and it might be added that these are the most difficult of all manipulations of the apparatus. Since the thin-walled bellows is easily ruptured by one or two bars over-pressure care must be taken during loading to keep the bellows motion within safe operating limits. Since the loading system can be relieved of pressure during the time of operation of the apparatus, it is easy to introduce new gas bottles to hold the reclaimed samples for analyses for impurities.

CHAPTER III

CALIBRATIONS AND CORRECTIONS

Pressure

The pressure gauges used in the present experiment have been periodically calibrated at the melting pressures of mercury at three different temperatures which are approximately -25° C, 0° C and 20° C. The melting pressures at these temperatures are taken to be the same as those previously reported[7] with the exception of the adoption of a more recent[11] value of 7569 bars at 0° C. The temperatures are measured and monitored by means of a platinum resistance thermometer which was manufactured and calibrated by the Leeds-Northrup Company. The H_2O triple-point resistance of the thermometer is periodically checked within our own laboratory. No significant resistance drift has occurred within four years.

The mercury samples are kept in a chamber which is submerged in a well-stirred naptha bath and thermostatted to the selected mercury freezing temperature. A 0.020 inch I.D. stainless steel capillary tube connects the mercury chamber to a pressure vessel which is thermostatted at 35° C and which contains the manganin pressure gauge. The solid-liquid mercury transition is detected by a resistance discontinuity technique using apparatus modeled after that of

Dadson and Greig[11]. The mercury is poured in vacuo into a thin-walled 0.03 inch I.D. teflon tube which is wrapped on an aluminum heat sink. An electrical current of about one milliampere is passed through the mercury thread and when the mercury freezes the change in the potential drop across the thread is detected potentiometrically. In actual practice several determinations of the resistance of the pressure gauge at the freezing pressures are made. The results at the lowest pressure calibration point show a scatter of about 2 bars which is probably due to temperature control difficulties. Since the slope of the melting curve of mercury is about 200 bars/°C, temperature instability of 0.01° C could easily produce the scatter. At higher temperatures the temperature control is better and the scatter of the calibration points is considerably reduced. The calibration results are summed up by representing the measured pressures as follows:

$$P = A + B(R-R_o) + C(R-R_o)^2 . \qquad (1)$$

Where A, B and C are determined by least squares analysis of the calibration points, R_o is the resistance of the pressure gauge at one bar pressure. The value of R_o drifts slowly with time possibly due to some slow oxidation of the resistance wire. The drift in a month time is usually about three to six parts per hundred thousand. This effect is of no consequence for the present work. Current values of R_o are used in Eq. (1). The constants for the pressure gauges used

in this work are very nearly: A = 1 bar B = 4020 bars/Ω and $C = 13$ bars/Ω^2. Due to the near linearity of the pressure gauge the constant B is the most significant of the three parameters. Different values of B result from calibrations at different times, although the variations in value have remained within 0.1 per cent over a three year period. This does not however mean that the pressures indicated by the gauge drift by this amount since the calibration constants are not independent of each other. The pressures obtained from Eq. (1) for fixed values of $(R-R_o)$ but with A, B and C from different calibrations taken several months apart differ by 2 bars at most at each of the calibration points. These differences are negligible except at the lowest pressures.

Thus in summary it appears that pressures determined by the manganin resistance gauge are accurate to about two bars which is due to calibration uncertainty plus unknown errors in the adopted fixed points. The precision of the measurements is about 0.4 bars as noted previously.

There are no corrections to be included with the use of Eq. (1) to obtain pressures from measured resistance changes, however care must be exercised to be sure that there is no significant leakage resistance at the point where the electrical leads pass through the pressure vessel. Leakage resistance of less than one Megohm at these places could parallel the resistance gauge and lead to an intolerable pressure uncertainty.

Temperature

The bellows chamber is thermostatted at 35° C in an oil bath and the only remaining temperature measurement is made at the constant volume chamber which is housed in a metal block thermostat. This measurement presents three problems: (1) Maintenance of spatial uniformity, (2) Stability with time and (3) Measurement with calibrated thermocouples.

In order to maintain spatial uniformity the metal block thermostat was provided with end heaters to compensate for heat loss through the pipe which connects constant volume chamber and bellows chamber. A special study was made to determine the power required for the end heaters to produce uniform temperature throughout the constant volume chamber. Four thermocouples were used for this study. One was placed within the bore of the constant volume chamber's pressure cell and three were inserted through the insulation and metal block and placed in contact with the exterior of the pressure vessel. The three exterior thermocouples were placed at the top, center and bottom of the hot cell. At each of the temperatures 35° C, 100° C, 200° C, 300° C, and 400° C the power distribution on the side and end heaters was varied until the interior thermocouple showed no temperature variation as it was moved over the length of the constant volume chamber. Then all the thermocouple readings and heater voltage settings were recorded and the thermocouples were intercompared at a single position. During this experimentation the end of the pipe which supports the

piezometer was water-jacketed and maintained at about 35° C in order to duplicate the actual conditions of use. In addition to correlating the exterior temperature distribution with the temperature of the pressure cell interior, the temperature in the pipe between the furnace and the water jacket was determined. This last information is needed for proper correction of the PVT data. The temperature difference between interior and exterior of the pressure vessel is quite small, amounting to about 2° C at 400° C, and then only near the bottom heater which compensates for most of the heat loss through the pipe. At 200° C the maximum temperature difference is approximately 0.5° C and diminishes rapidly with decreasing temperature. In any event the difference is considered to be a well-known function of temperature at each thermocouple position and only at 400° C does lack of knowledge of the difference amount to as much as 0.1° C. The construction of the furnace helps to insure that once established, the temperature correlation remains valid over a long period of time. The metal block without insulation weighs 35 pounds and the insulation which surrounds it is magnesia dispersed in a fiber matrix. The fiber prevents the insulation from settling out and permitting the furnace characteristics to change. The large mass and excellent insulation of the furnace help to maintain an equilibrium temperature but has the disadvantage of long equilibration times when temperature changes are needed.

The temperature control unit which was described in the previous chapter is capable of maintaining a fixed temperature of the furnace to within 0.02° C for periods of time up to 24 hours. The

stability is due in part to the use of thermally insulated wire wound resistors and a three-lead attachment for the resistance thermometer of the Wheatstone bridge of the control unit.

The task of calibrating thermocouples is always unfinished since the thermocouple emf at a given temperature drifts slowly with time. The thermocouples used in this experiment are chromel-alumel, insulated with magnesium oxide, and encased in stainless steel sheaths. The calibration procedure consists of recording the thermocouple emf at intervals of about 25° C between room temperature and 400° C. The temperatures are determined by the same platinum resistance thermometer used during pressure calibration. The thermocouples and platinum resistance thermometer are inserted into opposite ends of a special calibration furnace. Their temperature sensitive elements are in close proximity within the furnace. The calibration results are displayed graphically for each thermocouple in the form of a deviation curve. The thermocouple emf at each temperature is subtracted from the emf given in standard tables and the difference is plotted graphically versus temperature. The drift of thermocouple emf is most pronounced at temperatures above 200° C; consequently temperature measurements above 200° C are more uncertain than those at lower temperatures and the uncertainty increases with the time elapsed since the last calibration. Even though the thermocouple emf drifts it is possible to partly compensate for the effect on any particular PVT data run by interpolating the trend of the drift between different

calibrations of the thermocouples; one preceding the data run and one afterwards. The aging or drift appears to be a function of time rather than just the time spent in use at elevated temperatures.

The accuracy which can be obtained on temperature measurement with these thermocouples after all corrections are applied is estimated to be: 0.1° C at 100° C, 0.1° C at 200° C, 0.2° C at 300° C and 0.3° C to 0.4° C at 400° C. These estimates of accuracy correspond to the accuracy with which the corrections can be determined from the calibration graphs. The erratic nature of the deviations of the thermocouple emfs from either algebraic expressions or standard tables prevents any more accurate usage, however, for a few days after calibration the results are reproducible to about 0.1° C at any temperature up to 400° C.

Volumes

The volume measurements which are relevant to the present experiment consist of: (1) The absolute volume of the constant volume chamber and the capillary which connects it to the bellows and (2) Measurements of bellows volume changes.

Constant Volume Chamber and Capillary

The total volume of the constant volume chamber and capillary (which are shown in Fig. 1) is determined by filling them in vacuo with triply distilled and outgassed mercury. Precautions are taken to insure that no gas bubbles are trapped within the volume and that all the mercury is removed before any gases are loaded under experimental conditions.

The volume of constant volume chamber and capillary has been determined both before and after application of 10 kbar pressures and temperatures to 400° C with agreement on the volume measurement to 0.01 per cent which is about the expected accuracy of the measurement. Consequently, it appears that within 0.01 per cent there is no volume hysteresis due to the pressure and temperature cycles.

Several different constant volume chambers and capillaries have been used in gathering the experimental data since replacements have been made when leaks developed.

The determination of the capillary volume as a separate quantity is done by calculation using measured values of internal diameter and length of the capillary. In all cases the capillary volume is very nearly 0.33 cc and the constant volume chamber therefore approximately 10.20 cc.

The volumes of constant volume chamber and capillary must be corrected to account for thermal expansion when they are heated and for their compression under pressure. Literature values for the thermal expansion coefficient[12] and compressibility[13] of the stainless steel are sufficient for correction of the small volume of the capillary, however, the same quantities for the correction of the larger nickel constant volume chamber were each determined especially for this experiment.

The thermal expansion coefficient of nickel was measured directly by mounting a sample cut from the same stock as the constant

volume chamber in a furnace. The furnace cover was replaced with a pyrex sheet and several thermocouples were inserted through the back of the furnace. One thermocouple was used for temperature measurement and another for the temperature control. Outside the furnace a traveling microscope was mounted parallel to the specimen. The experiment was carried out in obvious fashion with the following results:

$$\frac{\Delta L}{L_{35}} = 13.82\times10^{-6}(T-35) + 1.655\times10^{-9}(T-35)^2 \ .$$

Where ΔL is the increase in sample length, L_{35} the length at 35° C and T is the temperature in degrees centigrade. Considering the limits of accuracy of the length measurements, the thermal expansions calculated using the above expression are estimated to be accurate to about one per cent.

The determination of the compressibility of nickel as a function of temperature required a considerably more sophisticated experimental arrangement. The measurements were made by Babb and Scott by an ultrasonic method and the results have been previously reported[14] but for completeness are reproduced in Table I.

The values in the table are the isothermal compressibilities at one atmosphere pressure. In practice these values are corrected linearly with pressure giving a compressibility decrease of two per cent at 10,000 bars at each temperature. The accuracy of the compressibilities in the table has been estimated to be about three per cent.

Table I. Compressibility of Nickel

T(° C)	Isothermal compressibility x 10^7(bar^{-1})
35°	5.38
100°	5.41
200	5.51
300	5.64
400	5.82

Bellows Volume Changes

The electrical system which is used with the bellows determines only the bellows length. The bellows calibration consists of a determination of bellows volume change as a function of the Kohlrausch slidewire position, which is equivalent to a change of volume versus change of length measurement. The invariance of circuit characteristics is required at least for the time interval between calibration and procurement of PVT data. This point will be discussed presently.

The calibration apparatus which is shown in Fig. 5 is essentially a manometer which encloses the bellows and its Wheatstone

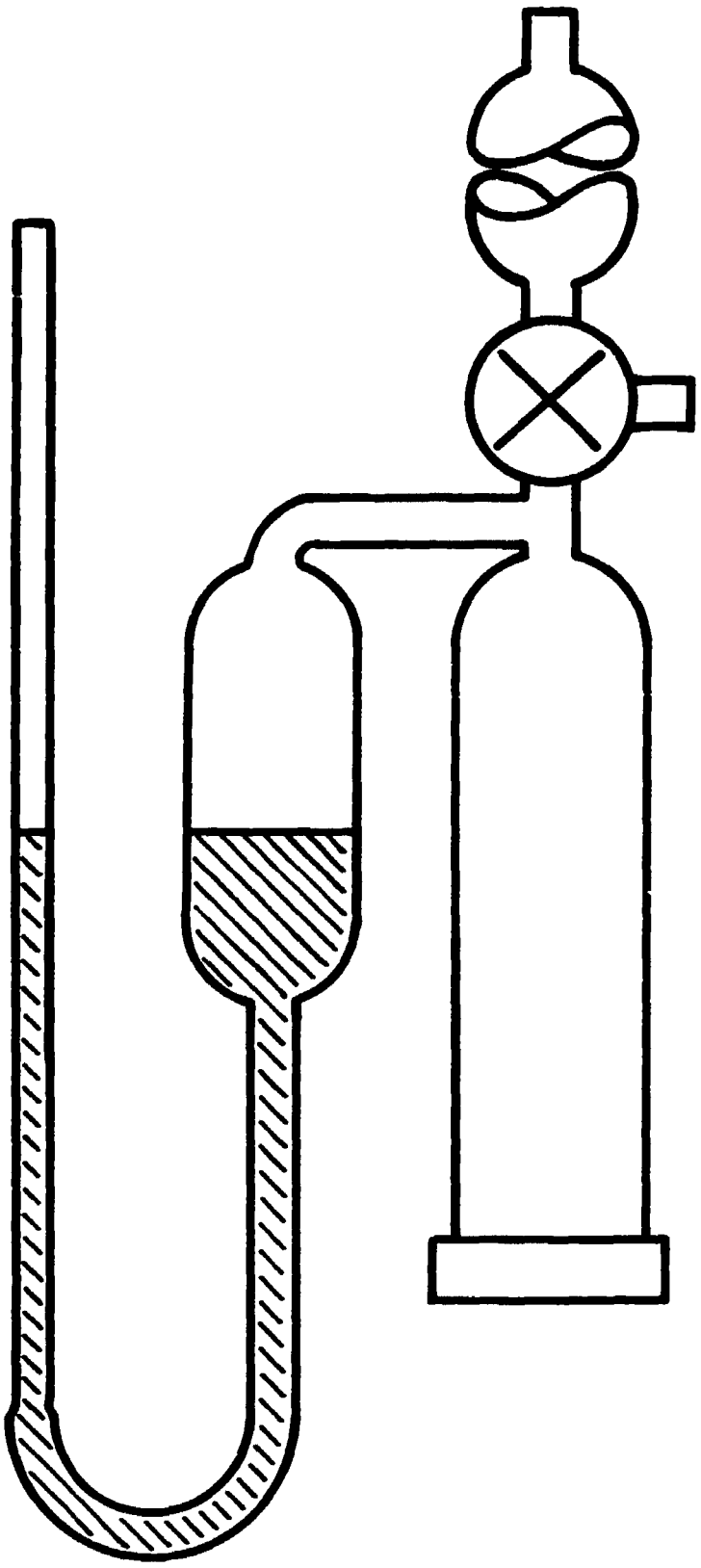

Figure 5. Bellows Calibration Manometer

bridge in carefully outgassed Octoil-S.* The Octoil-S transmits bellows volume changes to a mercury column in a precision bore glass capillary tube of 0.080277±0.000004 cm^2 internal cross-section. (The cross-section area of the glass capillary was obtained by releasing weighed increments of mercury from the column and measuring the length change of the column. Since the density of mercury is known at the working temperature the cross section area of the capillary can be determined and checked for uniformity along the tube length.)

The bellows volume changes which are displaced in the glass capillary are measured then by measuring the change in height of the mercury column with a cathetometer. The volume changes which are actually measured in this way are the volume changes on the exterior of the bellows, however these differ negligibly from the volume changes of the bellows interior due to the thin (0.0015 inch) walls of the bellows. A small correction must be applied to the measured mercury column height changes to compensate for the part of the bellows volume change absorbed by the compression of the Octoil-S as the mercury column height increases. If h_o is the lowest cathetometer setting, then the correction to be added in compensation for compression at h is:

$$\frac{(h-h_o)U_o\chi_o}{76a_t} .$$

---

*bis-diethylhexylsebacate

Where U_o is the volume of Octoil-S in the manometer, a_t is the cross section area of the glass capillary, χ_o is the compressibility of octoil in atmospheres^{-1} and $(h-h_o)$ is measured in centimeters. The compression of the mercury is negligible.

In order to duplicate the conditions of actual use, the entire calibration apparatus is housed in a well-decorated box that resembles a gutless grandfathers clock and thermostatted to 35° C in a stirred air bath. The maintenance of a uniform 35° C temperature prevents the occurrence of spurious volume changes due to thermal expansion or contraction of the manometer fluids. Finally, if h represents the cathetometer setting and D the Kohlrausch slidewire position then the calibration results can be displayed in the form:

$$h = h_o - E(D-D_o) + F(D-D_o)^2 \quad . \qquad (2)$$

Where h_o, E and F are constants determined by a least squares analysis of the measurements of D and h and D_o is the slidewire setting when the bellows is fully compressed against the end plugs. The point h_o is determined by least squares rather than by observation since a small flexing of the sides of the bellows occurs if the pressure inside the bellows is lowered below that needed to just achieve contact of the end plugs and the directly observed values of h_o are uncertain beyond the internal precision of the other calibration points.

Volume changes in the bellows can be obtained directly as functions of $D-D_o$ by multiplying Eq. (2) by a_t, the cross-section area of the glass capillary, and correcting for compression of the Octoil-S. Letting V be the bellows volume there follows:

$$V-V_o = a_t\left(1 + \frac{\chi_o U_o}{76a_t}\right)\left[-E(D-D_o) + F(D-D_o)^2\right] \quad . \qquad (3)$$

The internal precision of the volume changes is approximately 0.0007 cc which is well within the combined expected observation errors of 0.15 divisions in D and 0.005 cm on the cathetometer settings. Typical values of E and F are: $E = 0.0443$ cm/div and $F = 2.0\times10^{-7}$ cm/div^2. Their standard deviations as determined by routine statistical methods[15] are about 0.04 per cent and 7 per cent respectively. The quantity $\frac{\chi_o U_o}{76a_t}$ has the value 0.0016 taking $\chi_o = 7\times10^{-5}$/atm.[16]

The smallness of the F values, and their persistent presence caused much painstaking work to be done. It was at first thought that the non-linearity must be due to a systematic error in the calibration process, however, as the technique was perfected and the internal consistency of the measurements became greater, the non-linearities persisted and became quite well-defined. The glass capillary tube was checked for uniformity of cross-section, the electrical circuits were studied in detail and the temperature distribution within the calibration apparatus was mapped out. No effects appeared which could account for the non-linear bellows behavior and finally the reproducibility of the calibration results after subjecting the bellows to

pressure cycles to 10 kbar removed all lingering doubts about the calibration procedure. A simple geometric interpretation of the non-linearity is that as the bellows lengthens the convolutions open up and slightly increase the effective cross-section area of the bellows. Calculations based on this idea confirm the order of magnitude of the F values. Figure 6 exhibits the calculation for a particular bellows and shows the deviations from a linear least squares fit of h vs. D. A fit to Eq. (2) which is quadratic removes the curved pattern from the deviations.

Wheatstone Bridge Characteristics

As mentioned previously, the reliability of the calibration results depends on the invariance of the quantities $D-D_o$ over the time interval taken by calibration and procurement of PVT data. One must examine the construction of the bridge and external circuit to be assured of this invariance. The operating procedure for the circuit is shown schematically in Figs. 7A and 7B. One first manipulates the switches (See Fig. 3) S_2, S_3 and S_5 to obtain the configuration of 7A and then adjusts R_5 and/or R_6 and R_7 to obtain a null galvanometer. The switches are then changed to produce the configuration of Fig. 7B and a null is obtained by adjusting R_o. Using the notation for resistances of Figs. 7 and letting i_L be the total current passed by the Wheatstone bridge and i_R the current through the Kohlrausch slide-wire, then the first operation produces the equality

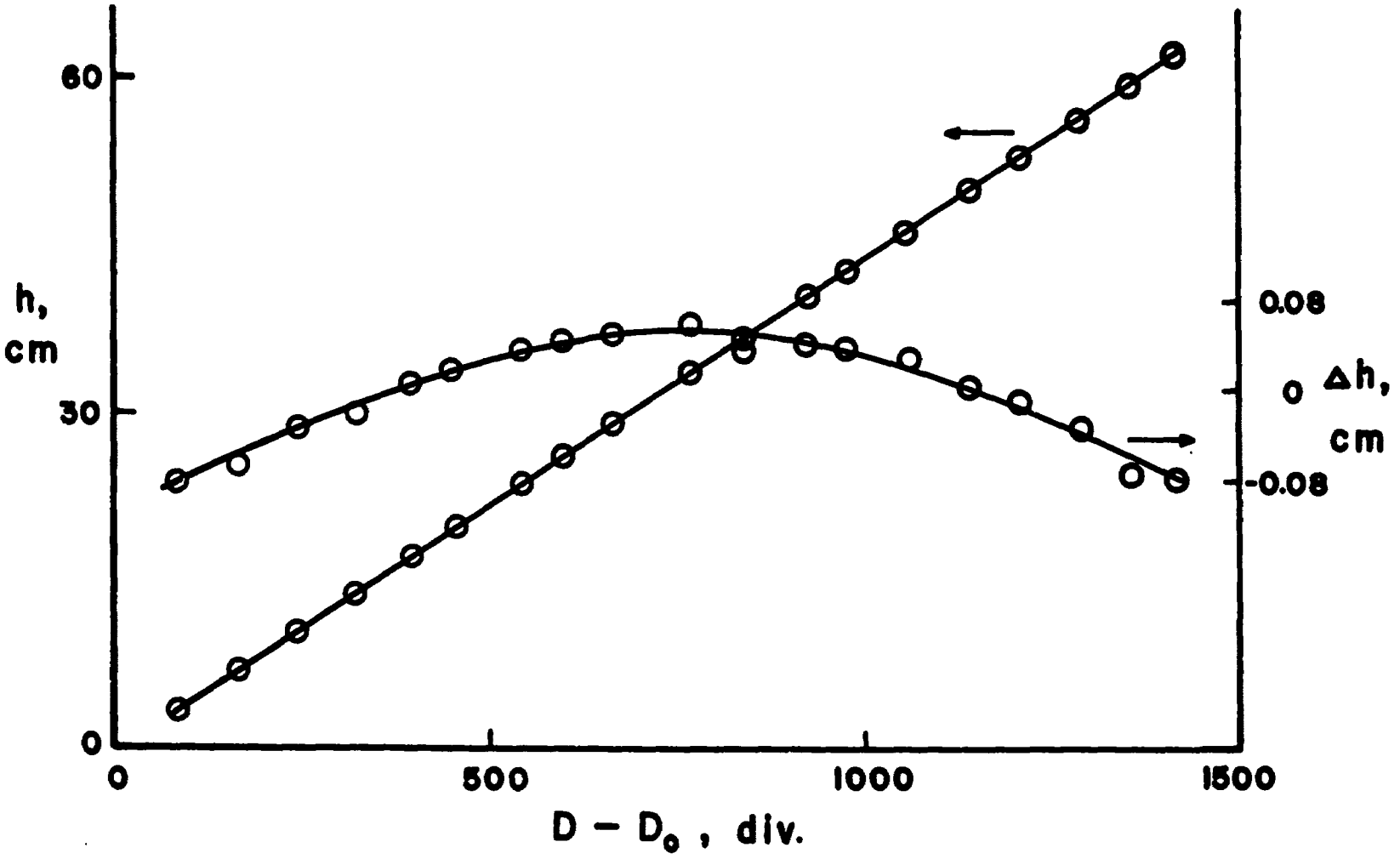

Figure 6. Bellows Calibration Results

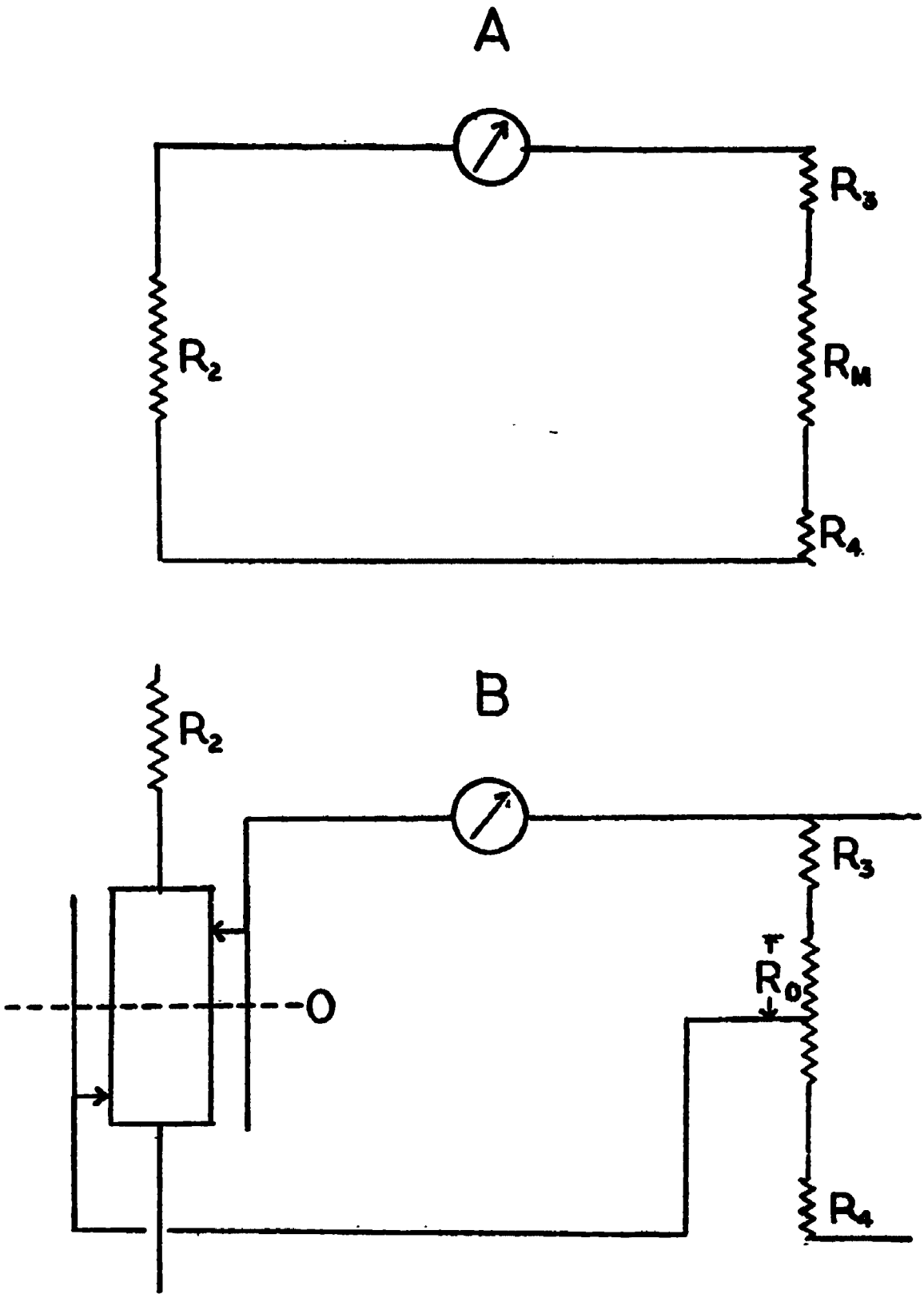

Figure 7. Circuit Configurations for Current Balance

$$i_L R_2 = i_R(R_m+R_3+R_4) \qquad (4)$$

and the second operation yields:

$$i_L \rho X = i_R(R_o+R_3) \quad . \qquad (5)$$

Where ρ is the resistance per unit length of the Wheatstone bridge slidewires and X the Wheatstone bridge wiper displacement from the null position. These equations may be solved for the ratio $\frac{R_o}{R_m}$ with the result:

$$\frac{R_o}{R_m} = (1 + \frac{R_3+R_4}{R_m}) \frac{\rho X}{R_2} - \frac{R_3}{R_m} \qquad (6)$$

The Kohlrausch slidewire D setting is defined by:

$$D = 1000(1 - \frac{R_o}{R_m}) \qquad (7)$$

This equation has been experimentally verified by direct measurement of D and measurements of R_o and R_m with the G-2 Mueller bridge. As noted previously, rms departures from the predictions of Eq. (7) and the measured values of D amount to about 0.15 divisions. Combination of Eqs. (6) and (7) yields:

$$D = 1000[1 - (1 + \frac{R_3+R_4}{R_m}) \frac{\rho X}{R_2} + \frac{R_3}{R_m}] \quad . \qquad (8)$$

R_3 and R_4 are small parasitic resistances associated with connections to the ends of the Kohlrausch slidewire. Their presence prevents the

external circuit from achieving a null output and this is reflected in Eq. (8). One can see that D>1000 would be required for X = 0. Since this is mechanically impossible there exists a region of indifference of width 2000 $\frac{R_0}{R_m}$ divisions in which no balance of the Wheatstone bridge and external circuit can be achieved. This reading discontinuity has been minimized by the use of heavy copper connections soldered to the slidewire and its value has been determined in three different ways. The first determination consisted of direct measurements of R_3 and R_m by means of the Mueller bridge. The second measurement was a direct one in which the width of the region of indifference was measured by micrometer displacement of the sliding contacts of the Wheatstone bridge. Finally a value was determined by a trial and error choice of the number of divisions which when added to Eq. (8) produce continuity for experimental measurements of D vs. X at the point X = 0. The width obtained was $\frac{2000R_3}{R_m}$ = 1.0 divisions in each case after the final modifications of the connections to the Kohlrausch slidewire were made.

The resistances appearing in Eq. (8) have the following values:

$$R_3 = R_4 = .0035\Omega$$

$$\rho = .549\Omega/\text{inch}$$

$$R_2 = .3526\Omega$$

$$R_m = 7.13\Omega$$

The smallness of the quantity $\frac{R_3+R_4}{R_m}$, plus the adjustment of the current ratio prevents any serious effects from room temperature variations of R_m thus permitting the Kohlrausch slidewire to stand in the open air with no thermostat required. Also the thermal insulation of R_2 coupled with the small temperature coefficient of resistance of manganin insures the constancy of the resistor R_2.

The resistivity ρ of the nichrome slidewires varies only under pressure since the bridge is thermostatted at 35° C during both bellows calibrations and runs with gases. The quantities $D-D_o$ which appear in the bellows calibration results can be expressed in the form:

$$D-D_o = \frac{dD}{dX}(X-X_o) \quad . \qquad (9)$$

Since the bellows volume changes at one atmosphere presumably always bear the same relationship to the bellows displacements $(X-X_o)$ then only the constancy of $\frac{dD}{dX}$ is required to insure that the bellows calibration in terms of the values $D-D_o$ remains accurate. The measurement of $\frac{dD}{dX}$ by a micrometer displacement of the bellows bridge is easily accomplished thus affording a convenient check on bellows calibration results when there are long time lapses between calibration and use of a bellows. Measurements of $\frac{dD}{dX}$ both before and after a run with the bridge under pressure also insures that the bridge is unaffected by the cycles under pressure. The value of $\frac{dD}{dX}$ as given by Eq. (8) is accurate to within the errors of measurement of the

quantities ρ and R_2 and the constancy of $\frac{dD}{dX}$ over periods of time up to six months has been observed. The statistical standard error of the micrometer observations of $\frac{dD}{dX}$ is about two parts in ten thousand and the variations over several months time remain well within this margin of error. The values of $\frac{dD}{dX}$ are periodically changed when the bridge is cleaned and the wires reset in tension which introduce changes in ρ, the resistivity of the wires. When the bridge wires are reset they are subjected to a pressure cycle above 5 kbar to anneal the strains introduced by cleaning.

Since bellows calibrations are obtained at one atmosphere pressure, a number of small corrections must be made on the volume changes using Eq. (3) in order to account for the effects of pressure on the Wheatstone bridge and the piezometer. The corrections due to the Wheatstone bridge are caused by contraction of the brass case and slidewires and changing wire resistivity under pressure. A literature value for the compressibility of brass[17] suffices for the first of these but the pressure coefficient of resistivity of the wires was determined experimentally and was found to receive a contribution from a change in tension on the wires. In order to accurately determine the necessary corrections for pressure effects on the Wheatstone bridge it was subjected to pressure with solid samples of brass, lead, and Armco Iron inserted in place of the bellows. To the first order of small quantities Eq. (8) lends itself to an interpretation of the results.

$$\Delta D = (D-1000)\frac{\Delta\rho}{\rho_o} + \left(\frac{dD}{dX}\right)_o \Delta X \qquad (10)$$

Here ΔD is interpreted as the change in D due to the small effects of pressure on the Wheatstone bridge, subscript zeroes refer to the same quantity at atmospheric pressure and ΔX is due to the relative motion between bridge wires and wiper due to the contraction of the case. Thus according to Eq. (10) when $D \approx 1000$ and a brass sample is used so that $\Delta X = 0$ is expected then one should observe no shift, i.e. $\Delta D = 0$. In actual fact a shift $\Delta D = 0.3$ divisions was obtained in the first 500 bars above atmosphere with no further increase to 10,000 bars. Upon release of pressure to about 9500 bars ΔD reversed to - 0.3 divisions and remained stationary until the pressure dropped below 500 bars. Finally, the initial setting was regained at one atmosphere. The source of this anomalous shift is still unknown, however its smallness and constancy of sign and magnitude for either monotonically increasing or decreasing pressures over the working pressure range relegate it to nuisance status only. The anomalous shift does appear in the PVT data as a small hysteresis between points taken with increasing pressure and those taken with decreasing pressure. The hysteresis width amounts to about 0.01 per cent in the gas densities determined in this work.

When the iron and lead samples were used instead of brass, again with $D \approx 1000$ so that contributions to ΔD should be due only to

relative motion, then ΔX in Eq. (10) should be given by $\Delta X = L\Delta\chi P$; where L is the sample length, $\Delta\chi$ the difference of linear compressibilities between brass and the sample and P the pressure in bars. Then the slope of the line ΔD as a function of pressure should be $(\frac{dD}{dX})_o L\Delta\chi$. The slopes actually measured agree to one per cent with those calculated by the preceding formula when Bridgman's[17,18] values for $\Delta\chi$ were used. Finally, using a brass sample so that $\Delta X = 0$ (except for the anomalous shift) and with D-1000 a large number of divisions then Eq. (10) becomes: $\Delta D = (D-1000)\beta P$ with $\frac{\Delta\rho}{\rho_o} = \beta P$ where β is the pressure coefficient of resistivity of nichrome. The slope of the line ΔD as a function of pressure is given by $(D-1000)\beta$. Thus the value of β was found to be 8.32×10^{-7}/bar. The correction for changing wire resistivity was anticipated before these measurements on solid samples were undertaken and a value $\beta = 7.05\times10^{-7}$/bar had been obtained by direct resistance measurement for a sample of unstrained wire from the same pool of lab stock. Consequently, the indirectly obtained value of $\beta = 8.32\times10^{-7}$/bar undermined confidence in the use of Eq. (10) to the extent that direct measurements were made of the bridge wire resistance under pressure. These measurements yielded $\beta = 8.323\times10^{-7}$/bar with the wires set in tension and $\beta = 6.98\times10^{-7}$/bar with tension relaxed. Finally, the change of resistivity with applied stress was measured for a sample of wire from the same spool. The tension coefficient of resistance thus obtained was $\xi = 1.3\times10^{-6}$/bar. If the effects of increasing pressure and decreasing tension were purely additive

one would expect the combination of both effects to yield:

$$\beta(\text{strained}) = \beta(\text{unstrained}) + Y\xi\Delta\chi \quad .$$

Where Y is Young's modulus for nichrome and ΔX the difference of linear compressibilities for nichrome and the brass frame over which the wires are stretched. Using Birdgman's[17,19] compressibilities for ΔX and the measured values of Y and ξ there follows; $Y\xi\Delta X \approx 3.1\times10^{-7}$/bar which is about a factor of two larger than is necessary to account for the difference between the previously given values of β.

When the bridge wires were reset in tension the first cycle under pressure was non-reproducible to the extent that the initial slope of resistance versus pressure curve corresponded to $\beta \approx 10\times10^{-7}$ (which agrees nicely with the sum of unstrained wire and tension contributions to β) but an annealing process began in the vicinity of 2000 bars and continued with increasing pressure until the value $\beta = 8.32\times10^{-7}$ /bar obtained reproducibly. It should be noted that 2000 bars corresponds to the yield strength of the nichrome. This curious annealing effect accounts for the constancy of β for the taut bridge wires over a three year period. It is thus concluded that the value of $\beta = 8.323\times10^{-7}$ /bar for the bridge wires in tension is both well-established and understood.

Volume Corrections

In order to sum up the corrections to be made on the volume changes computed using Eq. (3) it is necessary to establish a few

conventions. It should be clear that all corrections save the one on the cross-section area of the bellows are to be made relative to some starting position D on the slide wire since we are interested only in volume changes. Accordingly, let D_1 be the slidewire setting at the most expanded position of the bellows corresponding to P_1 which is the lowest pressure on the isotherm. Furthermore, D_1 is to be taken less than 1000 divisions if the bellows is on the expanded side of the Wheatstone bridge null position. According to this convention D_o, the fully compressed position, is the largest attainable thus accounting for the negative sign before the calibration constant E in Eq. (3). Equation (3) can be rewritten in terms of displacements from D_1 in the following way:

$$V_1-V = (1.0016)a_t\{[E + 2F(D_o-D_1)](D-D_1) - F(D-D_1)^2\} . \qquad (11)$$

Equation (11) serves as a convenient launch-pad for the discussion of the following corrections:

(1) Decrease of bridge wire resistance

(2) Shrinkage of brass bridge case

(3) Shrinkage of bellows cross-section area

(4) Shrinkage of stainless steel end plugs enclosed by the bellows.

The following notation will be adopted for this discussion:

$a_t = 8.0277\times10^{-2} \pm 4\times10^{-6}$ cm^2 -- glass capillary cross-section area

$\chi_N = 5.38 \times 10^{-7}$/bar -- cubic compressibility of nickel at 35° C

$\beta = 8.32 \times 10^{-7}$/bar -- pressure coefficient of resistivity of nichrome at 35° C

$L_5 = 4.75$ inch -- length of Wheatstone bridge case

$L_3 = 1.60$ inch -- length of wiper carriage of Wheatstone bridge

$L_4 = 1.50$ inch -- length of brass mounting post for nichrome bridge wire

$L_1 + L_2 \approx 1$ inch -- length of stainless steel between attachment points and bellows

$L_s = 1.10$ inch -- length of end plug enclosed by bellows

$\chi_B = 9.18\ 10^{-7}$/bar -- cubic compressibility of brass at 35° C

$\chi_s = 5.9\ 10^{-7}$/bar -- cubic compressibility of stainless steel at 35° C

$V_s = 4.5245\ cm^3$ -- volume of steel end plugs enclosed by bellows

$\frac{dD}{dX} \approx 1.6\ 10^3$div/inch -- Kohlrausch slide wire divisions per unit motion of bellows.

D_o = Kohlrausch slide wire setting with fully compressed bellows. $D_o > 1000$ by convention.

D_1 = slide wire setting at pressure P_1.

For the resistivity correction imagine the process of raising the pressure to compress the bellows to a displacement $D-D_1$ with $D_1 < D < 1000$. Then it should be clear that the quantity $D-D_1$ will be larger than just the amount corresponding to bellows motion due to

the decrease of wire resistivity. In order to correct $D-D_1$ to the value which corresponds only to bellows motion the following values of D should be used: $D = D_{obs} + (D_{obs}-1000)\beta P$. Thus $(D-D_1)_{obs} + (D_{obs}-1000)\beta P - (D_{1obs}-1000)\beta P_1$ corresponds only to bellows motion. Now as pressure increases and D traverses the point D = 1000 the preceding expression continues to correctly express the part of the observed differences which corresponds to motion of the bellows with the exception that the number of divisions which correspond to the width of the region of indifference of the external potentiometer must be added.

Another contribution which must be included is the shrinkage of the bridge case. An examination of the construction shown in Fig. 2 reveals that the shrinkage of the bridge case has the effect of making the relative motion between the bridge wires and bellows too small regardless of the direction of bellows motion. The correction consists of converting the relative motion due to shrinkage to divisions and adding it to the difference $D-D_1$. The addition required is:

$$\left(\frac{dD}{dX}\right)_o \left[\left(L_5-L_3-\frac{L_4}{2}\right)\frac{\chi_B}{3} - (L_1+L_2)\frac{\chi_S}{3}\right](P-P_1) \quad .$$

The correction for shrinkage of the bellows cross-section area must be carried out in two parts. Equation (11) must be multiplied by $(1-\frac{2}{3}\chi_N P_1)$ to account for the shrinkage of cross-section area of the bellows to pressure P_1. In order to complete the rest

of the correction imagine the bellows to be a cylinder of variable length. This should be a reasonable procedure since the effective cross-section area of the bellows is constant to about 0.1 per cent as its length changes. At any rate it is clear at least that the bellows will shrink in cylindrical symmetry. The volume change which must be added in compensation for the shrinking cross-section area is $L(a_1-a)$ where L is the length of the bellows at pressure P and a is its effective cross-section area, a_1 is the effective cross-section area at P_1. If L_s is the length of the stainless steel plug which is encased within the bellows then; $L = L_s + (\frac{dX}{dD})_o (D_o-D)$ and $(a_1-a) = a_o\frac{2}{3}\chi_N(P-P_1)$ where a_o is the bellows cross-section area at one atmosphere pressure. The equality of volume displacements within the bellows and in the calibration manometer yeilds the value of a_o;

$$a_o(\frac{dX}{dD})_o = a_t \frac{dh}{dD} \quad .$$

Then with sufficient accuracy for this small correction $\frac{dh}{dD} = [E + 2F(D_o-D_1)](1.0016)$. The completed correction for shrinkage of the bellows cross-section is:

$$L(a_1-a) = a_t(1.0016)[E + 2F(D-D_o)][L_s(\frac{dD}{dX})_o+(D_o-D)]\frac{2}{3}\chi_N(P-P_1) \quad .$$

Finally the correction for shrinkage of the stainless steel within the bellows is $V_s\chi_s(P-P_1)$. This last correction must be subtracted from the values of V_1-V since the shrinkage of stainless steel increases the bellows volume.

All the corrections can be summed up in the following form:

$$V_1 - V = A\{\alpha(D-D_1) + e(D-D_1)(P-P_1) + f(P-P_1)\} - b(D-D_1)^2 \tag{12}$$

$$\alpha = (1 - \frac{2}{3}\chi_N P_1)(1 + \beta P_1) \tag{13}$$

$$A = (1.0016)a_t[E + 2F(D_o - D_1)] \tag{14}$$

$$e = (\beta - \frac{2}{3}\chi_N) \tag{15}$$

$$f = \{[(L_5 - L_3 - \frac{L_4}{2})\frac{\chi_B}{3} - (L_1 + L_2)\frac{\chi_s}{3}](\frac{dD}{dX})_o - (1000 - D_1)\beta + [L_s(\frac{dD}{dX})_o + D_o - D_1]\frac{2}{3}\chi_N - \frac{\chi_s V_s}{A}\} \tag{16}$$

$$b = (1.0016)a_t F \ . \tag{17}$$

Equation (12) is convenient for calculations. The coefficients A, α, e, f and b can be calculated once the initial values P_1, D_o and D_1 are known and the computation of volume changes proceeds easily. Equation (12) expresses bellows volume changes only. For the isotherm at 35° C all parts of the piezometer are at the same temperature and the total piezometer volume change can be computed by adding the quantity to the coefficient f given by Eq. (16).

$$\frac{\chi_N V_u + \chi_s V_c}{A}$$

V_u = volume of constant volume chamber; V_c = volume of connecting capillary tube.

Typical values of the coefficients at 35° C are as follows:

$$A = 3.5 \times 10^{-3} \text{ cm}^3/\text{div}$$

$$\alpha = 1.0004$$

$$e = 4.7 \times 10^{-7}/\text{bar}$$

$$f = 2.5 \times 10^{-3} \text{ div/bar}$$

$$b = 2 \times 10^{-8} \text{ cm}^3/\text{div}^2$$

There is one more correction concerning bellows volume changes which arises when the constant volume chamber is heated to temperatures above 35° C. In order to reduce the data at the higher temperature the bellows volume must be known in order to determine the mass of gas within it using the previously determined densities from the 35° C isotherm. The problem encountered is the correction on bellows volume at a fixed D setting when the pressure is raised due to the heating of the upper chamber. There are competing processes involved in the volume correction:

(1) As the pressure increases with heating and resistivity drops the bellows must expand to keep D constant if D<1000 and must contract if D>1000.

(2) As the pressure increases the shrinkage of the case materials causes the null position of the bridge to creep toward the sliding contact if D>1000 and away from it if D<1000.

(3) The enclosed stainless steel end plugs shrink thereby increasing the bellows volume.

(4) The bellows cross-section area shrinks.

These corrections may be summed up as follows letting V_b be the bellows volume:

$$V_b(T) - V_b(35^\circ\ C) = (P-P_{35})\left[\chi_s V_s + A\left\{(1000-D)\beta - \left[L_s\left(\frac{dD}{dX}\right)_o + D_o - D\right]\frac{2}{3}\chi_N - \left[\left(L_5 - L_3 - \frac{L_4}{2}\right)\frac{\chi_B}{3} - (L_1+L_2)\frac{\chi_s}{3}\right]\left(\frac{dD}{dX}\right)_o\right\}\right] \tag{18}$$

P_{35} is the pressure at 35° C at the same value of D, A is given by Eq. (14) and all other symbols retain their usual meanings. Equations (12) through (18) are the basic equations for calculation of volume changes.

The last correction given by Eq. (18) is usually quite small, amounting to approximately 0.001 cc or less. This is less than one part in ten thousand of the piezometer volume.

CHAPTER IV

EXPERIMENTAL PROCEDURE

The first step in preparation to take isotherm data consists of evacuating the piezometer and gas loading system to about 10^{-2} mm-Hg and simultaneously heating the piezometer pressure vessel to 35° C. After the bellows chamber oil bath is stabilized at 35° C it is used to standardize the thermocouples for the metal block thermostat of the constant volume chamber. This standardization removes the possibility of 0.1° C uncertainty of the thermocouple readings and this temperature measurement therefore relies on the mercury thermostat of the oil bath alone. Usually 12 or more hours are spent in the process of evacuation and stabilization of the temperature, although the time could be considerably reduced if desired.

After the temperature control is established the initial setting D_o of the Kohlrausch slidewire is recorded with the bellows evacuated and the resistance R_o at atmospheric pressure of the manganin pressure gauge is measured. Then before admitting gas to the piezometer, the gas loading system is purged with the gas to be loaded under pressure and is re-evacuated. This precaution insures that any contaminants are removed from the connections to the gas sample bottle. The actual

loading of 10 to 12 atmospheric liters of the gas is then accomplished as described in Chapter II.

An important part of the experimentation with any gas consists of checking its behavior in the freeze valve. Normally, during the course of recording data the liquid nitrogen level in the freeze valve is maintained constant, however, either before or after the data is recorded the liquid nitrogen level is deliberately varied by as much as six inches in the dewar flask while efforts are made to observe a bellows volume change. This is usually done at several different pressures. The most unfavorable of these observations occurred on a run with argon when the pressure was raised to about 10,000 bars and about four inches of the dewar was then filled with liquid nitrogen. There was no effect observed at 10,000 bars but when the pressure was lowered to about 4,000 bars and the nitrogen deliberately boiled off, a volume change of about 8×10^{-4} cc appeared. Volume hysteresis in this amount would correspond to only 0.01 per cent in gas density and as mentioned before, the liquid nitrogen level is maintained to avoid the problem during the period of data accumulation. No other freeze valve volume changes have ever been observed.

One of the side benefits of initial experimentation with the freeze valve is that one or more cycles under pressure are accomplished thus serving to anneal any strains which could possibly (although improbably) have been introduced in the Wheatstone bridge wires during the assembly of the piezometer. As a matter of technique, the

Wheatstone bridge is cleaned and cycled under pressure before bellows calibrations are undertaken.

After the experiments with the freeze valve some 15 to 25 readings of the pressure gauge resistance and corresponding Kohlrausch slidewire settings are made. The temperature is also monitored and recorded during this period. As a general rule the temperature control is so stable that it is seldom that any adjustments of temperature are required. The measurements are spread over the useful stroke of the bellows from 50 to 400 bars apart depending on the pressure range and the gas which is being studied. Ten to fifteen minutes are allowed for thermal equilibration at each point and usually the variables to be recorded have stationary values for several minutes before their values are recorded. While thermal equilibrium is being attained at each setting, the previous measurement is plotted on large scale graph paper and checked for hysteresis or gas loss between points taken with increasing pressure and those taken with decreasing pressure. This also serves to eleminate gross reading errors. The experiment is aborted any time evidence of loss of gas appears. A typical plot of the raw data is shown for argon in Fig. 8.

After the five or six hours necessary for the accumulation of data at 35° C the metal block furnace for the constant volume chamber is heated and allowed to equilibrate at successively higher temperatures. When thermal equilibrium is established the accumulation of data at each temperature proceeds exactly as at 35° C. It usually

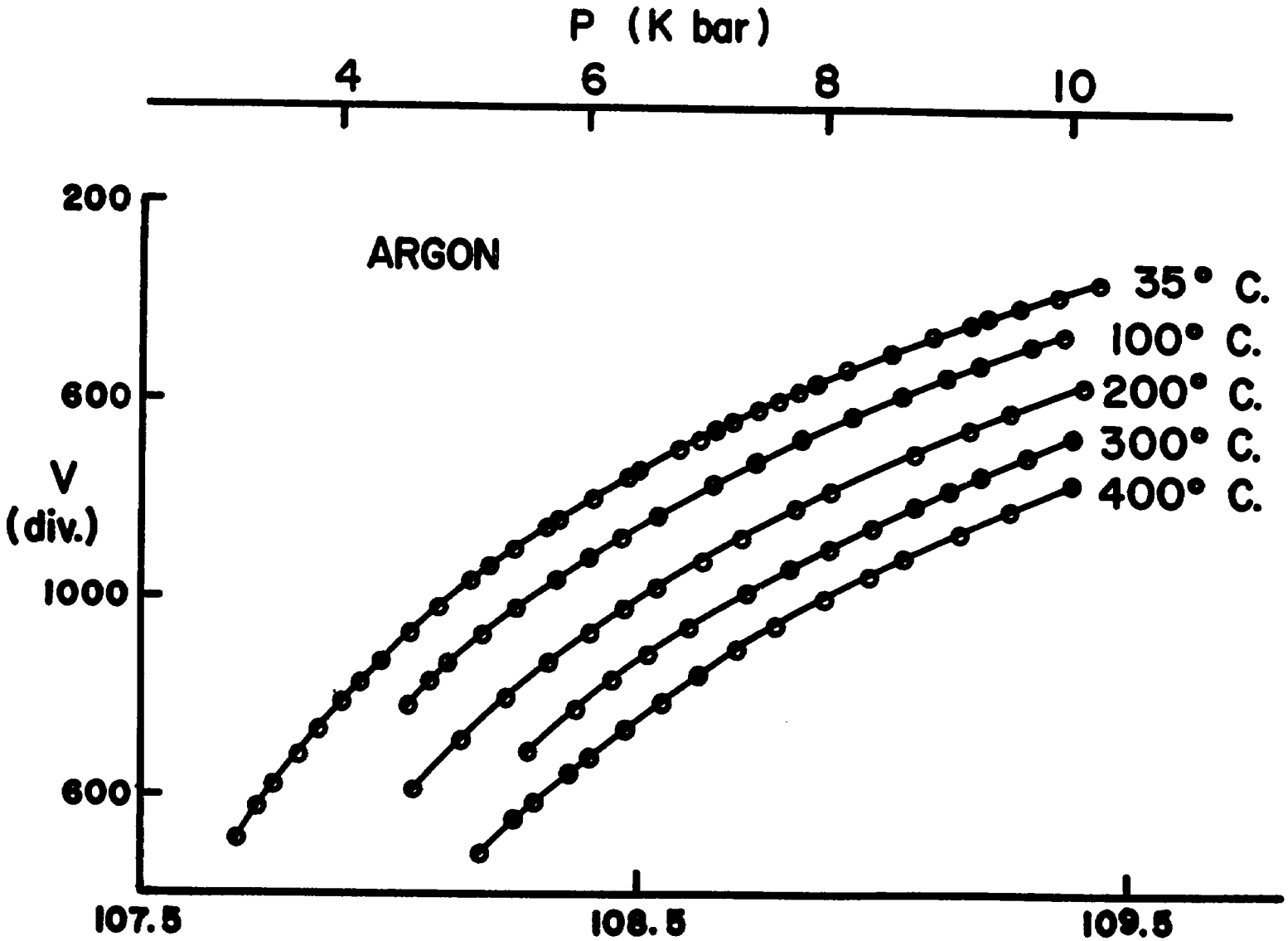

Figure 8. Raw Argon Data

requires at least five hours to run each isotherm after temperature control is established. Despite efforts to heat the furnace uniformly the periods of time required for the furnace to equilibrate grow from about two hours between 35 and 100° C to about five hours between 300 and 400° C. In view of the long time lags it is necessary to replenish the ice bath for the cold junctions of the thermocouples. This is usually done about one half hour before taking data on each isotherm. As a point of technique, the thermocouples are removed from the furnace during the heating periods to help prevent thermal aging. Another motivation for this procedure is that the thermocouples tend to develop shorts to their stainless steel sheaths at the places of close proximity to the heater windings of the metal block if they are left in place during the periods of rapid heating.

After the isotherm at 400° C is run the constant volume chamber is cooled back to 35° C with the aid of a water coolant in the thermometer wells of the furnace, and six to ten points are taken as a recheck to insure that no gas was lost from the piezometer during the runs at higher temperatures. If there is evidence of leakage the results of the run are discarded, but if not the gas is unloaded and stored in sample bottles pending analyses for impurities.

Usually at least two runs with different gas loads are necessary for the extension of isotherms from 1500-2000 bars to 10,000 bars. The first load usually begins at 1500 to 1600 bars and extends the isotherms to 4500-5000 bars. The second load overlaps the first, starting at

approximately 3000 bars and extending to 10,000 bars. Sometimes a third load at 35° C is used to overlap both the low and high pressure runs and provide better statistics for the data reduction. As a general rule the points taken in the range of the fiducial data are closely spaced along the isotherm in order to provide a more reliable judgement of the agreement between measured volume changes and the fiducial density differences. In addition, at least half the available 4 cc volume change which is permitted by the bellows is expended within the low pressure fiducial range. In this way the random errors of observation of the volume changes become negligible fractions of the total volume change which is used to span the fiducial data range.

CHAPTER V

DATA REDUCTION

The data which is taken consists of a number of pressure gauge resistance readings and the corresponding Kohlrausch slidewire settings at constant temperature. The resistance measurements are converted to pressures using Eq. (1) and the slidewire settings are converted to volume changes by means of Eq. (12). In view of the failure to observe significant volume changes in the freeze valve and a consideration of the physical processes involved which are described in the appendix, the reduction of data at 35° C proceeds upon the assumption that a constant mass of gas undergoes changes in volume within the piezometer. The equality of masses at pressures P_1 and P between which the volume change ΔV occurs yields the equation:

$$\rho_1 V_1 = \rho(V_1 - \Delta V) \quad . \tag{19}$$

Where ρ_1 and ρ are the gas densities at pressures P_1 and P respectively and V_1 the piezometer volume at pressure P_1.

In order to make use of Eq. (19) two fiducial densities ρ_f and ρ_1 are chosen corresponding to the pressures P_f and P_1. These are usually the highest and lowest pressures within the fiducial data range. Then V_1 can be obtained as well as the mass of gas $\rho_1 V_1$ in the

system. Usually P_f is the highest pressure on the isotherm for which fiducial data is available. After obtaining V_l the data between P_l and P_f is examined for systematic differences from the fiducial data. Generally there are none and Eq. (19) is recast in dimensionless Amagat units:

$$d_i = \frac{V_n}{V_l - \Delta V_{li}} \quad . \tag{20}$$

V_n is the Normal volume of gas and d_i the Amagat density obtained in the present work. Using preliminary values of V_n and V_l obtained from the preceding two point forced fit, the least squares best values of V_l and V_n are obtained for the range of overlap with the fiducial data by minimizing the quantity $\sum_i (d_i - \rho_i)^2$ where the ρ_i are fiducial Amagats densities. Figure 9 depicts the residuals $(d_i - \rho_i)$ as a function of pressure for Argon at 35° C. The fiducial below 2500 bars data was obtained from Michels, *et al.*[1] Points above 2500 bars correspond to extrapolation of Michels' work. The important feature of the figure is the statistical indistinguishability of points taken with increasing or decreasing pressures and the recheck points which were taken after the 400° C isotherm was run. This demonstrates the lack of any significant hysteresis. The per cent standard deviations of the values for V_l and V_n are usually on the order of 0.05 per cent. This reflects only the small scatter of the experimental points. V_n is not capable of determination by the experimental techniques described herein except through the use of fiducial data, however, there

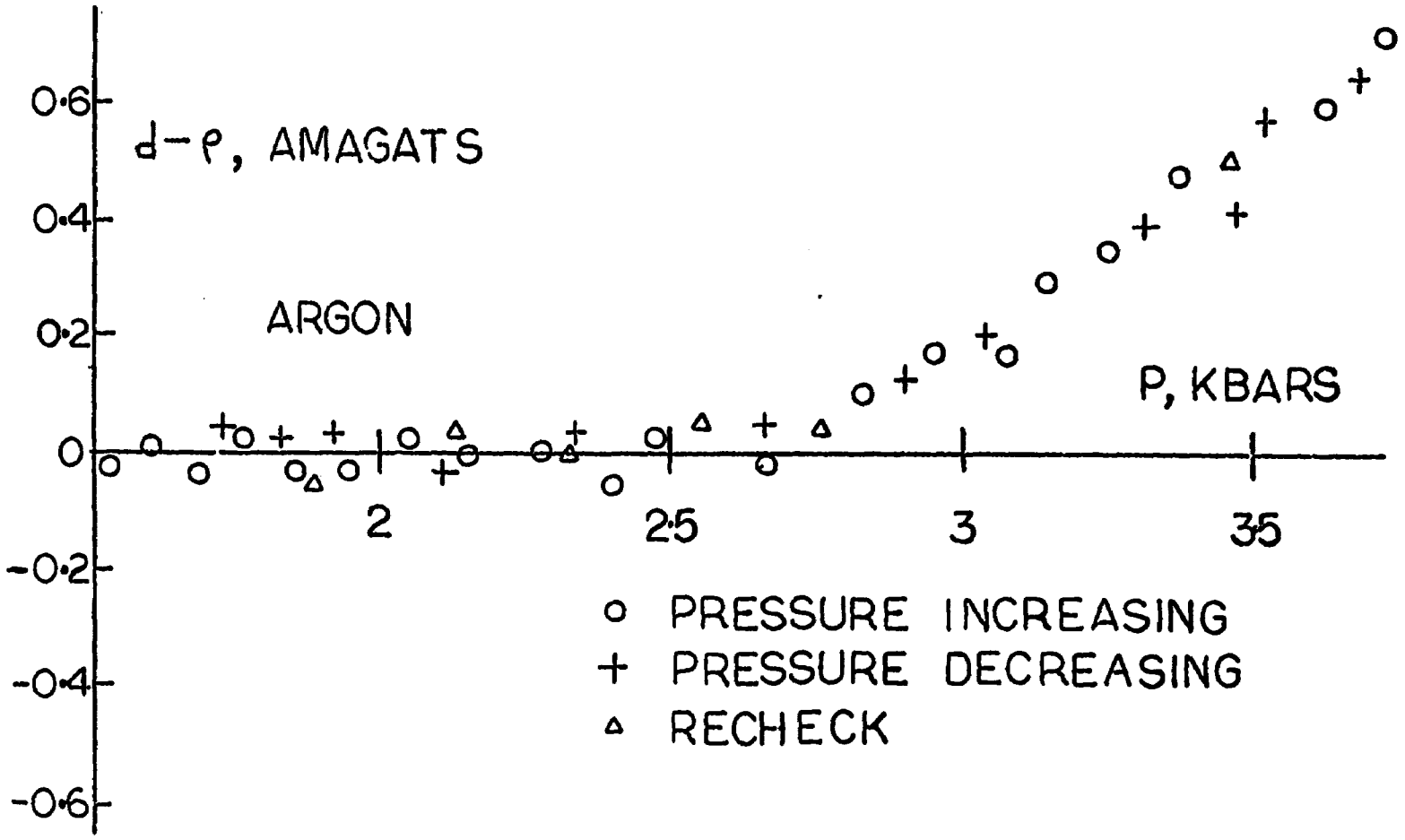

Figure 9. Residuals for 35° C Argon Fiducial Data Fit

are means of determining V_1 independently of the fiducial data from the requirements of internal consistency when two or more gas loads traverse a common pressure range. (See Appendix) It is also required that the values of V_1 determined by means of fiducial data agree reasonably with the external estimates of the piezometer volume; i.e., the volume obtained by addition of the estimated volumes of the various piezometer parts.

The quality of the fit to a set of fiducial data is quite independent of the accuracy of the values of V_1 and V_n as is demonstrated below. Equation (20) can be rewritten in the form:

$$d_i = \frac{\rho_1 a}{a - X_i} \quad , \tag{21}$$

where $a = \frac{\rho_f}{\rho_f - \rho_1}$ and $X_i = \frac{\Delta V_{1i}}{\Delta V_{1f}}$, where 1 = initial points, f highest pressure fiducial point, and i = measured point. This shows that the densities at 35° C calculated for this experiment in extension of existing fiducial data are expressed in terms of ratios of volume changes. If the bellows calibration was linear the calibration constants would drop out completely. Since the departures from linearity are small this indicates that the densities obtained at 35° C are practically independent of the volume calibration and depend mainly upon accurately matching the pressure and temperature scales of the fiducial data. Under the present experimental conditions the inequalities $0 \leq X_i \leq 2$ hold and a is approximately equal to 8.5. Values of X_i less than unity correspond to the fiducial range.

Density Interpolation

More than one gas load is required to extend the isotherms from 2 kbar to 10 kbar. This necessitates the use of densities determined by the low pressure load to resolve V_1 and V_n for the higher pressures once the fiducial range has been exceeded. Consequently, some convenient means of interpolating the experimental densities is necessary at 35° C as well as at higher temperatures. For this purpose a modified form of the Tait[20] equation has been adopted. The equation does not in any case fit the data within experimental precision but does fit well enough to be used in conjunction with a deviation curve. The form of the equation is:

$$d = d_o + C \ln \frac{P+B}{P_o+B} \quad . \qquad (22)$$

Where d_o, C, P_o and B are constants which are determined by force-fitting the equation to the experimental densities at three different pressures. The chief advantage of Eq. (22) for the present purposes lies in its simplicity. Given the pressures for which densities are desired the densities can be calculated quickly on a desk calculator and corrected using the deviation curve. Figure 10 illustrates the deviation between the predictions of Eq. (22) and the experimental data for Argon at 35° C. This figure shows that the equation is capable of fitting the data to about 0.1 per cent and also that the basic scatter in densities determined in this work is approximately 0.02 per

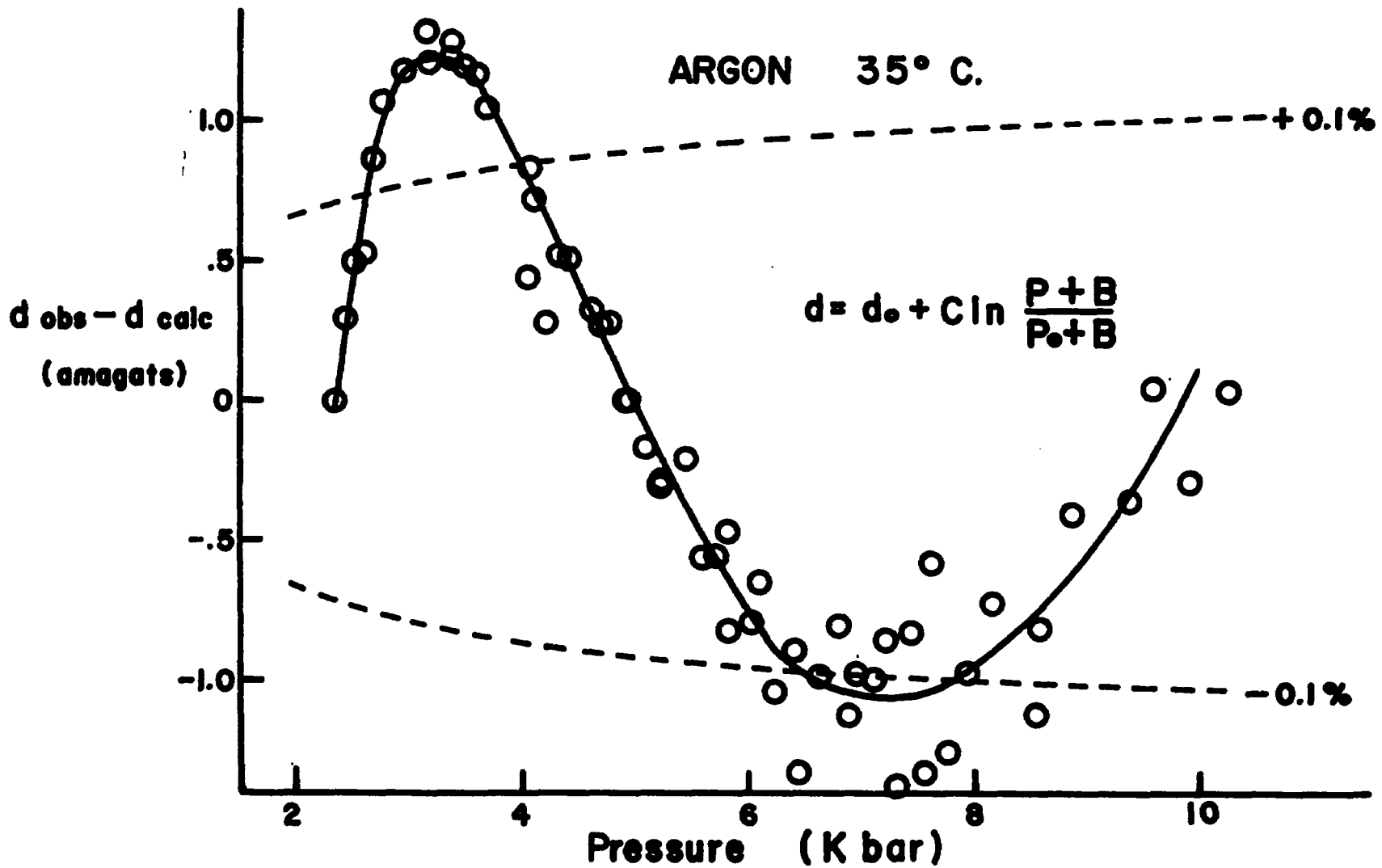

Figure 10. Deviation Curve for Modified Tait Equation

cent at pressures above 5 kbar and considerably less at lower pressures. The reason for the larger scatter at high pressures is not completely understood.

Temperatures above 35° C

The analysis of data at elevated temperatures is most conveniently carried out by mentally splitting the piezometer into three parts; a constant volume chamber of volume V_u, connecting capillary of volume V_c and length L, and a bellows with Volume V_b. Then the mass M of gas enclosed by the piezometer can be expressed in obvious notation:

$$M = M_u + M_b + M_c \quad . \tag{23}$$

Let ρ_c, ρ_b and ρ_u be the gas densities in the capillary, bellows and constant volume chamber respectively, and ρ_N the density of the gas at normal conditions. ρ_c is a function of position along the capillary due to the temperature gradient along its length. If y is the displacement along the capillary from the tip of the bellows (which is at 35° C) then the mass of gas in the capillary is given by:

$$M_c = V_c \int_0^L \rho_c \frac{dy}{L} \quad . \tag{24}$$

Also one can express ρ_c in the form:

$$\rho_c = \rho_b + (\rho_u - \rho_b) \frac{y}{L} + \rho_N f(y) \quad . \tag{25}$$

Here f(y) expresses the difference between the actual density variation along the capillary length and the linear function which precedes it in the equation. It is of course required that f(o)=f(L)=0. Insertion of Eq. (25) into the expression (24) yields:

$$M_c = V_c\left(\frac{\rho_b}{2} + \frac{\rho_u}{2}\right) + V_c\rho_N \int_o^L f(y)\,\frac{dy}{L} \quad . \tag{26}$$

Then since $\rho_b = \frac{M_b}{V_b}$, $\rho_u = \frac{M_u}{V_u}$ this becomes:

$$M_c = M_u\left(\frac{V_c}{2V_u}\right) + M_b\left(\frac{V_c}{2V_b}\right) + V_c\rho_N \int_o^L f(y)\,\frac{dy}{L} \quad , \tag{27}$$

comparing this last equation with Eq. (23) there follows:

$$M = M_u\left(1 + \frac{V_c}{2V_u}\right) + M_b\left(1 + \frac{V_c}{2V_b}\right) + V_c\rho_N \int_o^L f(y)\,\frac{dy}{L} \, . \tag{28}$$

Thus one obtains the mass of gas in the constant volume chamber:

$$M_u = \frac{M - M_b\left(1 + \frac{V_c}{2V_b}\right)}{1 + \frac{V_c}{2V_u}} - \frac{V_u V_c N}{V_u + \frac{V_c}{2}} \int_o^L f(y)\,\frac{dy}{L} \quad . \tag{29}$$

The Amagat density d_u which is defined to be $\frac{M_u}{\rho_N V_u}$ is given by:

$$d_u = \frac{V_n - d_b\left(V_b + \frac{V_c}{2}\right)}{V_u + \frac{V_c}{2}} - \frac{V_c}{V_u + \frac{V_c}{2}} \int_o^L f(y)\,\frac{dy}{L} \, . \tag{30}$$

As Eq. (30) stands it requires the a priori knowledge of density as a function of temperature for the evaluation of f(y).

Since this knowledge is one of the objects of the experiment
native approach is required. Limits on the value of the int
be established by considering the extreme cases in which the
is first assumed to be at 35° C over its complete length and
sumed to be at the higher temperature. Then taking $\frac{V_c}{V_u + \frac{V_c}{2}}$:
follows:

$$\frac{V_c}{V_u + \frac{V_c}{2}} \left| \int_0^L f(y) \frac{dy}{L} \right| < (0.01)(d_b - d_w)$$

Thus the integral over the capillary temperature distributi
small and in fact is smaller than indicated by the inequali
due to the nearly symmetric temperature differences from th
of the capillary. Considering the smallness of the integral
is initially ignored. Then the use of Eq. (30) with the in
neglected results in a set of densities as functions of tem
and pressure. Gas densities for each isotherm are then inte
at 500 bar intervals of pressure by means of Eq. (22) and a
curve similar to Fig. 10. The interpolated densities are th
by least squares techniques to parabolas centered near 100, 2
300° C. The multiple fits are necessary due to failure of th
to fit a quadratic expression. The quadratic functions are t
to evaluate $(\frac{\partial d}{\partial T})_p$, and densities as functions of temperature
bar intervals of pressure. Thus the density variation with t
along the capillary tube is determined and the neglected int

Here f(y) expresses the difference between the actual density variation along the capillary length and the linear function which precedes it in the equation. It is of course required that f(o)=f(L)=0. Insertion of Eq. (25) into the expression (24) yields:

$$M_c = V_c\left(\frac{\rho_b}{2} + \frac{\rho_u}{2}\right) + V_c\rho_N \int_o^L f(y)\,\frac{dy}{L} \quad . \tag{26}$$

Then since $\rho_b = \frac{M_b}{V_b}$, $\rho_u = \frac{M_u}{V_u}$ this becomes:

$$M_c = M_u\left(\frac{V_c}{2V_u}\right) + M_b\left(\frac{V_c}{2V_b}\right) + V_c\rho_N \int_o^L f(y)\,\frac{dy}{L} \quad , \tag{27}$$

comparing this last equation with Eq. (23) there follows:

$$M = M_u\left(1 + \frac{V_c}{2V_u}\right) + M_b\left(1 + \frac{V_c}{2V_b}\right) + V_c\rho_N \int_o^L f(y)\,\frac{dy}{L} \, . \tag{28}$$

Thus one obtains the mass of gas in the constant volume chamber:

$$M_u = \frac{M - M_b\left(1 + \frac{V_c}{2V_b}\right)}{1 + \frac{V_c}{2V_u}} - \frac{V_u V_c N}{V_u + \frac{V_c}{2}} \int_o^L f(y)\,\frac{dy}{L} \quad . \tag{29}$$

The Amagat density d_u which is defined to be $\frac{M_u}{\rho_N V_u}$ is given by:

$$d_u = \frac{V_n - d_b\left(V_b + \frac{V_c}{2}\right)}{V_u + \frac{V_c}{2}} - \frac{V_c}{V_u + \frac{V_c}{2}} \int_o^L f(y)\,\frac{dy}{L} \, . \tag{30}$$

As Eq. (30) stands it requires the a priori knowledge of density as a function of temperature for the evaluation of f(y).

Since this knowledge is one of the objects of the experiment an alternative approach is required. Limits on the value of the integral can be established by considering the extreme cases in which the capillary is first assumed to be at 35° C over its complete length and then assumed to be at the higher temperature. Then taking $\frac{V_c}{V_u + \frac{V_c}{2}} \simeq 0.02$ there follows:

$$\frac{V_c}{V_u + \frac{V_c}{2}} \left| \int_0^L f(y) \frac{dy}{L} \right| < (0.01)(d_b - d_u) \ .$$

Thus the integral over the capillary temperature distribution is quite small and in fact is smaller than indicated by the inequality above due to the nearly symmetric temperature differences from the midpoint of the capillary. Considering the smallness of the integral term it is initially ignored. Then the use of Eq. (30) with the integral term neglected results in a set of densities as functions of temperature and pressure. Gas densities for each isotherm are then interpolated at 500 bar intervals of pressure by means of Eq. (22) and a deviation curve similar to Fig. 10. The interpolated densities are then fitted by least squares techniques to parabolas centered near 100, 200 and 300° C. The multiple fits are necessary due to failure of the isobars to fit a quadratic expression. The quadratic functions are then used to evaluate $(\frac{\partial d}{\partial T})_p$, and densities as functions of temperature at 500 bar intervals of pressure. Thus the density variation with temperature along the capillary tube is determined and the neglected integral of

Eq. (30) is evaluated at the 500 bar intervals. The values of the integrals are then interpolated as functions of pressure and the densities at the measured pressures are individually corrected. Similarly, the values of $(\frac{\partial d}{\partial T})_P$ are interpolated as functions of pressure for each isotherm and are used to correct the individual densities to correspond to integral temperatures. This last procedure permits the comparison of data taken on different runs with different masses of gas. The necessity for correction to integral temperatures or at least corresponding temperatures is due to an inability to establish precisely the same stable temperature control position for different runs, although the temperature differences are usually only about 0.2 to 0.3° C. The correction for the capillary temperature distribution usually amounts to only about 0.08 per cent on gas density at the highest temperature and lowest pressure, however, its inclusion prevents a systematic error.

The volumes of the constant volume chamber and capillary which appear in Eq. (30) must be corrected for their thermal expansions and their compressions under pressure. This in turn requires a knowledge of the thermal expansion coefficient of nickel and also its compressibility as a function of temperature. The experimental determination of each of these quantities has been discussed. The determination of the bellows volume V_b which appears in Eq. (30) is obtained in the following way: The initial volume V_1 of the piezometer at the lowest pressure on the 35° C isotherm is obtained from least squares forced

fit to the fiducial data. Then the known volumes of constant volume chamber and capillary are subtracted leaving the bellows volume at the lowest pressure. The volume change to some slidewire setting D_1 for which a point is taken at high temperature can be computed using Eq. (12) and the correction (18) added to obtain the bellows volume at D_1 and temperature. Equation (12) with the coefficients evaluated for the higher temperature can then be used to find the bellows volume at any pressure.

The discussion thus far has assumed the existence of an isotherm at 35° C for the gases which have been tested. This is not always the case and indeed it has not been possible in some cases even to construct reliable fiducial data from the literature. Fortunately, in these instances fiducial data has been available at temperatures above 35° C but in order to use it one must invert Eq. (30) (again neglecting the integral in first approximation). Then if all volume changes both at 35° C and the higher temperature are calculated relative to the same value D_1 to the pressure P which is common to both isotherms Eq. (30) takes the form:

$$d_u = d_b\left(1 - \frac{\Delta V_b(35) + V_b(T,D_1) - V_b(D_1,35) + \Delta V_u + \Delta V_c - \Delta V_b(T)}{V_u + \frac{Vc}{2}}\right) \quad (31)$$

Where $\Delta V_b(35)$ is the bellows volume change between D_1 and pressure P at 35° C, $\Delta V_b(T)$ is the same quantity at temperature, $V_b(T,D_1)-V_b(35,D_1)$

is given by Eq. (18), and ΔV_u and ΔV_c are the enlargements of the constant volume chamber and capillary which are due to the thermal expansion and difference in compressibilities between the higher temperature and 35° C at pressure P. The volume changes at 35° C must be interpolated for use in Eq. (30); otherwise the introduction of fiducial densities for d_u permits the straightforward calculations of the "fiducial" 35° C densities d_b. The data reduction then proceeds along the lines previously developed.

Equation (31) reveals that densities at temperatures above 35° C depend essentially upon volume ratios which are experimentally determined rather than on the reducing parameters V_1 and V_n which appear in the analysis. The volume ratio given in the equation is internally consistent to the extent that both bellows volume changes and volumes of constant volume chamber and capillary are calibrated in terms of the density of mercury samples which came from the same laboratory container in each case.

Correction for Inaccurate Fiducial Data

Equations (21) and (31) suggest a scheme for correcting the densities given in this thesis for inaccuracies in the fiducial data. The integrity of these measurements can be preserved within experimental error by preserving the values of X_i of Eq. (21) and the volume ratios given by (31). If new fiducial densities ρ_1 and ρ_2 corresponding to pressures P_1 and P_2 are assumed at 35° C and d_1 and d_2 are tabular

values given within these pages then the corrected values of d will be given by:

$$d_{corr} = \frac{\rho_1 d_i}{d_i(1-r) + r d_1} \quad . \tag{32}$$

Where d_i are the data table entries reported herein and

$$r = \frac{d_2(\rho_2-\rho_1)}{(d_2-d_1)\rho_2} \quad .$$

The correction at higher temperatures can then be obtained as follows:

$$\frac{d_{corr}(P,T)}{d_{corr}(P,35^{\circ}C)} = \frac{d(P,T)}{d(P,35^{\circ}C)} \quad . \tag{33}$$

Such corrections obviously should be undertaken with the largest possible value for the difference $\rho_2-\rho_1$, since the two point fit essentially establishes not only the magnitude of the densities but also the slope of the isotherm.

CHAPTER VI

EXPERIMENTAL RESULTS

Argon

The experimentation with argon occupied by far the largest portion of time spent in obtaining the experimental results. The argon runs were used in the process of de-bugging the experiment chiefly because it was the simplest of the molecules studied and because it freezes at atmospheric pressure at a temperature above the boiling temperature of liquid nitrogen. For nitrogen a back-pressure must be kept on the freeze valve or it will open with spectacular results. The earliest runs with argon were made before a thorough understanding of the bellows calibration requirements was obtained. Needless to say, the resulting data inspired a thorough study of the bridge corrections and several versions of the great microvolt hunt.

The fiducial data which were adopted for the argon reduction were from Michels *et al.*[1] It was necessary to interpolate these data to construct a 35° C isotherm. This was done in two ways: first a multiple point Lagrangian interpolation of the original data, followed by a least squares polynomial fit to a virial expansion; second, a

multiple point Lagrangian interpolation of the virial coefficients given by Michels *et al.* The difference between these two approaches is negligible for the present purposes since it amounts to less than 0.01 per cent.

The virial equation which was used for the representation and interpolation of the fiducial data can be expressed in the form:

$$PV = \sum A_k \rho^k \quad .$$

The 35° C virial coefficients which were used to provide the fiducial data used in the present work on argon are given below:

$$A_0 = RT = 1.14417134 \text{ bar-amagats}$$
$$A_1 = -0.69558047 \times 10^{-3}$$
$$A_2 = 2.28813875 \times 10^{-6}$$
$$A_3 = 1.66043811 \times 10^{-9}$$
$$A_4 = -2.44483945 \times 10^{-12}$$
$$A_5 = 11.01996818 \times 10^{-15}$$
$$A_6 = -2.6902406 \times 10^{-18}$$

The most confounding of the early bad results was due to the reliance upon the fiducial data to a full 3000 bars. The measured volume changes simply failed to fit over the full range. This inspired the error analysis of the next chapter before it was realized that Michels measurements on the nearest isotherms at 25° C and 50° C extended only to about 2300 bars. When the fiducial range was restricted

to points below 2500 bars remarkable agreement resulted as is shown in Fig. 9. Above 2500 bars the results deviate from the extrapolated densities from the fiducial virial expansion. This is not due to a fault with the fiducial data; just the extrapolation is not valid.

The earliest data exhibited about twice the random scatter — shown in Fig. 9 due to lack of polarity reversing switches on the bridge circuit. Variable thermal emfs were responsible for the larger scatter. In the face of the additional scatter, a forced fit to 3000 bars produced what appeared to be a parabolic systematic pattern in the residuals $d_i-\rho_i$. These features provoked the careful study of the bellows calibration and the installment of the polarity reversal switches. In addition, heavy busses were provided for the ends of the Kohlrausch slidewire to minimize the region of indifference of the external circuit. Finally, the last three runs with argon produced data with excellent reproducibility and acceptably small scatter. The reproducibility at 35° C is always forced over a portion of the pressure range due to reliance each time on fiducial data. At other temperatures the agreement between results from different runs is not forced and after the densities from different runs have been corrected to the corresponding integral temperatures the complete results can be compared by means of the deviations from the modified Tait equation. Results from different runs reproduce within the scatter of the points over the common pressure range. This range of comparison is sometimes as great as 4 to 5 kbar. The reproducibility is much better than could

be expected if temperature measurements taken at different times were as uncertain as they were estimated to be in Chapter III or if different bellows and constant volume chamber calibrations were inconsistent to more than 0.1 per cent.

Unfortunately, the data at 100° C does not agree quite so well with the data of Michels *et al.* The divergence in densities is small; the 100° C densities obtained in the present experiment are about 0.6 amagats larger than those of Michels *et al.* It is shown in the next chapter that this is about a factor of three beyond the expected error of the present experiment. This small difference in densities corresponds to about 1.0 per cent difference in the gas thermal expansions as measured in this work and as measured by Michels *et al.* Since the thermal expansion measurement is a direct one in the present work it is difficult to expect even 0.3 per cent error on this determination.

Another indication of small inconsistencies between this work and that of Michels *et al.* is given by the initial piezometer volume V_1 which is resolved using the fiducial densities. It is possible by a technique outlined in the Appendix to obtain the initial volume independently of fiducial data. The independently determined value agrees to within 0.2 per cent of a value obtained by addition of the volumes of the individual parts of the piezometer while both values are about 0.7 per cent larger than the value obtained using the fiducial data. The indication in this last case is that the quantity a which appears in

Eq. (21) is too small by perhaps 0.2-0.3 per cent. Assuming the lowest fiducial point to be accurate, then the densities at 10,000 bars obtained in this work could be in error by 0.3--0.4 per cent due to establishment of an erroneous slope of the isotherm in the fiducial range. As a result of this uncertainty it is felt that accuracy greater than 0.4 per cent on the largest densities in Tables II, III and V cannot be claimed. The small lack of agreement with the work of Michels *et al.* caused the expenditure of considerable effort to check both the internal consistency and absolute accuracy of the present work. It is believed now that the discrepancy is due to some physical effect rather than error of measurement. One possible source of the disagreement is the van der Waals interaction between the argon and the mercury used by Michels *et al.* to compress their gas. This interaction has been discussed by Jepson and Rowlinson[21] in some order of magnitude calculations for relatively low pressure. They conclude that the effect can be large, however, the calculations are not accurate enough to be used for correction of the experimental work and the author is unaware of any experimental determinations of the effect.

Argon has been the subject of experimentation by other workers. Bridgman[22] studied it twice; his first work gave volume changes from 2 kbar to 15 kbar while his later work evaluated the density at 2 kbars from which the densities at higher pressures could be evaluated. The densities given by Bridgman are about 6 to 7 per cent lower than the ones reported herein. This is probably due to the argon dissolving

in the kerosene which was used as a pressure transmitting fluid thus resulting in volume changes for a mass of gas smaller than Bridgman thought. Babb has corrected Bridgman's isothermal data by assuming that the kerosene was saturated with argon at 2 kbars. Then by using the data of Michels *et al.* to fit the volume change measurements new densities were determined. The results still differ by around 1.0 per cent from those of the present work presumably due to a pressure dependent solubility of argon in kerosene.

More recently Polyakov and Tsiklis[23] have published data for argon over the same pressure and temperature ranges as the present work. Their data differs from this work by 2 to 3 per cent, with the disagreement being a slight function of pressure and nearly the same at each temperature. Their method consisted of loading a pressure vessel with gas measuring its volume, removing it and measuring the volume at one atmosphere then repeating the process with a steel displacing slug in the pressure vessel. The difference in volumes of gas is the volume of gas displaced by the slug. All elastic distortions of the pressure vessel are cancelled by this procedure, however, plastic distortions such as could occur in the pressure seals could lead to systematic error. Their pressure calibration must be regarded as inferior to the one in the present experiment since their manganin gauges were calibrated at a single point despite widespread knowledge[24] of the nonlinear behavior of manganin. In addition, their work was undertaken with poor temperature control and the compressibility used for

their displacing slug was for a material similar to, but not the same as the actual slug. The compressibility was not corrected for the effects of temperature.

The measurements of Lecocq[25] of the isotherms to 950° C and 1000 bars serve to fill in part of the region not covered in the present work although neither set of results can be extrapolated easily enough or well enough for meaningful comparisons to be made.

By way of comparison with theory, Cure and Babb[26] have numerically integrated the Percus-Yevick equation for the 55° C isotherm of argon using a modified Buckingham model intermolecular potential function. They compared their results with the same calculations for a Lennard-Jones[27] potential and also with a Monte-Carlo calculation[28] using the Lennard-Jones potential. In all cases the divergences between the various calculations are small in comparison with their disagreements with the present experiment. The disagreement between theory and experiment is most pronounced at high densities and reaches about 10 per cent. There could be many explanations for this result, however, a clear division of the problem is presently impossible. Briefly, it remains to be determined whether or not the potential energy of interaction of molecules at high densities can be assumed pairwise additive. Even if pairwise additivity is valid it seems clear that better representations of intermolecular potentials will be required. This is sometimes demonstrated by a lack of ability to effect agreement between calculations and experiment for both the

transport properties and low order virial coefficients for gases using the same assumed intermolecular potential function. Finally, it is by no means established that the current statistical mechanical formulation of the dense fluid state is capable of describing dense fluids and this statement applies doubly to approximate theories such as the Percus-Yevick approximation.

Argon Data Tables

The data in the following tables has been gathered in several runs on research grade argon obtained from the Matheson company. The least pure of the samples showed impurity levels of less than one part per million hence all results were averaged without regard to impurities and were interpolated by means of the modified Tait equation and deviation curves to form Tables II and III. The parameters for the modified Tait equations which were used are given in Table IV. The original points upon which the interpolated data were based are given following Table IV. They are arranged, within a given temperature, in groups of individual runs in the order in which they were taken and separated by lines. Individual runs are arranged chronologically and represent runs with different bellows, thermocouple and pressure gauge calibrations. Early data taken before the system was de-bugged are not included and some half dozen points have been eliminated as being bad readings. An extra decimal place has been carried on the original data since the random scatter is about 0.1 to 0.15 amagats.

Figures 11, 12 and 13 follow the tables of raw data and depict the argon isotherms, isochores and isobars respectively.

An interesting aspect of the data in Table III is the changing sign of $(\frac{\partial Z}{\partial T})_d$ ($Z = \frac{PV}{RT}$) within the experimental temperature range. This behavior is to be expected but has apparently not been noted by other workers. Over the range covered here the locus of points such that $(\frac{\partial Z}{\partial T})_d = 0$ is given by:

$$Z = 4.859 - 0.0053T \qquad (T \text{ in } ^\circ C) \quad .$$

This is a straight line within the rather broad limits of error. The maxima on the isochores is so broad that the locus of maxima is not well known. Along this locus the so-called internal pressure vanishes - i.e. the thermal pressure $T(\frac{\partial P}{\partial T})_d$ is balanced by the external pressure. This locus is called either the Joule line or the Amagat line.

Table II. Densities of Argon at Integral Pressures

Pressure Bars	Temperature, °C				
	35	100	200	300	400
				Density Amagats[a]	
1500	614.7				
2000	671.9	-618.0			
2500	715.7	665.6	600.8	547.9	503.1
3000	751.5	704.5	642.4	591.3	547.6
3500	782.0	737.3	678.0	628.3	585.7
4000	808.5	765.8	708.8	660.6	619.0
4500	832.0	791.1	736.2	689.4	648.7
5000	853.2	813.8	760.7	715.2	675.4
5500	872.7	834.5	783.0	738.6	699.6
6000	890.6	853.5	803.3	760.1	721.8
6500	907.2	871.0	822.1	779.8	742.2
7000	922.8	887.4	839.5	798.0	761.2
7500	937.5	902.8	855.9	815.1	779.0
8000	951.4	917.3	871.3	831.2	795.7
8500	964.5	931.1	886.0	846.5	811.5
9000	977.0	944.1	899.9	861.0	826.4
9500	988.9	956.5	913.1	874.7	840.6
10000	1000.2	968.4	925.6	888.0	854.1

[a]For this work one amagat unit of density = 4.4647×10^{-5} mole/cm^3 from Ref. 1. The difference between this value and that given by Baxter and Starkweather [Proc. Nat. Acad. Sci. 12, 699 (1926), 14, 57 (1928)] is negligible for the present purposes.

Table III. Pressures of Argon at Integral Densities

Density Amagats	Temperature, °C				
	35[a]	100[a]	200	300	400
				Pressure Bars	
500	863	1170			2468
550	1093	1466		2523	3030
600	1394	1845	2491	3112	3707
650	1790	2323	3100	3829	4524
700	2308	2937	3850	4700	5509
750	2976	3714	4775	5760	6700
800	3833	4690	5915	7058	8133
850	4920	5906	7317	8618	9845
900	6278	7407	9004		
950	7947	9234			
1000	9985				

[a]The values above the line in these two columns were calculated from Michels *et al.*(1) Due to the inconsistency of thermal expansion mentioned in the text the 100° column is not smooth: the virial expansion would predict 2330 bars at 650 amagats.

Table IV. Parameters in the Modified Tait Equation

	35°	100°	200°	300°	400°
P_o(bars)	2500	2500	2500	2500	2500
d_o(Amagats)	715.64	665.62	600.82	547.90	503.12
B(bars)	555.70	346.65	244.07	246.95	279.65
C(Amagats)	229.56	234.60	246.57	258.34	268.38
RMS dev.[a] (Amagats)	0.82	0.60	0.44	0.36	0.19

[a]This is the rms deviation of the equation with cited parameters from the observed experimental points in the range 2500 - 10,000 bars.

P bars	d amagats						
35.00°C		35.00°C Contd.		35.00°C Contd.		35.00°C Contd.	
1191	568.32	6538	908.42	2127	684.05	5253	863.24
1259	579.19	6782	916.04	2315	700.45	4691	840.43
1295	585.19	7035	922.85	2545	718.96	4090	812.85
1339	591.86	7333	932.37	2760	735.05	----------	
1409	602.11	7577	939.39	----------		54.85° C	
1486	612.71	7818	946.09	4195	817.86	3662	777.07
1566	623.45	----------		3176	762.86	2564	705.79
1658	634.75	1537	619.59	3497	781.81	2751	719.84
1749	645.34	1612	629.15	3865	800.66	2933	732.50
1843	655.86	1682	637.62	4044	810.27	3130	744.26
1944	666.27	1760	646.63	4367	825.97	3337	758.46
2045	676.88	1851	656.62	3354	773.54	3564	771.70
2154	686.38	1946	666.50	3683	792.02	3800	784.74
2270	696.94	2046	676.37	4605	836.65	4172	803.50
2406	708.24	2163	687.30	5106	857.48	4454	817.55
2550	719.78	2281	697.73	5724	880.87	4746	830.20
2689	730.24	2400	707.69	6391	903.71	5034	842.26
2848	739.68	2558	720.67	7095	925.73	5386	856.29
2969	749.67	2749	734.25	7767	944.76	5723	868.82
----------						----------	
2346	703.17	2938	747.25	8560	965.72	6077	881.44
2425	709.70	3147	760.69	7237	930.09	6469	894.61
2504	715.99	3375	774.39	6100	894.15	6865	907.14
2590	722.47	3622	788.24	6798	916.86	7279	919.51
2674	728.91	3883	801.92	8175	956.17	7753	933.12
2763	735.42	4161	815.55	10245	1005.65	----------	
2958	748.77	4439	828.33	9611	991.84	95.25° C	
3158	761.63	4058	810.60	8889	974.55		
3369	774.39	3466	779.61	7440	936.00	2834	695.95
3596	787.35	3026	753.02	5450	871.00	3013	709.04
3823	799.79	2665	728.21	4847	846.88	3221	722.92
4074	812.16	2324	701.39	----------		3433	736.48
4346	824.99	2102	681.68	5826	884.70	3646	749.18
4629	837.67	1866	660.36	6465	906.22	3881	762.44
4942	850.90	1718	641.83	7620	941.00	4134	775.91
5245	862.94	2405	708.10	8586	966.71	4397	788.92
5593	876.03			9917	998.32	4680	802.45
5849	885.14	----------		9380	986.22	4989	815.91
6034	891.71			7940	949.79	5295	829.00
6243	898.64	1980	669.87	6964	921.84	5625	842.19

P bars d amagats (Contd.)

95.25° C Contd.

P	d
5972	854.98
6311	867.26
6320	867.56
6652	878.61
7116	894.64
7492	905.12
7949	918.17
8387	930.44

100.40° C

P	d
1811	596.51
1918	608.71
2052	623.17
2209	638.95
2574	671.52
2809	690.04
3050	707.55
3339	726.88
3686	748.00
4064	769.03
4493	790.51
4275	779.95
3499	737.12
2707	682.44
2133	631.62

100.10° C

P	d
4947	811.60
4510	791.51
4769	803.44
5473	833.35
6055	855.36
6629	875.43
7442	900.98
8215	923.21
8994	943.98
9268	950.80
9704	961.35
9980	967.88
8629	934.46
7810	911.89
7081	889.84
6319	864.73
5785	845.21
5201	822.24

200.19° C

P	d
3272	662.61
3481	676.67
3703	690.85
3934	704.67
4188	719.47
4432	732.61
4699	746.16
4981	759.74
5300	774.42
5567	785.60
5865	798.03
6124	808.01
6474	820.95
7178	845.20
7773	864.31
8413	883.12
9000	899.60
9454	911.59

200.20° C

P	d
2247	576.57
2421	593.11
2606	610.06
2796	626.15
3024	644.21
3281	662.97
3566	682.21
3901	702.78
4267	723.54
4681	745.13
5150	767.46
5352	776.47
4079	713.33
3411	671.99
2906	635.17
2513	601.94

200.13° C

P	d
5578	777.78
4618	742.54
5013	761.22
5732	792.73
6565	817.08
7755	865.75
8585	882.48
9185	904.70
10139	928.95
9545	914.18
8731	892.45
8052	872.82
7341	850.77
6616	826.04
6076	806.09

300.00° C

P	d
2528	550.29
2784	573.38
2945	586.74
3178	604.97
3478	626.69
3781	646.96
4114	667.45
4477	688.08
4868	708.57
5370	732.59
5933	757.29
6702	787.46
5098	720.27
4276	677.12
3600	635.38
3076	597.25

300.10° C

P	d
5559	741.11
5982	759.11
6893	794.06
7713	822.13
8383	842.98
9020	861.39
10052	889.33
9678	880.30
9295	869.15
8737	853.88
8054	832.85
7352	810.11
6537	781.61

399.90° C

P	d
2833	533.57
4241	633.74
3888	612.06
3593	597.33
3314	572.16
3051	551.74
6656	748.37
6076	725.04
5621	705.17
5168	683.88
5458	697.67
5902	717.58
6369	737.03
7297	771.80
7831	790.54
10036	854.96
9528	841.57
9106	829.55
8671	816.92
8369	807.52
8010	795.99
7618	783.03
6949	759.35

P bars	d amagats						
35.00°C		35.00°C Contd.		35.00°C Contd.		35.00°C Contd.	
1191	568.32	6538	908.42	2127	684.05	5253	863.24
1259	579.19	6782	916.04	2315	700.45	4691	840.43
1295	585.19	7035	922.85	2545	718.96	4090	812.85
1339	591.86	7333	932.37	2760	735.05	----------	
1409	602.11	7577	939.39	----------		54.85° C	
1486	612.71	7818	946.09	4195	817.86	3662	777.07
1566	623.45	----------		3176	762.86	2564	705.79
1658	634.75	1537	619.59	3497	781.81	2751	719.84
1749	645.34	1612	629.15	3865	800.66	2933	732.50
1843	655.86	1682	637.62	4044	810.27	3130	744.26
1944	666.27	1760	646.63	4367	825.97	3337	758.46
2045	676.88	1851	656.62	3354	773.54	3564	771.70
2154	686.38	1946	666.50	3683	792.02	3800	784.74
2270	696.94	2046	676.37	4605	836.65	4172	803.50
2406	708.24	2163	687.30	5106	857.48	4454	817.55
2550	719.78	2281	697.73	5724	880.87	4746	830.20
2689	730.24	2400	707.69	6391	903.71	5034	842.26
2848	739.68	2558	720.67	7095	925.73	5386	856.29
2969	749.67	2749	734.25	7767	944.76	5723	868.82

2346	703.17	2938	747.25	8560	965.72	6077	881.44
2425	709.70	3147	760.69	7257	930.09	6469	894.61
2504	715.99	3375	774.39	6100	894.15	6865	907.14
2590	722.47	3622	788.24	6798	916.86	7279	919.51
2674	728.91	3883	801.92	8175	956.17	7753	933.12
2763	735.42	4161	815.55	10245	1005.65	----------	
2958	748.77	4439	828.33	9611	991.84	95.25° C	
3158	761.63	4058	810.60	8889	974.55		
3369	774.39	3466	779.61	7440	936.00	2834	695.95
3596	787.35	3026	753.02	5450	871.00	3013	709.04
3823	799.79	2665	728.21	4847	846.88	3221	722.92
4074	812.16	2324	701.39	----------		3433	736.48
4346	824.99	2102	681.68	5826	884.70	3646	749.18
4629	837.67	1866	660.36	6465	906.22	3881	762.44
4942	850.90	1718	641.83	7620	941.00	4134	775.91
5245	862.94	2405	708.10	8586	966.71	4397	788.92
5595	876.03	----------		9917	998.32	4680	802.45
5849	885.14			9380	986.22	4989	815.91
6034	891.71			7940	949.79	5295	829.00
6243	898.64	1980	669.87	6964	921.84	5625	842.19

P bars — d amagats (Contd.)

95.25° C Contd.

P	d
5972	854.98
6311	867.26
6320	867.56
6652	878.61
7116	894.64
7492	905.12
7949	918.17
8387	930.44

100.40° C

P	d
1811	596.51
1918	608.71
2052	623.17
2209	638.95
2574	671.52
2809	690.04
3050	707.55
3339	726.88
3686	748.00
4064	769.03
4493	790.51
4275	779.95
3499	737.12
2707	682.44
2133	631.62

100.10° C

P	d
4947	811.60
4510	791.51
4769	803.44
5473	833.35
6055	855.36
6629	875.43
7442	900.98
8215	923.21
8994	943.98
9268	950.80
9704	961.35
9980	967.88
8629	934.46
7810	911.89
7081	889.84
6319	864.73
5785	845.21
5201	822.24

200.19° C

P	d
3272	662.61
3481	676.67
3703	690.85
3934	704.67
4188	719.47
4432	732.61
4699	746.16
4981	759.74
5300	774.42
5567	785.60
5865	798.03
6124	808.01
6474	820.95
7178	845.20
7773	864.31
8413	883.12
9000	899.60
9454	911.59

200.20° C

P	d
2247	576.57
2421	593.11
2606	610.06
2796	626.15
3024	644.21
3281	662.97
3566	682.21
3901	702.78
4267	723.54
4681	745.13
5150	767.46
5352	776.47
4079	713.33
3411	671.99
2906	635.17
2513	601.94

200.13° C

P	d
5578	777.78
4618	742.54
5015	761.22
5732	792.73
6565	817.08
7755	863.73
8585	882.48
9185	904.70
10139	928.93
9543	914.18
8731	892.45
8052	872.82
7341	850.77
6616	826.04
6076	806.09

300.00° C

P	d
2528	550.29
2784	573.38
2945	586.74
3178	604.97
3478	626.69
3781	646.96
4114	667.43
4477	688.08
4868	708.57
5370	732.59
5933	757.29
6702	787.46
5098	720.27
4276	677.12
3600	635.38
3076	597.25

300.10° C

P	d
5559	741.11
5982	759.11
6893	794.06
7713	822.13
8383	842.98
9020	861.39
10052	889.33
9678	880.30
9295	869.15
8737	853.88
8054	832.85
7352	810.11
6557	781.61

399.90° C

P	d
2833	533.57
4241	633.74
3888	612.06
3593	597.33
3314	572.16
3051	551.74
6656	748.37
6076	725.04
5621	705.17
5168	683.88
5458	697.67
5902	717.58
6369	737.03
7297	771.80
7831	790.54
10036	854.96
9528	841.57
9106	829.55
8671	816.92
8369	807.52
8010	795.99
7618	783.03
6949	759.35

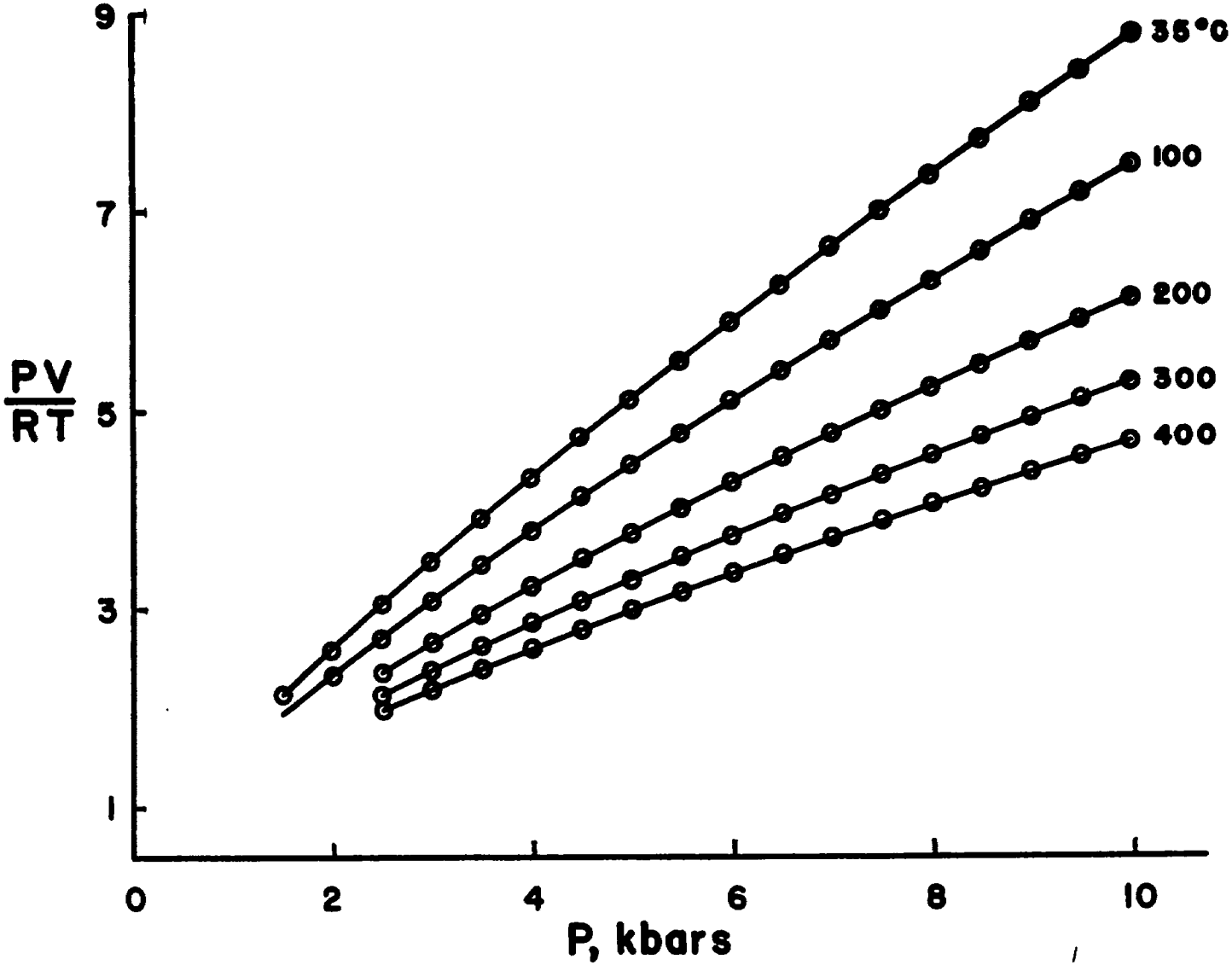

Figure 11. Isotherms of Argon

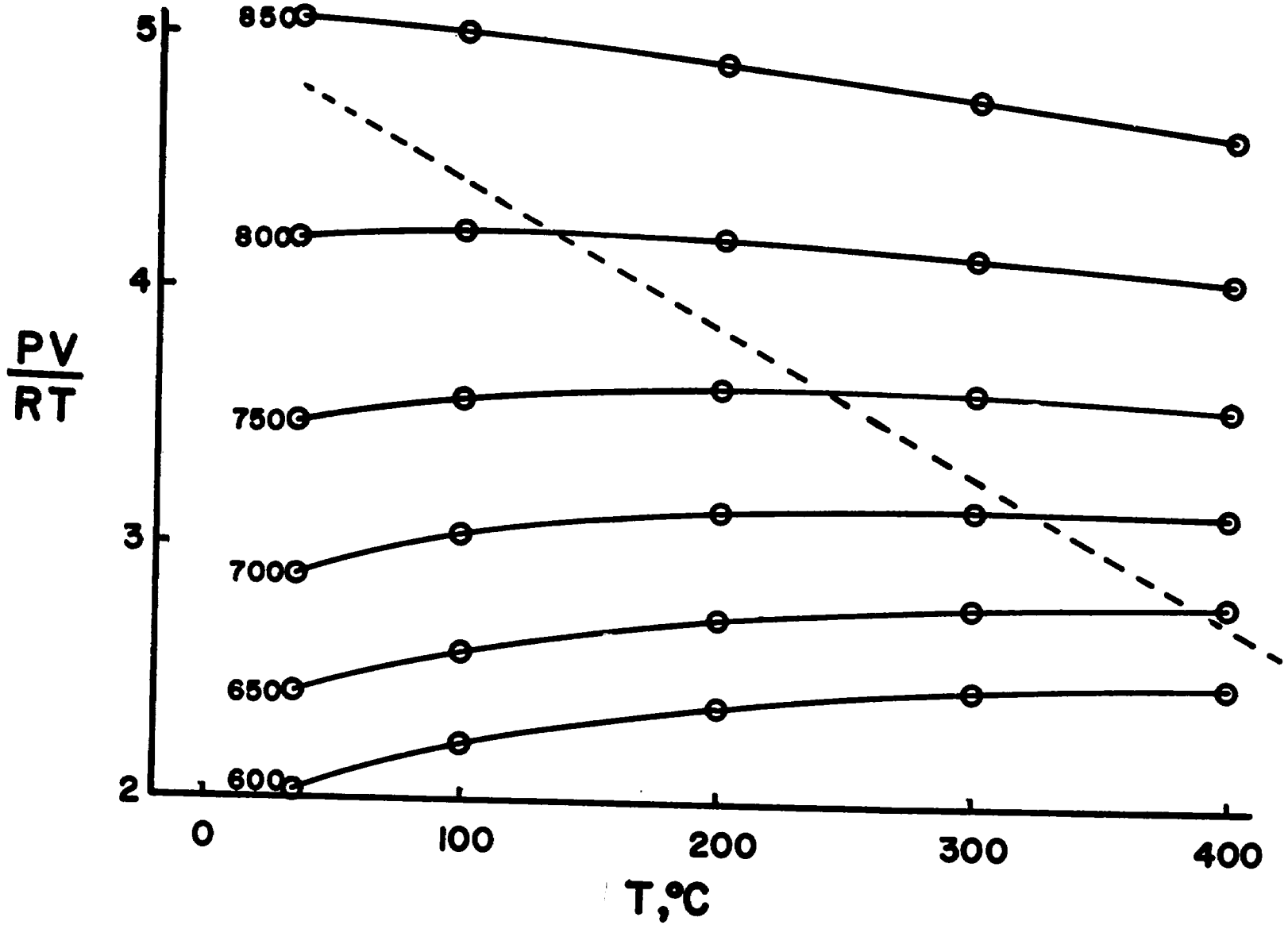

Figure 12. Isochores of Argon

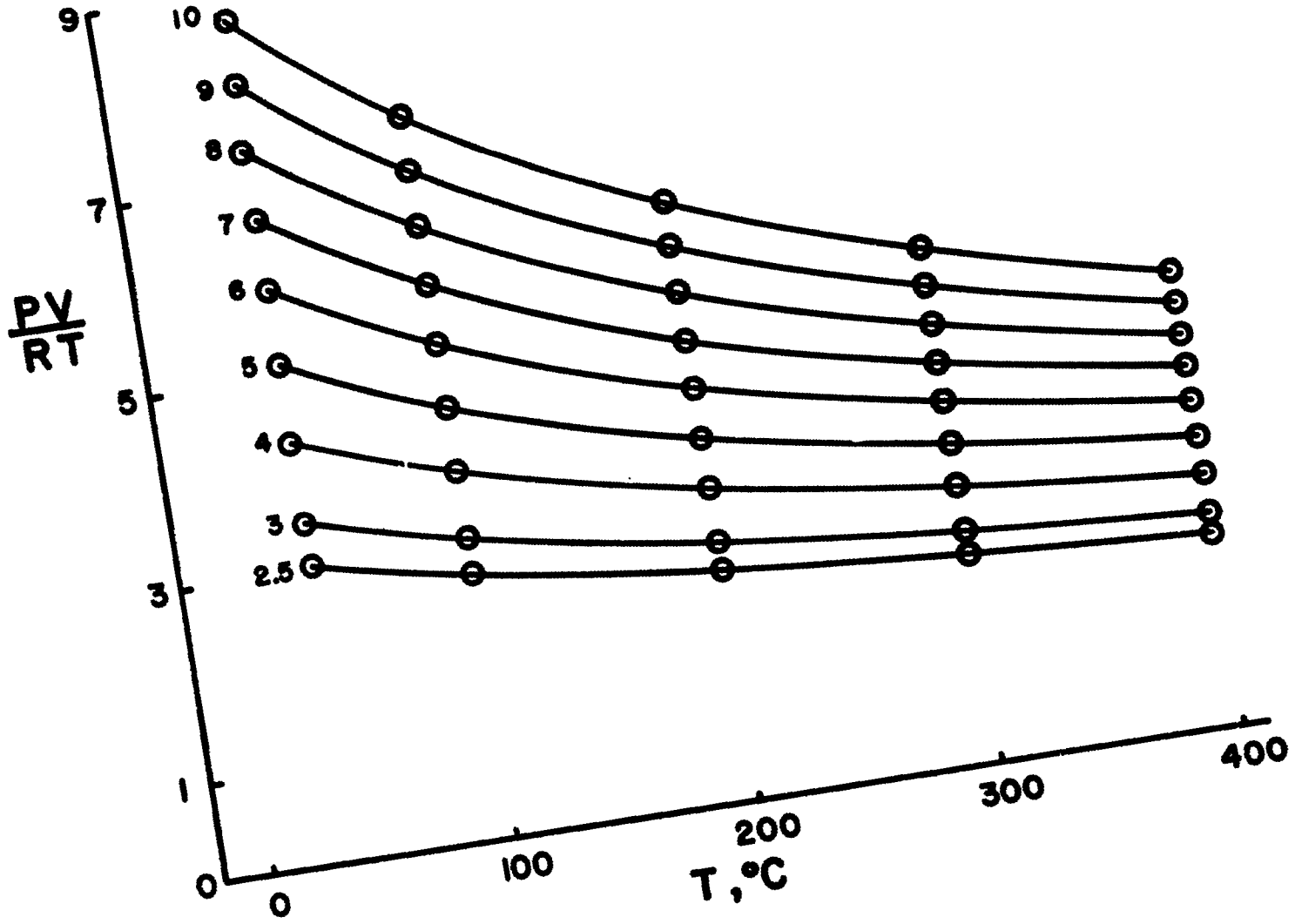

Figure 13. Isobars of Argon

Nitrogen

In contrast to the simple spherical and chemically inert argon molecule, nitrogen represents the next step in molecular complexity and was therefore a logical second choice among the gases studied. It is diatomic, homonuclear and relatively chemically inert.

The fiducial 35° C data was again taken from the work of Michels *et al.*[29] whose isotherms were represented in the following modified virial form:

$$P(V-\alpha) = \sum A_k \rho^k \quad .$$

Michels *et al.* tabulated the values of the polynomial coefficients A_k and the value of α at 35° C intervals of temperature. It was therefore necessary to interpolate their results in order to construct a 35° C isotherm. It was decided that the laborious least squares fitting of a virial expansion to the Lagrangian interpolated raw data of Michels *et al.* could be avoided since this procedure had proven to be unnecessary in the case of argon. Instead, the polynomial coefficients A_k given by Michels *et al.* were multiple point Lagrangian interpolated for 35° C. Then the raw data was Lagrangian interpolated and a value of α was determined by fitting these interpolated data by least squares technique to the modified virial expansion using the interpolated values of A_k. The values of the constants which were determined in this fashion for 35° C are as follows:

$$\alpha = 5.84083 \times 10^{-4} \text{ amagats}$$

$$A_0 = 1.143597 \text{ bar amagats}$$

$$A_1 = -0.822444 \times 10^{-3}$$

$$A_2 = 3.237504 \times 10^{-6}$$

$$A_3 = -0.700062 \times 10^{-9}$$

$$A_4 = 6.754749 \times 10^{-12}$$

The use of the modified virial expansion with the cited parameters is probably not valid for pressures above 2200 bars since the nearest isotherms at 25° C and 50° C upon which the interpolation was based were not extended much beyond this pressure. As a result of this, the fitting of volume changes to the fiducial data was terminated at 2200 bars and the densities at higher pressures obtained in the present work deviate markedly from results obtained by extrapolation of the fiducial polynomial. It was also shown in the work of Michels *et al.* that deviations between the polynomial predictions and the measured points became abruptly large near the end of their pressure range. In any case the volume changes measured in the present work fit the adopted fiducial densities extremely well over a 600 bar pressure interval with an rms scatter in densities of 0.02 amagats.

Nitrogen has been studied by a number of other workers; among them is Bridgman[30] whose results extend to rather high pressures but are known to be in error and will not be considered here. Benedict[2] in Bridgman's laboratory made a more careful study of nitrogen to 6000 bars and 200° C. More recently Tsiklis has twice[30,31] made measurements on nitrogen by two somewhat different methods. In addition to

these direct determinations, Michels *et al.*[32] have published tables which were obtained by combining their results with those of Benedict.

The agreement of the present work with Michels *et al.* at 35° C is forced due to adoption of their work for fiducial densities. It was necessary to interpolate the results of Benedict for the 35° C comparison shown in Fig. 14. The ordinate $\Delta\rho$ of the figure is the difference between Amagat densities obtained in the present work and the densities given by others. The line in the upper half plane which is labeled VE is a comparison of the present work with points given by the modified virial expansion of Michels *et al.* The lowest line which is labeled BE is a comparison with the results of Benedict. The solid line which is labeled CBE is a comparison with Benedict's work with a correction made on his pressure scale. Benedict's manganin gauges were calibrated against a free piston gauge to 1500 bars and at the melting pressure of mercury at 0° C. Unfortunately Benedict used the Bridgman value for the 0° C melting point of mercury thus correction of his pressure scale to a more correct[11] 0° C calibration point is necessary. This simple pressure scale correction is shown on the CBE curve to bring the results of Benedict to agreement with the present work within his claimed experimental error of 0.2 per cent.

At 100° C there is a slight density difference of about 0.5 Amagats between this work and that of Michels *et al.* The discrepancy is qualitatively the same as was shown by the argon data and as was suggested previously, it may be due to the interaction of mercury with the gases studied by Michels *et al.* The agreement with Benedict is improved

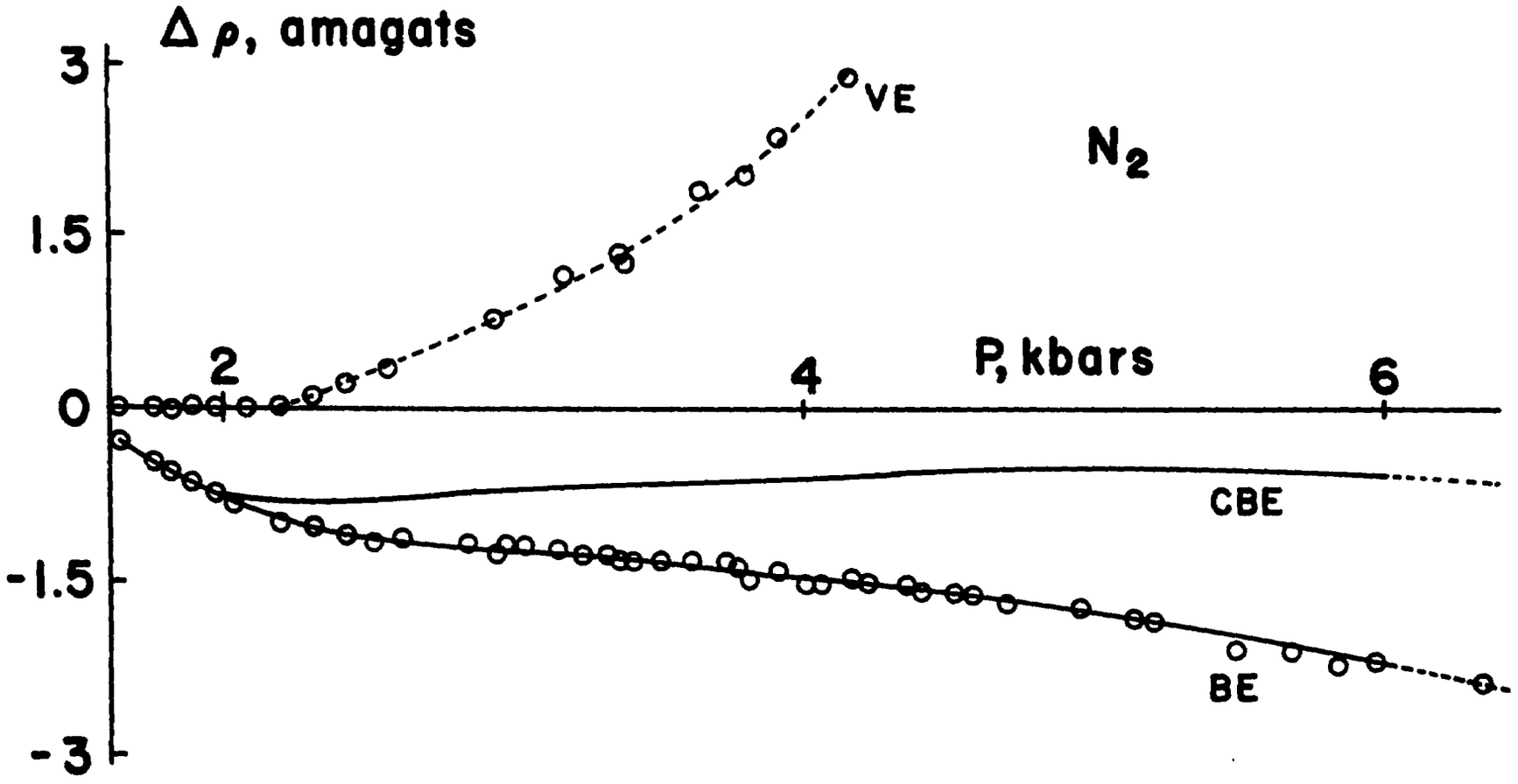

Figure 14. Comparison of Nitrogen Data

at 100° C and low pressures and the comparison with his work when corrected for pressure scale errors remains within his claimed experimental error to 6000 bars.

At 200° C the temperature range of Michels *et al.* is exceeded and there are no further comparisons with the fiducial work. At 2000 bars and 200° C the comparison with Benedict is fairly poor, showing a disagreement of 2.5 Amagats in density. As pressures increase the agreement improves markedly and above 3500 bars the densities are in excellent agreement. Throughout the whole temperature range common to the present work and that of Benedict and at pressures above 3500 bars the thermal expansion measurements agree within experimental error. Thus over the common range the agreement of the present work with that of Benedict is within his claimed experimental error except at the lowest pressures and 200° C, and at the highest pressures the agreement is remarkable.

The data of Tsiklis and Polyakov[31] cover the same temperature and pressure range as this work. The divergences between their densities and the present ones are erratic with pressure and systematic in temperature. The differences are: less than 0.7 per cent at 100° C, less than 0.5 per cent at 200° C and 300° C and at 400° C increase with pressure from a low of about 0.3 per cent at 2500 bars to a high of 1.6 per cent at 10,000 bars. Their most recent data is in good agreement with the earlier work of Tsiklis.[30] The densities of Tsiklis and Polyakov are higher than those obtained in this work at a given pressure

at 100 and 200° C and are lower at 300 and 400° C. These authors claim an accuracy of 0.3 per cent for their work, however most of the objections which were given to their claims of accuracy for argon measurements remain valid in the case of the nitrogen data. In addition to those objections already stated their nitrogen had about 0.5 per cent impurity. Taking these things into account it appears that the data of Polyakov and Tsiklis are in agreement with the present work within the combined experimental errors except at 400° C. This divergence is too large and is perhaps traceable to neglect of the second degree term of the thermal expansion of their displacing slug.

Finally, the results of Michels *et al.*[32] which supposedly are combinations of the data of Michels *et al.*[29] and Benedict can be compared with the present work. Michels *et al.* constructed these data by arbitrary adjustments of the results of Benedict, sometimes by as much as 1.5 per cent. The corrections which were made on Benedicts data were greater than the divergences between his results and the extrapolation of the virial expansions given by Michels *et al.*[29] The highly suspicious nature of the combined results has been noted before[5] and the comparison with the present work is relatively poor. Thus the composite data should not be used, for it disagrees with all the direct experimental results.

Babb[14] has extrapolated the results of this work to -22.45° C in order to compare with the Percus-Yevick calculation[26] results. As was the case with argon the agreement is within calculational error at low densities and at higher densities rises above 10 per cent.

Nitrogen Data Tables

The data in Tables V and VI have been constructed in the same way as for argon. Several runs on research grade nitrogen from the Matheson Company were averaged without regard to impurities to form the interpolated tables. The nitrogen contained 4.5 parts per million of argon.

Table VII gives the parameters used in the modified Tait equation for interpolation of the data. Following Table VII the original data upon which the interpolated points were based is given. Figures 15, 16 and 17 follow the raw data and depict the nitrogen isotherms, isochores, and isobars respectively. As in the case of argon the "Amagat Line" or "Joule Line" passes through the experimental region and is indicated in Fig. 16. The locus of the curve is given by: $Z = 4.93493 - 0.82926T + 0.06852T^2$ where $Z = \frac{PV}{RT}$ and T is in °C. Again the maximum on the isochores is so broad that the locus is not well known.

Considering the agreements which exist among the results of several independent investigations, the densities given in the tables are probably accurate to about 0.3 per cent over the full pressure and temperature ranges.

Table V. Densities of Nitrogen at Integral Pressures

Pressure Bars	Temperature, °C				
	35	100	200	300	400
	Density Amagats[a]				
1500	521.9				
2000	572.3	530.6	478.0		
2500	611.3	572.1	521.3	479.7	445.1
3000	643.3	606.0	557.2	516.8	482.4
3500	670.7	634.9	587.8	548.6	514.7
4000	694.6	660.2	614.5	576.5	543.2
4500	716.0	682.6	638.4	601.2	568.7
5000	735.4	702.9	659.9	623.4	591.8
5500	753.0	721.5	679.4	643.8	612.9
6000	769.4	738.6	697.5	662.6	632.3
6500	784.7	754.4	714.3	680.0	650.3
7000	799.0	769.4	729.9	696.2	667.0
7500	812.5	783.3	744.6	711.4	682.7
8000	825.2	796.5	758.5	725.8	697.4
8500	837.2	809.0	771.6	739.4	711.4
9000	848.7	820.9	784.1	752.4	724.7
9500	859.7	832.2	796.1	764.8	737.2
10000	870.2	843.1	807.5	776.6	749.5

[a]For this work one amagat unit of density = 4.4636×10^{-5} mole/cm^3.

Table VI. Pressures of Nitrogen at Integral Densities

Density Amagats	Temperature, °C 35[a]	100[a]	200	300	400
			Pressure Bars		
450	1003	1305			2562
475	1152	1490		2442	2895
500	1325	1704	2243	2762	3265
525	1527	1940	2550	3122	3674
550	1760	2220	2892	3524	4128
575	2031	2540	3282	3973	4631
600	2347	2905	3721	4475	5189
625	2704	3321	4213	5036	5806
650	3115	3795	4765	5661	6492
675	3586	4326	5383	6354	7251
700	4120	4926	6072	7122	8092
725	4726	5601	6839	7971	9012
750	5412	6356	7692	8905	10022
775	6178	7199	8632	9930	
800	7036	8139	9669		
825	7994	9178			
850	9059	10320			
875	10236				

[a]The values above the line in these two columns were calculated from Michels' *et al.*[29]. Due to the inconsistency of thermal expansion mentioned in the text the 100° column is not smooth: the expansion would predict 1948 bars at 525 amagats.

Table VII. Parameters in the modified Tait Equation

	Temperature, °C				
	35°	100°	200°	300°	400°
d_0 (Amagats)	572.30	530.61	478.00	479.72	445.11
P_0 (Bars)	2000	2000	2000	2500	2500
B (Bars)	556.213	450.718	430.119	236.783	245.821
C (Amagats)	210.036	215.496	226.188	236.783	245.821
RMS dev.[a]	1.09	1.00	0.71	0.49	0.29

[a]This is the rms deviation in amagats of the equation which cited parameters from the observed experimental points over the range P_0 to 10,000 bars.

P Bars	d Amagats				
35.00° C					
1643	537.96	6692	790.32	3751	647.66
1758	549.81	3215	655.63	3100	611.93
1816	555.45	3407	665.99		
1888	562.27	3410	665.95	5111	707.20
1972	569.87	3404	665.70	4594	686.56
2083	579.42	3614	676.43	3964	658.34
2192	588.25	3769	683.92	3441	631.47
2309	597.38	3998	694.42	3705	645.34
2423	605.80	4218	704.18	4279	672.42
2569	616.04	4398	711.75	5764	730.48
2940	639.76	4580	719.21	6649	758.80
3388	664.88	5140	740.43	7392	780.20
3912	690.63	5673	758.79	8232	802.16
4517	716.65	6338	779.88	8950	819.52
-4161	701.75	7001	799.00	10050	844.03
3624	676.88	7890	822.39	9489	831.98
3177	653.54	8830	844.77	7791	790.95
2742	627.63	9805	866.08	6190	744.54
2028	574.69	9457	858.81		
2303	596.92	9100	850.91	**200.00° C**	
2608	618.72	8479	836.75	2248	500.41
3803	685.43	8165	829.28	3091	563.39
3367	663.75	7601	815.08	2613	530.15
2970	641.62	7286	806.85	2241	499.84
2422	605.71	5963	768.37	2432	515.70
2525	612.97	10115	872.55	2818	544.79
2615	619.15	4837	729.29	3426	583.51
2839	633.63			4013	615.17
3235	656.66	**100.40° C**		4329	630.40
3506	670.99	2623	580.77	4896	655.52
4059	697.19	2254	552.66	4573	641.65
4694	723.66	1960	526.62	3738	600.92
5489	752.54	2112	540.66		
5839	764.20	2445	567.73	**199.80° C**	
5197	742.46	2849	596.20	4226	625.59
4955	733.68	3385	628.39	5050	661.94
4353	709.93	4069	663.20	5724	687.78
3734	682.29	4774	693.83	6306	707.90
3040	645.74	4383	677.48	7085	732.49

199.80°C Contd.

8015	758.92
8896	781.65
10052	808.73
9622	799.00
9183	788.70
8458	770.71
7513	745.12
6710	721.12
5840	692.06
5356	674.20
4602	643.03

300.15° C

3866	569.29
3526	550.11
2987	515.94
2552	483.76
2769	500.41
3259	533.68
4406	596.38
4872	617.78
4172	584.97

300.00° C

4405	596.79
4697	610.21
5440	641.57
6116	666.72
7006	696.38
7670	716.36
8483	738.96
9300	759.91
9989	776.39
9598	767.14
8897	749.83
8065	727.65
7336	706.57
6572	682.40
5808	655.59
5067	626.37

400.22° C

4267	557.07
3965	541.22
4897	586.69
4542	570.29
3512	513.23
3043	485.29
2835	470.63
3285	501.38
3766	530.17

399.90° C

4843	584.80
5188	599.87
6069	634.54
6672	656.12
7442	680.81
8351	707.26
9237	730.81
9968	748.71
9522	738.00
8759	718.38
7939	695.71
7023	667.79
6366	645.72
5614	617.79
5650	619.05

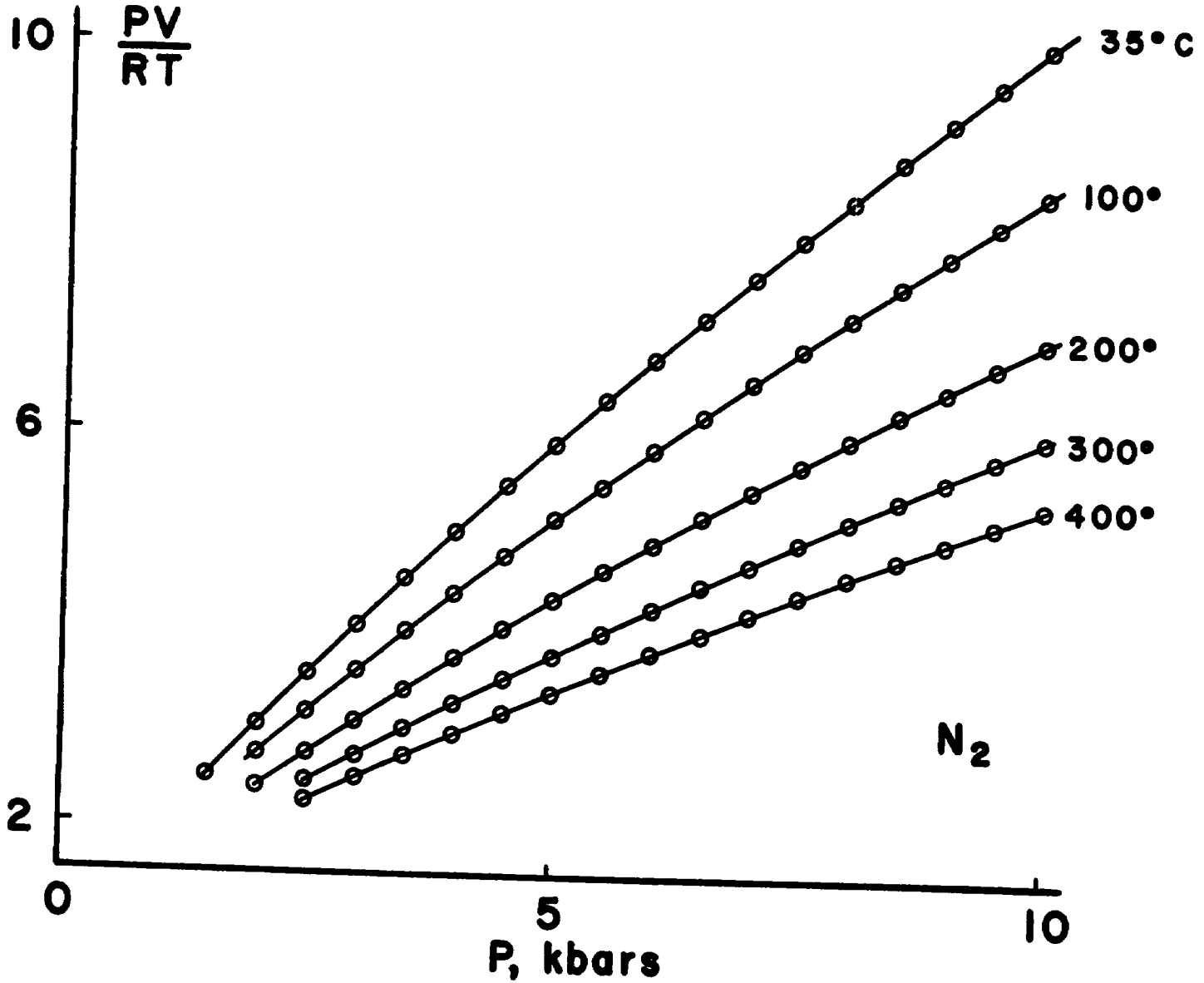

Figure 15. Isotherms of Nitrogen

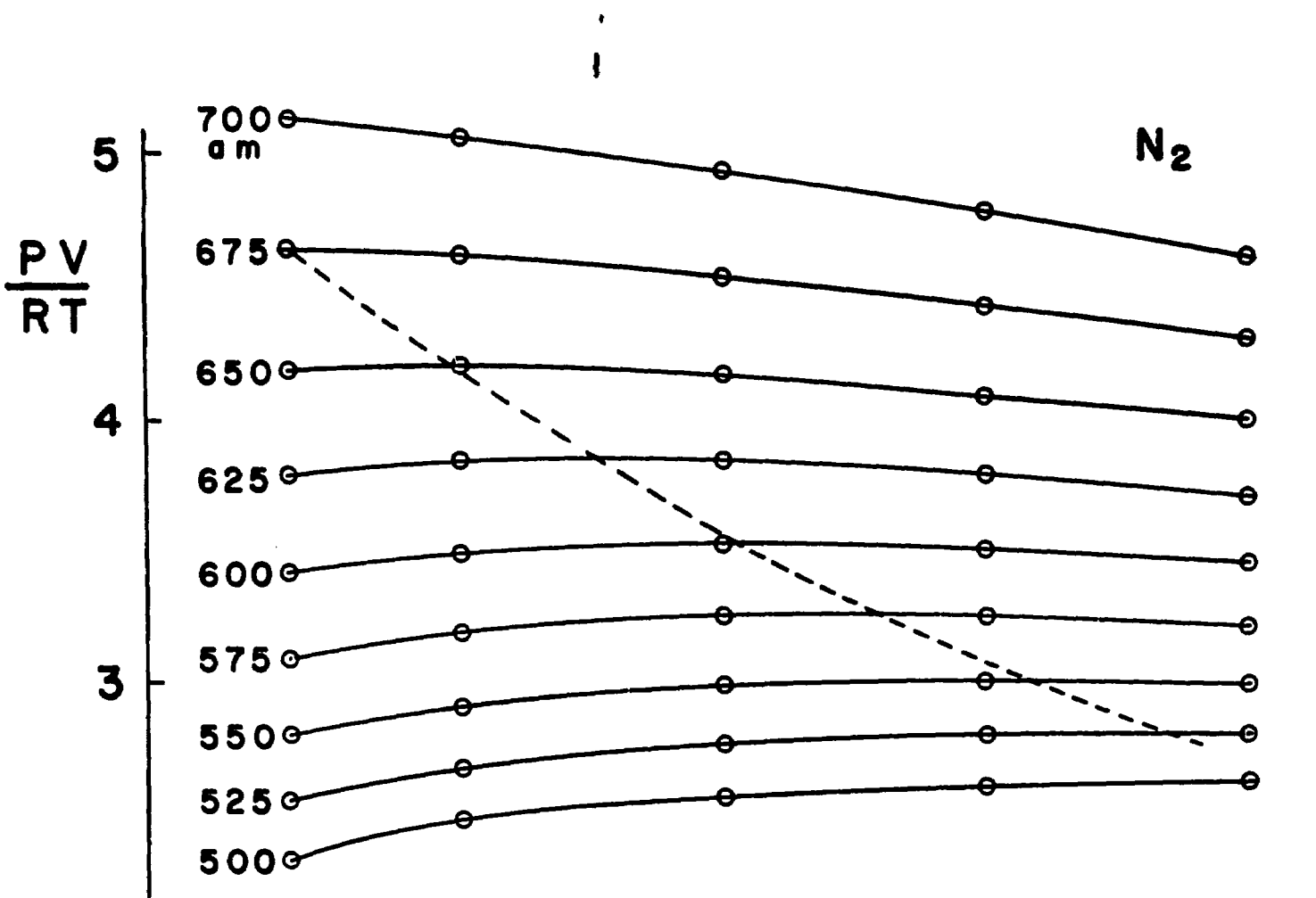

Figure 16. Isochores of Nitrogen

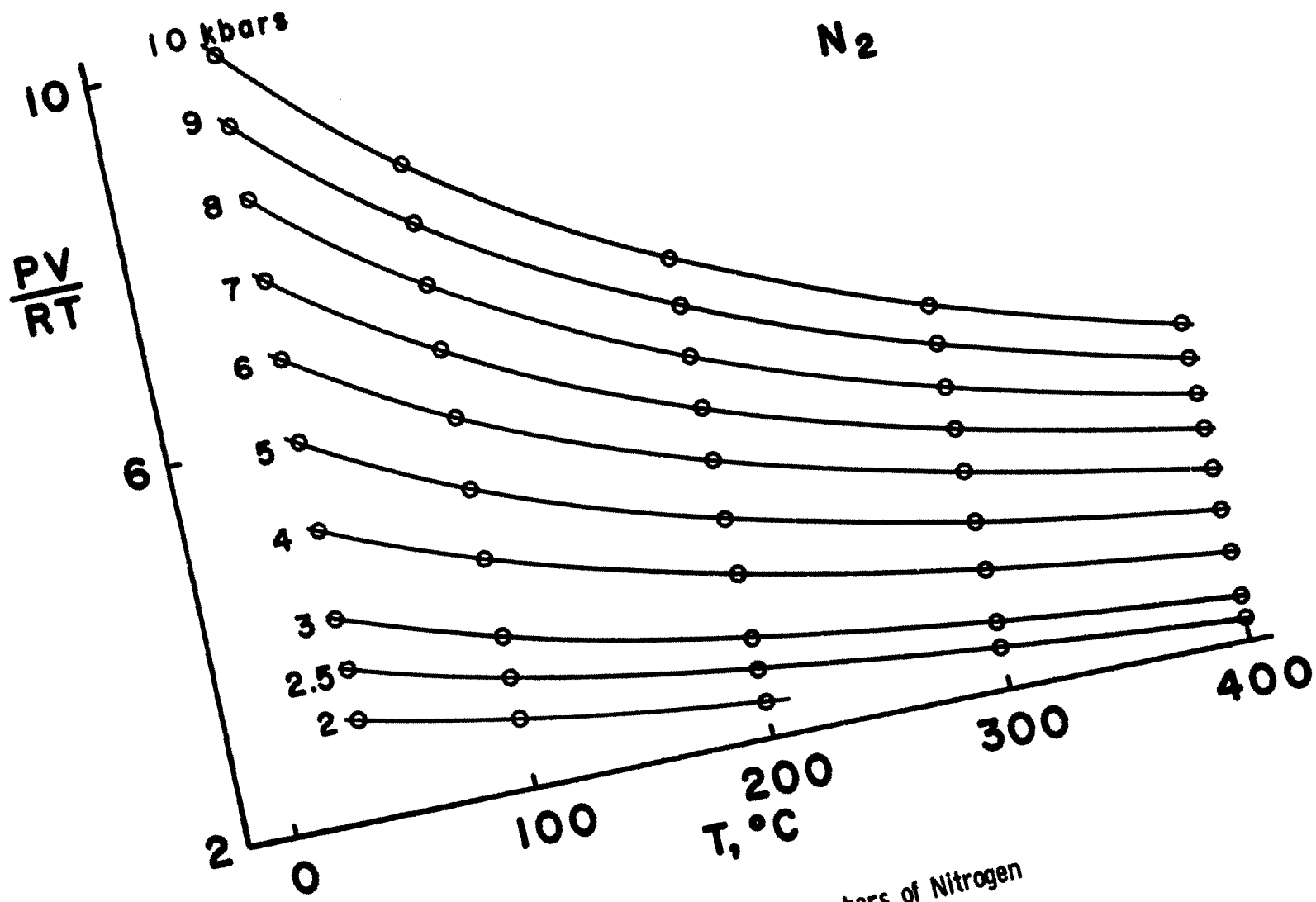

Figure 17. Isobars of Nitrogen

Propene

Interest in the density of propene at high pressure is occasioned by the possibility of its use as a pressure transmitting fluid.[33] Propene was the only substance investigated where any of the isotherm temperatures were below the critical point. The experimental procedure was essentially the same as before but the data reduction was more complicated due to the impossibility of constructing a reliable 35° C fiducial isotherm from the existing literature. Accordingly, the 100° C isotherm for propene given by Michels *et al.*[34] was adopted for fiducial data fitting. The virial expansion given by Michels *et al.* at 100° C is based upon only two points within the fiducial pressure range, the highest one being at 2328 bars. Thus it was necessary to make the fiducial fit to points below 2300 bars and in order to get a large enough volume change within the fiducial range, the lowest pressure points were taken at pressures of only about 1000 bars.

It is quite fortuitous that the present work on propene was accomplished on a single sample load taken with the same bellows and constant volume chamber used for nitrogen. The piezometer was undisturbed between the runs and it therefore was possible to obtain comparisons of the initial piezometer volumes which were obtained from fits to fiducial data for different gases. The excellent comparison (0.1 per cent) between the volumes yielded by the two different fiducial attachments lends a large measure of confidence to the fitting procedure at 100° C and removes any doubt associated with reliance

upon a fiducial virial expansion which is based upon so few points. The volume of the system obtained in both cases was, as in the case of argon, a little smaller than the actual volume obtained by either external estimates or analyses based upon overlapped isotherm data. (See Appendix) The consistency which is thus implied for both this work and the work at the van der Waals laboratory is noteworthy.

For propene there is no data other than that from the van der Waals laboratory available for comparison. As mentioned before it was thought impractical to try to construct a fiducial 35° C isotherm, however, the results obtained in the present work at 35° C appear to agree very reasonably with the extrapolated results of Michels *et al.* There is no way to make a decent comparison at 200° C; first because no reasonable procedure was found for fitting the Michels *et al.* results through both the liquid and gas regions in order to extrapolate them to 200° C, and second, the propene polymerized at 200° C. A total of about 1 per cent of the volume of the sample was lost through the polymerization process. It was necessary to discard the constant volume chamber after the run with propene since it contained carbon deposits on its inner walls. Since a reaction had taken place none of the recheck runs normally made were of any value, however, the lack of any volume hysteresis at 100° C suggests that no reaction occurred at any pressure at 100° C. The data at 200° C was reduced under the assumption that no polymerization occurred upon heating to 200° C. This seems reasonable since the pressure was only about 4000 bars

during the heating period and the reaction rate increased greatly at the highest pressures. If some reaction did occur then a spurious volume change would be taken away from the normal expansions encountered upon heating a gas and the densities given in the data tables for 200° C would be too large.

The propene used in this experiment was CP grade and from the same lot on which the melting point[33] and viscosity data[35] have previously been reported. The data is presented in Tables VIII, IX and X and the isotherms are shown in Fig. 18.

The interpolated points which appear in Tables VII and VIII at 200° C and high pressures have been partially corrected for the volume hysteresis due to polymerization. A gradual correction was applied between 5 and 10 kbar amounting to about 2 Amagats at 10,000 bars. The original points have been reported with no correction for polymerization.

Methane

Methane was chosen for investigation by virtue of its being the simplest of the hydrocarbons. The fiducial data for methane were taken from the work of Deffet and Ficks[36] who presented isotherm data in tabular form at 50.63° C, 101.34° C and 151.88° C. It was decided to fit to the fiducial data at 101.35° C rather than try to extrapolate their results to 35° C. Accordingly, the tabular fiducial data at 101.34° C were fitted to a modified Tait equation and interpolated with the aid of a deviation curve. Some smoothing of the

Table VIII

Densities of Methane and Propene at Integral Pressures

Pressure bars	CH_4 Temperature, °C			Density[a] amagats	C_3H_6 Temperature, °C		
	35°	100°	200°		35°	100°	200°
1000					323.2	(301.5)	
1500	520.6	478.4			338.3	319.2	295.9
2000	558.7	520.7	470.6		350.1	332.9	311.5
2500	588.4	553.6	507.0		360.0	344.0	324.5
3000	613.0	580.6	537.0		368.6	353.6	335.5
3500	634.2	603.6	562.0		376.2	361.9	344.8
4000	652.9	623.7	583.7		383.0	369.4	353.0
4500	669.6	641.6	603.2		389.3	376.2	360.3
5000	684.8	657.8	620.7		395.1	382.5	367.2
5500	698.9	672.6	636.7		400.5	388.3	373.6
6000	711.8	686.4	651.4		405.5	393.7	379.5
6500	724.0	699.3	665.0		410.3	398.7	385.0
7000	735.4	711.3	677.9		414.7	403.5	390
7500	746.2	722.7	689.9		419.0	408.0	395
8000	756.4	733.3	701.3		423.1	412.3	400
8500	766.1	743.5	712.1		427.0	416.4	404
9000	775.4	753.1	722.3		430.7	420.3	408
9500	784.3	762.3	732.0		434.4	424.1	412
10000	792.9	771.3	741.3		438.0	(427.9)	416

[a] One amagat of density = 4.4723×10^{-5} moles/cm^3 for CH_4 and = 4.5439×10^{-5} moles/cm^3 for C_3H_6.

Table IX. Pressures of Propene at Integral Densities.

Density Amagats	Temperature, °C 35°	100[a]	Pressure Bars 200° C
300		976	1626
320	(916)	1524	2315
340	1567	2307	3236
360	2500	3379	4478
380	3774	4797	6045
400	5454	6635	8030
420	7621	8960	

[a]The values above the line were determined from the virial expansion.

Table X. Pressures of Methane at Integral Densities

Density Amagats	Pressure Bars		
	Temperature, °C		
	35°	100°	200°
475		1464	2058
500		1739	2399
525	1558	2062	2792
550	1875	2443	3255
575	2270	2894	3796
600	2732	3422	4422
625	3276	4041	5138
650	3928	4762	5959
675	4677	5594	6895
700	5552	6540	7952
725	6553	7619	9150
750	7699	8852	
775	8996	10232	

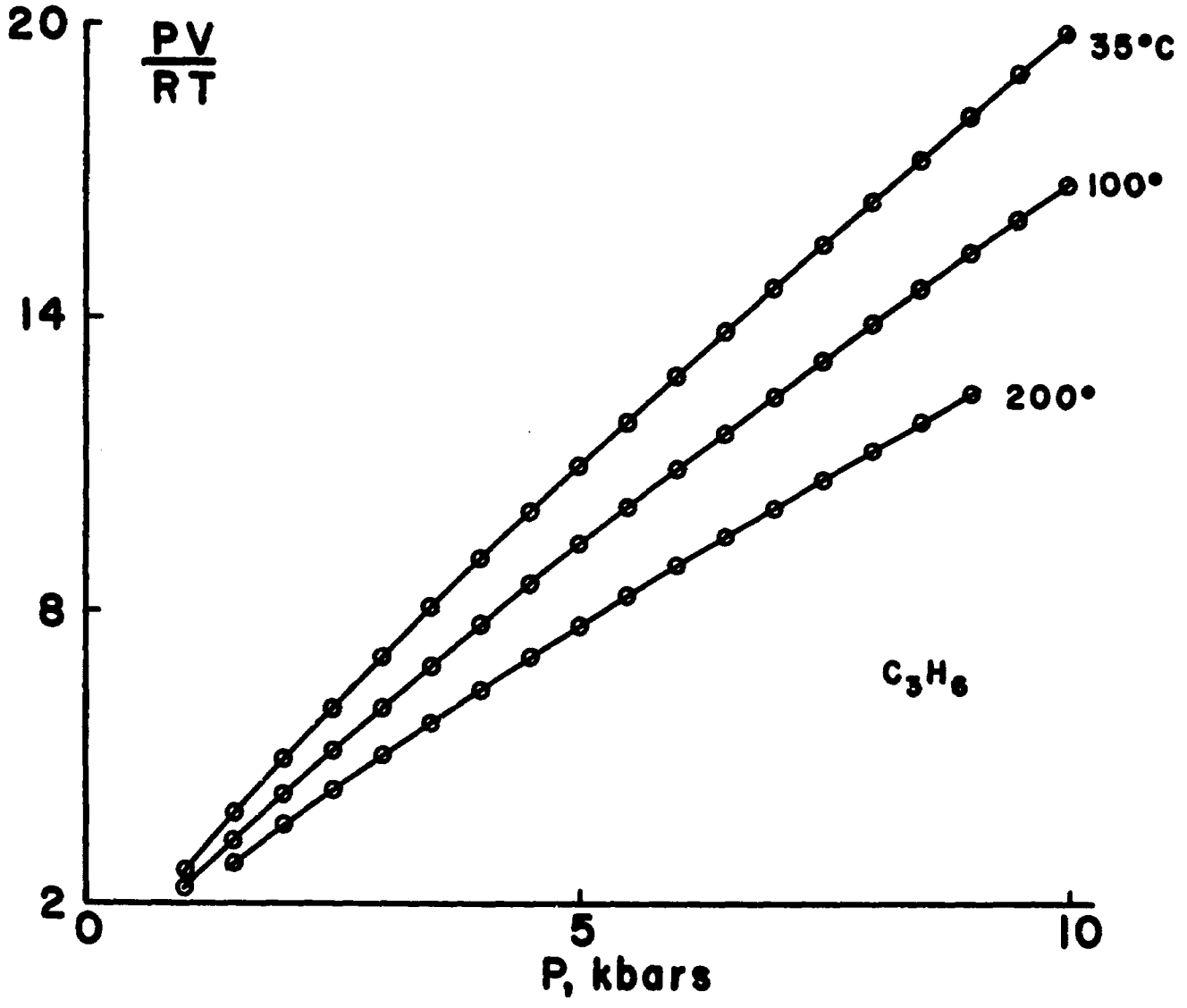

Figure 18. Isotherms of Propene

fiducial points was necessary in order to achieve a reliable interpolation. The actual experimental temperature setting which was used for the isotherm in the fiducial range was 101.36° C. It simply wasn't worth the effort which would have been required to eliminate the 0.02° C temperature difference from the fiducial isotherm and no corrections were made for this small temperature discrepancy. The quality of fit of the volume changes measured in this work to the adopted fiducial densities is not as good as was obtained for other gases, and the initial volume of the piezometer which obtained from the fit to fiducial data was distinctly lower than that obtained from the use of fiducial data for other gases. The initial volume obtained was at least 1.5 per cent smaller than the estimated actual volume. Considering the success of fitting the propene data at 100° C, the data fitting procedure at high temperatures is quite unlikely to be responsible for any of the discrepancies encountered. Since the fiducial data provided by Deffet and Ficks is the only isotherm data reported from their laboratory it is possible that inexperience of those workers led to some minor systematic errors in their work. Thus it is probable in the case of the methane data that an eventual revision of the densities given herein will be undertaken when superior fiducial data becomes available. A scheme was given in the chapter dealing with data reduction whereby the present work can be easily corrected for inaccuracies in the adopted fiducial points.

The highest temperature at which isotherm data was taken for Methane was 200° C. After the polymerization of propene it was decided that caution was the better part of valor and the temperatures were kept low enough to avoid repeating the destruction of a calibrated constant volume chamber.

The methane data is a source of considerable satisfaction. Due to unfortunate mechanical problems both the bellows and constant volume chamber were replaced between the low pressure and high pressure loads of methane. This meant that two completely separate calibrations were used for the piezometer on the two runs. The agreement of the two sets of data over their common pressure range is magnificent. This gives concrete experimental evidence for the internal consistency of the present work.

The present work on methane was accomplished using two samples of gas, both from Phillips Petroleum Company and both of purity greater than 99.95 mole per cent.

Data Tables

The combined data for methane and propene are given in Tables VIII, IX, X and XI. Tables VIII, IX and X were constructed in the same manner as for other gases and the constants for the modified Tait equation are given in Table XI. Following Table XI are the original points upon which the interpolated data were based. Figures 18 and 19 show the isotherms of propene and methane respectively.

Table XI

Parameters in the Modified Tait Equation

T, °C	CH_4 35°	100°	200°	C_3H_6 35°	100°	200°
(Bars) P_o	1500	1500	2000	1000	1000	1500
(Amagats) d_o	520.56	478.37	470.56	323.19	301.45	295.85
(Bars) B	616.49	403.25	362.69	1430.7	1043.8	935.53
(Amagats) C	168.85	172.46	183.12	74.129	74.930	80.08
RMS dev.[a] (Amagats)	1.37	1.34	0.75	0.72	0.89	-

[a] This is the rms deviation of the predictions of the equation with the parameters shown from the original data points. The 100° CH_4 figure includes corrections for thermal expansion from the observed temperatures of 101.36° C. No figure is given for the 200° C_3H_6, since the original data show polymerization.

C_3H_6

35.00°		199.90°	
965	321.76	4193	355.85
1255	331.45	4817	364.72
1457	337.14	5310	371.19
2054	351.25	3489	344.58
2727	363.98	2879	332.97
3279	372.87	1702	302.50
4108	384.42	2308	319.85
5615	401.70	5988	379.96
7109	415.68	7291	393.97
9241	432.50	7956	400.18
8562	427.35	9074	410.52
7776	421.30	8303	404.57
6233	407.74	6629	389.02
8371	426.00	2913	337.56
4866	393.60		

100.02°	
4881	381.16
6256	396.32
7723	409.94
9143	421.50
9685	425.47
8419	415.69
7004	403.34
5515	388.35
3446	361.16
2268	339.20
1906	330.60
1613	322.64
1365	314.94
1154	307.31
1255	311.05
1485	318.72
1762	326.76
2087	334.98
2481	343.67
2944	352.65
4188	372.12

CH_4

35.00° C

1504	520.89
1587	527.95
1617	530.45
1732	539.57
2005	558.99
2168	569.33
2599	593.60
3115	618.16
3739	643.43
4539	670.90
5034	685.80
4119	657.06
3416	630.87
2870	607.05
2392	582.46
1887	550.93
6783	730.62
8674	769.43
7656	749.40
5899	709.26
4990	684.52
4074	655.47
3324	627.12
3344	627.89
2927	609.71
2541	590.64
2738	600.67
3166	620.39
3592	637.79
4350	664.81
5025	685.61
6013	712.26
6771	730.28
7590	748.04
8341	763.02
9049	776.24
9659	787.07
10155	795.43
9374	782.19
8621	768.39
7952	755.41
7142	738.53
6361	720.69
5709	704.39
5342	694.50
4690	675.56
4091	656.06
3804	645.88
4099	656.29

101.36°

1575	484.67
1694	495.45
1787	503.33
1912	513.27
2038	522.72
2345	543.46
2755	567.11
3043	581.98
3763	613.79
4118	627.51
4928	654.86
5474	671.33
4489	640.73
3385	598.00
2556	556.19
2184	533.04
4149	628.73
4561	643.00
5005	657.39
5967	685.04
8150	735.94
8901	750.73
10075	772.18
9657	764.55
9169	755.99
8322	739.49
7571	723.71
7201	715.50
6766	705.17
6350	694.97
5540	673.18

200.00°

1973	468.38
2195	485.68
2498	506.85
3178	546.10
3925	580.56
4690	610.00
5339	631.63
5795	645.52
4994	620.73
4327	596.73
3592	566.05
2857	529.10

200.02°

7795	696.76
8358	709.14
10127	743.56
9680	735.48
9265	727.52
8776	717.78
7108	680.46
6477	664.54
5881	648.03
5240	628.51
4569	605.64
4896	617.17
5671	641.82
6213	657.33
6820	673.34
7451	688.78

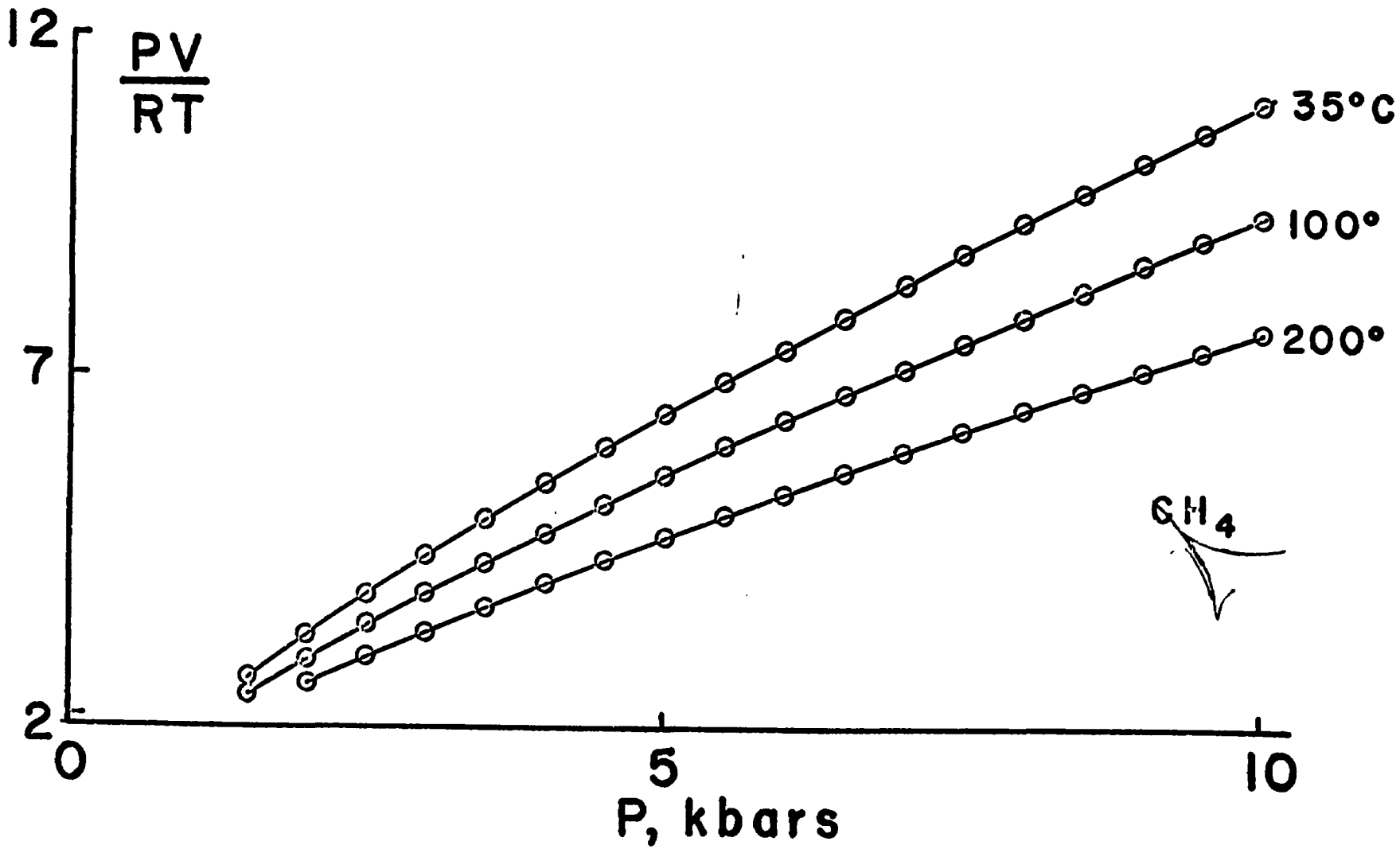

Figure 19. Isotherms of Methane

CHAPTER VII

ERROR ANALYSIS

The magnitude of random density errors as mentioned in previous chapters is about 0.02 per cent. It is conceivable that systematic errors of greater consequence exist within the data and these possibilities are to be explored now. Throughout the discussion it will be assumed that fiducial densities are errorless quantities thus only the errors introduced by the present experiment are contemplated. Errors in the pressure and temperature scales will be reflected in the densities in an attempt to answer the question: At a given pressure and temperature, how well is the density known?

Temperature 35° C

Equation (21) demonstrates that a possible major source of error is defused by the reliance upon ratios of volume changes at 35° C. Systematic errors enter these ratios only through the corrections to volume changes which are not linear functions of the bellows length.

If contributions due to error are indicated by the lower case Greek letter δ then Eq. (21) can be expanded to the first order

of errors in the volume ratio X_i as follows:

$$\frac{\delta d_i}{d_i} = \frac{X_i}{a-X_i}\left[\frac{\delta(\Delta V_{1i})}{(\Delta V_{1i})} - \frac{\delta(\Delta V_{1f})}{\Delta V_{1f}}\right] . \qquad (34)$$

It is evident that the errors vanish for i = 1 (since $X_1 = 0$) and i = f which implies a forced fit at these points. For other values of i the quantity in parentheses will depart systematically from zero if the volume changes are systematically erroneous. The maximum errors should occur for $X_i = 2$ which corresponds to the maximum available volume change, however, a relative maximum in the fiducial range occurs for $X_i = \frac{1}{2}$. The value of a is fixed by the fraction of the initial piezometer volume which is spent in the fiducial range.

The question to be answered now is: Can a systematic volume error remain undetected within the fiducial range and yet have serious effects at higher pressures? The answer can be given by expressing the parenthetic term of Eq. (34) in terms of errors δe, δf and δb of the coefficients of Eq. (12). The coefficient e which is a difference between pressure coefficient of resistivity of michrome and two thirds the compressibility of nickel may be in error by as much as 5 per cent since the separate quantities are known each to about 2 per cent. The coefficient f consists mainly of the corrections for compression of the entire piezometer. The competing effects of decreasing nichrome resistivity and shrinking bridge case very nearly are cancelled within this coefficient. Then since the compressibilities in

question are known to an estimated 2 per cent, errors in f should be in the range 2-3 per cent.

Equation (34) can be rewritten in the form:

$$\frac{\delta d_i}{d_i} = \frac{X_i}{a-X_i}\left[|1-X_i|\ \frac{\delta b}{b}\frac{b(D_f-D_1)}{A} + \delta e|P_i-P_f| + \delta f\left|\frac{P_i-P_1}{D_i-D_1} - \frac{P_f-P_1}{D_f-D_1}\right|\right] \qquad (35)$$

The following conditions correspond to $X_i = \frac{1}{2}$ for a load of argon starting at P_1=2000 bars.

$D_i-D_1 \simeq 300$ div

$D_f-D_1 \simeq 600$ div

$P_i-P_f \simeq 600$ bars

$P_f-P_1 \simeq 1200$ bars

$A \simeq 3.5 \times 10^{-3}$ cm^3?div

$e \simeq 4.7 \times 10^{-7}$/bar

$f \simeq 2.5 \times 10^{-3}$ div/bar

$b \simeq 2 \times 10^{-8}$ cm^3/div

$$a = \frac{V_1}{\Delta V_{1f}} = 8.5$$

If the errors in e and f are overestimated to be 10 per cent and 5 per cent respectively and the error in b is taken as 7 per cent corresponding to the standard deviation from the bellows calibration then Eq. (35) yields $\frac{\delta d_i}{d_i} = 6 \times 10^{-6}$ for $X_i = \frac{1}{2}$. Thus it must be concluded that systematic errors of the kind considered are completely undetectable. The next step, however, requires the estimate of error for $X_i = 2$ which corresponds to about 5000 bars. Taking $D_i-D_1 = 1200$ div, $P_i-P_f = 2000$ bars and all other quantities with the same values as before there obtains $\frac{\delta d_i}{d_i} = 3 \times 10^{-4}$. The addition of a systematic error

for a gas load which extends the isotherm to 10,000 bars would give a maximum error $\frac{\delta d}{d} \approx 6 \times 10^{-4}$ due to errors of volume measurement at 35° C. Unfortunately the answer to the question previously offered is a resounding yes.

Other systematic errors which can be easily estimated are those which arise from failure of the pressure and temperature scales in the present experiment to match those of the fiducial data. The pressure effect is not expected to be serious since the low pressure calibration point for the gauge used was established by Michels who also provided most of the fiducial data. The use of fiducial data requires first that the measured pressures and temperatures be assumed free of error, then the corresponding fiducial densities are obtained. The effects of pressure and temperature error would then be revealed by a poor fit of the measured volume changes to the fiducial densities. Assuming then that the pressure and temperature errors are δP and δT respectively, the error in the assumed fiducial density ρ would be:

$$\frac{\delta\rho}{\rho} = \chi\delta\rho + \beta\delta T \ , \qquad (36)$$

where χ is the gas compressibility and β the coefficient of thermal expansion. With sufficient accuracy for the present discussion, both χ and β can be expanded in quadratic functions of density which will fit well enough to cover the entire fiducial range.

$$\chi_i = \chi_1 + \left(\frac{\rho_f}{\rho_i}\chi_f - \frac{\rho_1}{\rho_i}\chi_1\right)\left(\frac{\rho_i-\rho_1}{\rho_f-\rho_1}\right) + \frac{\gamma}{\rho_i}(\rho_i-\rho_1)(\rho_i-\rho_f) \qquad (37)$$

$$\beta_i = \beta_1 + \left(\frac{\rho_f}{\rho_i}\beta_f - \frac{\rho_1}{\rho_i}\beta_1\right)\left(\frac{\rho_i-\rho_1}{\rho_f-\rho_1}\right) + \frac{\alpha}{\rho_i}(\rho_i-\rho_1)(\rho_i-\rho_f) \qquad (38)$$

γ and α are constants which can be determined by means of the fiducial data. Then assuming accurate volume change ratios X_i Eq. (21) can be expanded to first order in the errors due to P and T with the result:

$$\frac{\rho_i-d_i}{d_i} = \frac{X_i(X_i-1)}{a - X_i}\left\{\left(\chi_f-\chi_o-\frac{\gamma\rho_f}{a}\right)\delta P + \left(\beta_f-\beta_o-\frac{\alpha\rho_f}{a}\right)\delta T\right\} \quad . \qquad (39)$$

The vanishing of the errors at X = 0 and X = 1 implies again that a two point forced fit has been employed and Eq. (39) expresses only the observable density error. For a = 8.5 and $0<X<2$ the systematic error curve is approximately parabolic with a relative maximum near X = ½ which is the middle of the fiducial range. The coefficients of δP and δT are functions essentially of the lowest pressure on the isotherm. If this lowest pressure P_1 is around 1500 bars then for the gases Argon, Nitrogen and Methane:

$$\chi_f - \chi_1 - \frac{\gamma\rho_f}{a} \approx 3\times10^{-4}/\text{bar} \qquad \beta_f-\beta_1-\frac{\alpha\rho_f}{a} \approx 10^{-3}/^\circ\,\text{C} \quad .$$

It is believed unlikely that δP could exceed 3 bars or that δT could be as much as 0.3° C, however if these values are used in

Eq. (39) with X = ½ the result is: $\frac{\rho_i - d_i}{d_i} \simeq 4 \times 10^{-5}$. Systematic errors this small are of course unobservable in the face of the larger random scatter. Nonetheless, the error increases with increasing pressure and attains the value 4×10^{-4} at X = 2 which corresponds to 4500-5000 bars. For a second gas load which begins at about 3000 bars and continues to 10,000 bars, the coefficients of δP and δT in Eq. (39) become negligibly small thus preventing any further contributions to error with each succeeding gas load. In addition, the pressure and temperature scales conform on the overlapped runs above the fiducial range. Thus the systematic error introduced in the fiducial range continues to grow with pressure only by virtue of the error in the initial slope of the isotherm. The magnitude of error is approximately the ratio of densities at 10,000 bars and 3,000 bars multiplied by the maximum error contributed by the first load. This reaches a magnitude of 0.1 per cent. It is an annoying but unchangeable fact that systematic errors can remain undetected in the fiducial range and yet grow rather large at elevated pressures. It is believed, however, that the margins of experimental error used in the estimates have been quite liberal. Thus in summary the combined systematic density errors which have been considered start at zero in the fiducial range due to the forced fit and grow approximately linearly with density to about 0.16 per cent at the highest pressures.

Temperatures Above 35° C

Although Eq. (31) neglects the capillary temperature distribution it correctly expresses all but about 0.03 per cent of the density of gas in the constant volume chamber. It serves therefore for the discussion of errors at elevated temperatures and can be rewritten as:

$$d_u = d_b\left(1 - \frac{\Delta V_b+\Delta V_u+\Delta V_c}{V_u + \frac{V_c}{2}}\right) \quad . \tag{40}$$

$\Delta V_b+\Delta V_u+\Delta V_c$ is the total expansion of the piezometer which occurs upon heating from 35° C to temperature at constant pressure. Subscripts b, c and u refer to bellows, capillary and constant volume chamber respectively. The first order expansion of errors in d_u due to the various density and volume errors is:

$$\frac{\delta d_u}{d_u} = \frac{\delta d_b}{d_b} + \left(\frac{d_b}{d_u} - 1\right)\left[\frac{\delta(\Delta V_b)}{\Delta V_b+\Delta V_u+\Delta V_c} + \frac{\delta\left(V_u + \frac{V_c}{2}\right)}{V_u + \frac{V_c}{2}}\right] + \frac{\delta(\Delta V_u+\Delta V_c)}{V_u + \frac{V_c}{2}} \tag{41}$$

The quantity $\frac{\delta\left(V_u + \frac{V_c}{2}\right)}{V_u + \frac{V_c}{2}}$ which appears above is the error of calibration of the volumes of constant volume chamber and capillary. Its value of 1×10^{-4} is negligible in comparison with the term which precedes it. The ratio $\frac{\delta(\Delta V_u+\Delta V_c)}{V_u + \frac{V_c}{2}}$ represents the errors of evaluation of the thermal expansion and compression of constant volume chamber and capillary tube. Due to the smallness of volume of the connecting capillary there are no

stringent accuracy requirements for its volume correction. Thus the last term consists essentially of errors on corrections to the constant volume chamber. The compressibility χ_N of nickel is known to within 3 per cent over the working pressure and temperature ranges. The effect of error in nickel compressibility at 35° C has already been examined (estimated at 5 per cent) and is included in the $\frac{\delta d_b}{d_b}$ of Eq. (41). As a result, the errors in ΔV_u due to compressibility must be expressed in terms of the errors in the difference $\chi_N(T)-\chi_N(35)$. The thermal expansion coefficient e_N is known to about 1 per cent. Thus incorporating these estimates Eq. (41) can be rewritten:

$$\frac{\delta d_u}{d_u} = \frac{\delta d_b}{d_b} + \frac{\delta(\Delta V_b)}{V_u + \frac{V_c}{2} - \Delta V_b - \Delta V_u - \Delta V_c} + 0.03[\chi_N(T)-\chi_N(35)]P + 0.01\, e_N(T-35) \qquad (42)$$

Using the maximum difference in compressibilities of nickel and P = 10,000 bars it follows that the compressibility correction at elevated temperature differs negligibly from the one at 35° C which is incorporated in $\frac{\delta d_b}{d_b}$ in the above equation. Thus Eq. (42) can be simplified and the effect of temperature error included:

$$\frac{\delta d_u}{d_u} = \frac{\delta d_b}{d_b} + \frac{\delta(\Delta V_b)}{V_u + \frac{V_c}{2} - V_v} + \beta\delta T + (0.01)e_N(T-35) \qquad (43)$$

β = thermal expansion coefficient for the gas.

The reason for not including a pressure error as well as the temperature error δT is due to the reproducibility of the pressure measurements at both 35° C and higher temperatures whereas the temperature errors are independent at each temperature. Furthermore, the effects of pressure and temperature errors in the fiducial range have been considered previously and are included in $\frac{\delta d_b}{d_b}$. It should be noted that Eqs. (40) through (43) apply to isobaric processes; consequently, there are no contributions due to behavior of the gas in the freeze valve. This remains the same along each isobar. Since β and the volume changes ΔV_b vary only slightly for different gases the evaluation of Eq. (43) for Argon is sufficient for the estimate of errors. It is especially interesting to evaluate Eq. (43) at low pressures where $\frac{\delta d_b}{d_b}$ is negligible and at 100° C where comparisons with the same data set from which the 35° C fiducial data was obtained are often possible. In particular, for Argon at 100° C and 2000 bars the parameters in Eq. (43) have the following estimated values.

$$\delta(\Delta V_b) = 1.8\times10^{-3}\ \text{cm}^3 \qquad \Delta T = 0.1^\circ\ \text{C}$$

$$V_u + \frac{V_c}{2} - \Delta V_b = 9.6\ \text{cm}^3 \qquad \beta = 1.7\times10^{-3}/^\circ\ \text{C}$$

$$e = 4.1\times10^{-5}/^\circ\ \text{C} \qquad T-35 = 65^\circ\ \text{C}$$

The estimate of error $\delta(\Delta V_b)$ given above should be about a factor of two too large. Under these conditions the maximum error would be $\frac{\delta d_u}{d_u} \approx 3\times10^{-4}$ which corresponds to approximately 0.2 Amagats. When the

volume changes ΔV_b exceed about 1.0 cm^3 the errors $\delta(\Delta V_b)$ are taken to be 0.1 per cent of ΔV_b corresponding to the expected errors due to calibration and corrections. The predictions of Eqs. (35), (39) and (43) may be summed up in the following table:

TABLE XII

$\frac{\delta d}{d}$ x 100 % Argon

Bars	35° C	100° C	200° C	300° C	400° C
2500	0	0.03	0.04	0.05	0.09
6000	0.08	0.11	0.11	0.12	0.13
10,000	0.16	0.19	0.20	0.20	0.22

CHAPTER VIII

Summary

Within these pages a detailed description of experimental apparatus and procedure has been given along with rather extensive tables of the results obtained and estimates of accuracy. It would be gratifying to report that the behavior of the substances studied was well understood and could be simply represented, however this is not the case. In contrast to the lengthy machine calculations which are fashionable these days, the author joined a lengthy procession of predecessors who sought understanding of the dense fluid state hopefully through the empirical study of the experimental results. Although the effort was by no means wasted in terms of the gain in factual knowledge, the author discovered nothing which would simplify either the understanding or the representation of dense fluid behavior. The best equation of state for hot dense gases of which the author is aware is the modified Tait equation given within these pages. It was born of the necessity for data interpolation on this project and is due entirely to the effort of S. E. Babb, Jr. The equation works increasingly well at higher pressures and temperatures and may represent a limiting form of equation of state for hot dense gases although there is as yet no theoretical explanation for its success.

During the period of time occupied by this research there were some advances in empirical knowledge of dense fluids. The most noteworthy was Holleran's[37] discovery of a linear relationship between density and temperature of a gas along the line $\frac{PV}{RT} = 1$. The Boyle temperature and close-packed solid density are parameters which enter the new relation. With these parameters and a third which apparently corresponds to a range of intermolecular interaction a new and highly accurate law of corresponding states[38] was formulated which holds for simple molecules. The range of correspondence apparently includes the solid, liquid and gas phases, however tests with complex molecular structures have yet to be attempted. The success of the modified Tait equation and Holleran's unit compressibility law and law of corresponding states are added to a growing wealth of knowledge which must sometime be encompassed by theory. The theorists burden is a heavy one indeed.

At the conclusion of any research it is profitable to look back and see what has been done and inquire as to how it could have been done better or more completely. Some considerations of this sort follow.

The work has relied upon fiducial data provided by other workers. At the inception of this research it was felt that the accurracy of the fiducial data was great enough to present no problems, however, the minor inconsistencies which were encountered would indicate that some means of divorcing this experiment from reliance upon fiducial

data should be found. The solution would require the use of something other than a freeze valve for the lowest pressures and perhaps a gas displacement technique for obtaining the initial piezometer volume. A different valve and additional plumbing would permit a weight determination of the mass of gas in the piezometer.

Even if this work could be divorced from the fiducial data it would be extremely interesting to directly measure the effect of the gas-mercury van der Waal's interaction. As long as workers persist in the use of mercury as a pressure transmitting medium the need for this knowledge will remain.

An obvious advantage of the technique used in this work is that the gases are not kept in the presence of contaminants and there are no resilient seals in the piezometer. With the additional advantage of continuous readings available it becomes clear that the type of apparatus employed in this work is overwhelmingly better than any other in existence for the determination of high-pressure isotherm data. If anyone objects to this claim for reasons of accuracy it should be noted that a number of improvements can be made in each of the pressure, volume and temperature measurements without altering the basic design. Although the manganin pressure gauge used in this work is a very good one, the errors of calibration contribute a major portion to the total error. This could be eliminated by comparison with a dead weight gauge in the low pressure range. It would be possible through the use of a potentiometer more accurate than the

Kohlrausch slidewire and the simple expedient of a more precise cathetometer to reduce the scatter in the volume measurements and calibration. The capillary which connects the constant volume chamber and bellows could be reduced in diameter and lengthened to permit the use of a larger and more uniform furnace and more accurate temperature measuring devices such as a resistance thermometer.

All things considered it should be possible with some expenditure of funds to reduce the scatter in the measurements by an order of magnitude and to increase the absolute accuracy of the results by the same amount.

BIBLIOGRAPHY

1. A. Michels, H. Wijker and K. Wijker, Physica 15, 627 (1949) and many works at both earlier and later dates.
2. M. Benedict, J. Am. Chem. Soc. 59, 2224 and 2233 (1937).
3. P. W. Bridgman, Proc. Nat. Acad. Sci. 9, 370 (1923) and Proc. Amer. Acad. Arts and Sci. 70, 1 (1935).
4. J. Bassett and Dupinay, Comptes Rendus 191, 1295 (1930).
5. A. G. Blake, R. H. Bretton and B. F. Dodge, A.I.Ch.E.I. Chem. E., Symposium Series (London) 2, 105 (1965).
6. D. S. Tsiklis and A. I. Kulikova, Zh. Fiz. Khim. 39, 1756 (1965).
7. M. D. Boren, S. E. Babb, Jr. and G. J. Scott, Rev. Sci. Instr. 36, 1456 (1965).
8. P. W. Bridgman, Proc. Amer. Acad. Arts and Sci. 66, 185 (1931).
9. S. E. Babb, Jr., Rev. Sci. Instr. 35, 917 (1964).
10. S. E. Babb, Jr., J. Appl. Phys. 38, 3167 (1967).
11. R. S. Dadson and R.G.P. Greig, Brit. J. Appl. Phys. 16, 1711 (1965).
12. Handbook of Chemistry and Physics, 39th Ed. Chemical Rubber Publishing Co., Cleveland, Ohio.
13. P. W. Bridgman, Proc. Am. Acad. Arts and Sci. 77, 212 (1949).
14. S. E. Babb, Jr., G. J. Scott, C. D. Epp and S. L. Robertson, Rev. Sci. Instr. (in press) Also Stanley E. Babb, Jr., Stanley L. Robertson and G. J. Scott. Final Report on National Science Foundation Grants GP-1847 and GP-5839 (1968).

15. W. E. Deming, "Statistical Adjustment of Data", John Wiley and Sons, Inc., New York 1943, p. 167 ff.

16. American Society Mechanical Engineers (1953) Research Publication, Pressure-viscosity Report Vol. I and II, American Society of Mechanical Engineers; New York.

17. P. W. Bridgman, Proc. Am. Acad. Arts and Sci. 66, 196 (1931).

18. P. W. Bridgman, Proc. Am. Acad. Arts and Sci. 58, 219 (1923).

19. P. W. Bridgman, Proc. Am. Acad. Arts and Sci. 58, 189 (1923).

20. P. G. Tait, Scientific Papers (Cambridge University Press, New York, 1898) Vol. 2. See also G. Tamman, Z. Phys. Chem. 17, 627 (1895).

21. W. B. Jepson and J. S. Rowlinson, J. Chem. Phys. 23, 1599 (1955).

22. P. W. Bridgman, Proc. Nat. Acad. Arts and Sci. 59, 173 (1924); *ibid.* 70, 1 (1935).

23. E. V. Polyakov and D. S. Tsiklis, Zh. Fiz. Khim 41, 2370 (1967).

24. Stanley E. Babb, Jr., "High Pressure Measurements", E. C. Lloyd and A. A. Giardini eds. Butterworths, Washington 1963, p. 115.

25. A. Lecocq, J. Rech. du C.N.R.S. 11, 55 (1960).

26. J. C. Curé and S. E. Babb, Jr., J. Chem. Phys. 48, 2045 (1968).

27. A. A. Broyles, J. Chem. Phys. 35, 493 (1961).

28. W. W. Wood and F. R. Parker, J. Chem. Phys. 27, 720 (1957).

29. A. Michels, H. Wouters and J. de Boer, Physica 3, 585 (1936).

30. D. S. Tsiklis, Doklady 79, 289 (1951).

31. D. S. Tsiklis and E. V. Polyakov, Doklady 176, 308 (1967); [English translation Soviet Physics-Doklady 12, 901 (1968)].

32. A. Michels, R. J. Lunbeck and G. J. Wolkers, Physica 17, 801 (1951).

33. L. E. Reeves, G. J. Scott and S. E. Babb, Jr., J. Chem. Phys. 40, 3662 (1964).

34. A. Michels, T. Wassenaar, P. Louwerse, R. J. Lunbeck and G. J. Wolkers, Physics 19, 287 (1953).

35. S. E. Babb, Jr. and G. J. Scott, J. Chem. Phys. 40, 3662 (1964).

36. L. Deffet and F. Ficks, "Advances in Thermophysical Properties at Extreme Temperature and Pressures", S. Gratch, editor, A.S.M.E. New York, 1965, p. 107.

37. Eugene M. Holleran, J. Chem. Phys. 47, 5318 (1967).

38. Eugene M. Holleran, J. Phys. Chem. 72, 1230 (1968), also Eugene M. Holleran and Gary J. Gerardi, *ibid.* 72, 3559 (1968).

39. P. H. Lahr and W. G. Eversole, J. Chem. Eng. Data 7, 42 (1962).

40. R. K. Crawford and W. B. Daniels, Phys. Rev. Letters 21, 367 (1968).

APPENDIX

Independent Determination of the Piezometer Volume

When two different sample loads span a common pressure range and the piezometer has not been disassembled between the runs it is possible to determine the initial piezometer volume at the lowest pressure on the 35° C isotherm independently of fiducial data. If the raw data from the two runs is plotted on the same graph, such as Fig. 10, the highest pressure 35° C isotherm would occupy a position similar to the 400° C isotherm shown in that figure. The effect is the same in both cases since gas is added to the bellows.

Accordingly, let D_1 be the Kohlrausch slidewire setting at the lowest pressure P_1 on the 35° C isotherm and let P_2 be the pressure on the second gas load corresponding also to D_1. Then a volume change ΔV_{12} occurs when the smaller gas load is raised to pressure P_2. For pressures above P_2 there is a pressure range common to both loads of gas. Within this common pressure range let ΔV_1 represent the volume changes in the smallest gas load beginning with pressure P_2. Then if ΔV_2 represents the volume changes beginning from P_2 for the larger gas load there follows:

$$\frac{\Delta V_1}{M_1} = \frac{\Delta V_2}{M_2} \quad . \tag{44}$$

Where M_1 is the mass of gas in the small sample and M_2 is mass of gas in the large sample. The above equation and the measured volume changes serve to determine the mass ratio $\frac{M_2}{M_1}$.

It is also required that the data reduction yield a unique density at each pressure. Thus if V_1 is the initial piezometer volume corresponding to the slidewire setting D_1 there follows:

$$\frac{M_1}{V_1-\Delta V_{12}-\Delta V_1} = \frac{M_2}{V_1-\delta V-\Delta V_2} \quad . \tag{45}$$

Here δV is a correction on the piezometer volume similar to that given by Eq. (18) due to the initial piezometer volume being slightly smaller due to pressure effects at D_1 on the high pressure load. The last two equations can be solved for the initial volume V_1 with the result:

$$V_1 = \frac{\frac{M_2}{M_1}\Delta V_{12} - \delta V}{\frac{M_2}{M_1} - 1} \quad . \tag{46}$$

The foregoing discussion illustrates the principles involved in an independent determination of the piezometer volume. These considerations were stimulated by small discrepancies which appeared in the values of V_1 obtained by the least squares fitting to fiducial data, some of which was provided for the higher pressure runs by this experimental work.

In actual practice it requires considerable effort to determine the mass ratio $\frac{M_2}{M_1}$ given by Eq. (44). In the first place the volume changes on one load must be obtained by interpolation since only rarely do the measured pressures correspond exactly on two different runs. Second, some means of eliminating random scatter in the data must be found. A reasonable procedure in this last case consists of fitting the interpolated volume changes ΔV_1 to the values of ΔV_2 to obtain a least squares best value of $\frac{M_2}{M_1}$. (This was actually done in the case of argon.) A more direct procedure is possible, however, since the least squares fit to fiducial data randomizes the scatter in volume changes to first order. Thus one can use the modified Tait equation to interpolate densities and then use the densities to interpolate volume changes. These considerations then lead to a more convenient expression of Eq. (46) which can be given in the following form:

$$V_1 = V_1' + \frac{(V_1'-V_2')- V}{(\frac{V_{n2}}{V_{n1}} - 1)} \qquad (47)$$

V_1' and V_{n1} are the least squares best values of V_1 and V_n which are obtained through the use of Eq. (20) for the lowest pressure run and V_2' and V_{n2} are their counterparts on the larger sample load. Thus the left member of Eq. (47) gives an initial volume which is independent of the fiducial data. It should be noted that the role of statistical errors of this determination is displayed as clearly as possible

by the above equation. The major contribution is expressed in the difference $V_1'-V_2'$. The combined standard deviations of these quantities usually amounts to about 0.01 cc while the denominator of the right member usually has a value of about 2×10^{-1}. Thus the volume determined by Eq. (47) is only statistically accurate to about 0.3 per cent. As far as any systematic errors in the present work are concerned the effects would be the same for both the fits to the fiducial data and for the use of Eq. (47). Both approaches are based upon ratios of volume changes, consequently the initial volumes given in each case should be directly comparable.

The following comparison is given for the piezometer volume for argon at 1537 bars and 35° C:

I 16.97±0.08 cm^3--addition of volumes

II 16.99±0.05 cm^3--given by Eq. (47)

III 16.870±0.006 cm^3--fiducial data fitting

The large uncertainty on the external estimate I is due to the difficulties involved in estimating the freeze valve capillary volume and the fully compressed volume of the bellows. A very similar comparison obtains for the nitrogen data.

Discussion of Freeze Valve Characteristics

The assumption was made for the purpose of data reduction that a constant mass of gas at 35° C was responsible for the measured volume changes. This assumption needs to be examined with appropriate consideration of the processes which occur in the freeze valve.

At the lowest pressure P_1 on the 35° C isotherm the capillary tube is blocked at a position slightly above the liquid nitrogen level in the dewar flask and at a temperature corresponding to the melting temperature of the solid at pressure P_1. If there was no compression or extrusion of the solid plug and if the fluid above the plug behaved as if it were all at 35° C then there would be no problems at all associated with the freeze valve, however, one must consider the variations of density within the capillary in order to demonstrate that the departures from the 35° C behavior of the gas are negligible.

The freeze valve capillary tubing traverses a temperature variation from 77° K at the liquid nitrogen level to room temperature in a length of about two to three inches. About fourteen additional inches of capillary stand at room temperature and connect the freeze valve to the piezometer which is thermostatted at 35° C. Within the region of high temperature gradient a solid gas plug exists submerged under a region of liquid which then extends up the capillary until the critical temperature is reached. Above the critical point a gas density gradient exists until the room temperature portion is reached.

When the pressure is increased the solid-liquid interface rises, with the solid volume growing at the expense of the gas in the piezometer and the liquid above the interface. This effect introduces a volume change in the piezometer in excess of the volume change for the gas at 350° C, however, this spurious volume change is partially compensated by virtue of the gas in the room temperature portion of the capillary being less compressible than the gas at 35° C.

If the liquid nitrogen level in the dewar flask is kept constant and it is assumed that the temperature varies linearly within the capillary between 77° K and room temperature, then it is possible to calculate the excess volume change within the capillary by integrating over the density distribution in the capillary. For this calculation let V_c be the capillary tube volume between the initial solid plug position and the 35° C portion of the piezometer. Then if $V_n(P)$ is the normal volume of gas within the capillary at pressure P, the excess of normal volume ΔV_n of gas which is lost from the 35° C portion of the piezometer will be:

$$\Delta V_n = [V_n(P)-V_n(P_1)] - [d(P,35)-d(P_1,35)]V_c, \qquad (48)$$

d(P,35) denotes the Amagat density of gas at 35° C and pressure P. The quantity $V_n(P)-V_n(P_1)$ is given by:

$$[V_n(P)-V_n(P_1)] = \frac{X}{Y}\frac{V_c}{221}\left\{\int_{T_m(P_1)}^{T_m(P)}[d_s(P,T)-d_L(P_1,T)]dT\right.$$

$$+\int_{T_m(P)}^{T_c}[dg(P,T)-d(P_1,T)]dT+\int_{T_c}^{25^\circ C}\left.[dg(P,T)-dg(P_1,T)]dT\right\}$$

$$+[dg(P,25)-dg(P_1,25)]\left(\frac{Y-X}{Y}\right)V_c \quad . \qquad (49)$$

Here room temperature has been taken to be 25° C, subscripts s, L, and g refer to solid liquid and gas, respectively. X is the length of capillary over which the temperature gradient exists and Y is the length between the initial solid plug position and the 35° C portion of the piezometer. $T_m(P)$ is the melting pressure of the solid at pressure P and T_c the critical temperature of the substance.

Equations (48) and (49) have been evaluated for argon. The data of Lahr and Eversole[39] were interpolated and integrated graphically for the evaluation of the integrals in Eq. (49). The major contributions to $V_n(P)-V_n(P_1)$ come from the first and last terms of the right member of Eq. (49). The other integrals could have been safely neglected.

The differences ΔV_n given by Eqs. (48) and (49) are: 0.01 cm^3 at 2000 bars, 0.25 cm^3 at 5000 bars, and 0.62 cm^3 at 10,000 bars. These values are certainly negligible fractions of the 10 to 12 liter normal volumes of the gas within the piezometer. Use of the more

recent argon melting point data of Crawford and Daniels[40] would not substantially alter the results obtained.

Equations (48) and (49) neglect the depression of the solid in the capillary which is due to the compressibility of the solid phase, however, this should not be of any consequence. The experimental results also rule out the possibility of extrusion of the solid for this would introduce a hysteresis which would be detected in the recheck runs at 35° C if the extrusion amounted to as much as one centimeter in the capillary.